REPUBLIC OF TURKEY

YILDIZ TECHNICAL UNIVERSITY

GRADUATE SCHOOL OF NATURAL AND APPLIED SCIENCES

COUPLING A WATER BALANCE MODEL WITH A GROUNDWATER FLOW MODEL AND ITS APPLICATION ON ERGENE BASIN

Emmanuel RUKUNDO

DOCTOR OF PHILOSOPHY THESIS

Department of Civil Engineering

Program of Hydraulics

Advisor

Prof. Dr. Ahmet DOĞAN

May, 2019

REPUBLIC OF TURKEY

YILDIZ TECHNICAL UNIVERSITY

GRADUATE SCHOOL OF NATURAL AND APPLIED SCIENCES

COUPLING A WATER BALANCE MODEL WITH A GROUNDWATER FLOW MODEL AND ITS APPLICATION ON ERGENE BASIN

A thesis submitted by Emmanuel RUKUNDO in partial fulfillment of the requirements for the degree of **DOCTOR OF PHILOSOPHY** is approved by the committee on 20.05.2019 in Department of Civil Engineering, Hydraulics Engineering Program.

Prof. Dr. Ahmet Doğan

Yildiz Technical University

Advisor

Approved By the Examining Committee

Prof. Dr. Ahmet Doğan, Advisor
Yıldız Technical University _____

Prof. Dr. Hayrullah AĞAÇCIOĞLU, Member
Yıldız Technical University _____

Prof. Dr. Abdüsselam ALTUNKAYNAK, Member
Istanbul Technical University _____

Assoc. Prof. Dr. Berna AYAT AYDOĞAN, Member
Yıldız Technical University _____

Assoc. Prof. Dr. Mehmet ÖZGER, Member
Istanbul Technical University _____

I hereby declare that I have obtained the required legal permissions during data collection and exploitation procedures, that I have made the in-text citations and cited the references properly, that I haven't falsified and/or fabricated research data and results of the study and that I have abided by the principles of the scientific research and ethics during my Thesis Study under the title of coupling a water balance model with a groundwater flow model and its application on Ergene basin supervised by my supervisor, Prof. Dr. Ahmet DOĞAN. In the case of the discovery of a false statement, I am to acknowledge any legal consequence.

Emmanuel RUKUNDO

Signature

This study was financially supported through Scientific Research Projects of Yildiz Technical University with project Grant number 2015-05-01-KAP04, as well as partially supported by the Scientific and Technological Research Council of Turkey (TUBITAK) Grant number 115Y008.

.

Dedicated to my Late Parents and Sister

and my Beloved Wife

ACKNOWLEDGEMENTS

First of all, I thank the Almighty God for His endless Grace and Blessing on me during all these years here at Yildiz Technical University and in all my life.

I would like to express my thanks and gratitude to the Scientific and Technological Research Council of Turkey (TUBITAK) for granting me the scholarship to study for a Ph.D. degree in Turkey at Yildiz Technical University and for all their financial support.

I express my sincere gratitude to Prof. Dr. AHMET DOĞAN for having given me an opportunity to work under his guidance and provided the necessary resources for the achievement of the objective of this research. My thanks are also addressed to all Professors of Civil Engineering department especially the Hydraulic division at Yildiz technical University for their intellectual training.

I am grateful to Prof. Dr. Frank Wendland and Dr. Frank Hermann at Forschungszentrum Jülich for providing the mGROWA model and their assistant during the mGROWA model development in the Ergene River catchment.

I am highly grateful to my classmates for their support and encouragement during this research.

I would like to thank also my wife Rosette BAGWANEZA for her valuable moral and love she showed me during this academic Journey. I wish to express special thanks to the family of NGIRUMPATSE Straton, to the family of KARANGWA Vedaste and to the family of KAYIRANGA Vivens for their moral and financial support during my studies. It is here to express my thanks for their special understanding.

We say thanks, although neither the words nor the pages are enough to express our gratitude to everyone who, near or far, participated in our building and contributed to the achievement of this work.

Emmanuel RUKUNDO

TABLE OF CONTENTS

LIST OF SYMBOLS

θ_{pwp}	Soil water moisture at the permanent wilting point
K_{LN}	Crop coefficient
X_i	Original variable i
q_{cr}	Capillary rise
q_t	Total runoff in the grid cell
e	Euler number
E	Residual matrix
E_f	Nash-Sutcliffe index
et_0	Grass reference evapotranspiration
eta	Actual evapotranspiration
h	Potentiometric head
i	Index of the days in a month
K	Hydraulic conductivity
p	Precipitation in grid cell
q_d	Direct runoff
q_r	Groundwater recharge
r	Plant-specific factor
s	Soil moisture
st	Merged station-based daily value

t	Number of days in that month
W	Water source and /or sinks
X	Standardized matrix of variables
Zi	Standardized variable i
θ	Actual soil water content
θa	Plant's available soil water content at field capacity
β	Slope
γ	Aspect
μ	Mean value

LIST OF ABBREVIATIONS

BAS	Basic package
BCF	Block-centered flow package
BFI	Base flow index
CORINE	Coordination of information on the environment
DEM	Digital elevation model
DRN	Drainage package
ETV	Evapotranspiration package
GHB	General head boundary package
HBF	Horizontal flow barrier package
LU	Lower-upper
MoMLR	Monthly Mean Low water discharge for prolonged long period of years
OC	Output control package
PCA	Principal component analysis
RCH	Recharge package
RIV	River package
WEL	Well package

LIST OF FIGURES

LIST OF TABLES

ABSTRACT

Coupling a Water Balance Model with a Groundwater Flow Model and its Application on Ergene Basin

Emmanuel RUKUNDO

Department of Civil Engineering

Doctor of Philosophy Thesis

Advisor: Prof. Dr. Ahmet DOĞAN

Groundwater is of great importance to support the ecosystem life on planet earth. The reliable simulation of groundwater recharge and identification of its dominant influencing factors is indeed the key control to understand the groundwater system, its potential accessibility, and its sustainability. During this research, a GIS grid based water budget model (mGROWA) was applied to estimate the long-term groundwater recharge and other water balance quantities based on basin characteristics such as hydro-climatic data, land cover, soil textures, geology, and topography. The study was performed in Ergene river catchment (11000 km^2) which is one of the Mediterranean basins located in Turkey. The model simulations were done for the spatial resolution of the grid cell of 100 m for the period of 20 years (1991-2010). The hydrograph separation techniques, based on the base flow indices (BFI), were applied to split up the modeled total runoff into two main components namely groundwater recharge and direct runoff depending on the catchments attributes (e.g. geology, groundwater depth). The model was validated in 10 sub-catchments possessing long-term daily stream records. Thereafter, the statistical methods including Pearson correlation method and principal component

analysis (PCA) were integrated for assessing the most controlling basin factors that are influencing the groundwater recharge. Simulated groundwater recharge rates were displayed as long-term yearly mean and as long-term monthly levels with the purpose of denoting periodic variation of groundwater recharge.

mGROWA has shown the ability for estimating the spatial and temporal variability of groundwater recharge with high confidence, however, it does not simulate the distribution of hydraulic heads. Against this background, a new method for integrating the mGROWA, with the regional subsurface water flow model (MODFLOW) was adopted. The recharge values resulted from mGROWA was provided to MODFLOWas input data, in a steady state, and the simulated groundwater depths by MODFLOW become the input file of mGROWA. In this coupling, the iteration ends when acceptable groundwater heads are reached.

The model validation and statistical analysis have indicated that the differences between simulated and observed values are generally under 20% and no valid inconsistency was observed. PCA revealed that the recharge variation is mostly influenced, in order of significance, by vegetation land cover, soil textures, and climate variables. The generated results may conclusively contribute to the establishment of quantitative status of groundwater system exploitation and enhancement of water resource management policy of the study area. In addition, this study draws special attention to the advantage of applying coupled procedures to adjust and validate the recharge rates as input data of the upper boundary in sub-surface water flow models.

Keywords: Ergene catchment, Recharge, Water budget components, Catchments characteristics, and Principal component analysis

ÖZET

Su Bütçesi Modeli ile Yeraltı Suyu Akım Modelinin Bağlanması ve Ergene Havzasında Uygulaması

Emmanuel RUKUNDO

Inşaat Mühendisliği Bölümü

Doktora Tezi

Danışman: Prof. Dr. Ahmet DOĞAN

Yeraltı suyu, dünya ekosistemini desteklemesi dolayısıyla büyük bir öneme sahiptir. Yeraltı suyu beslemesinin güvenilir modellerinin yapılması ve buna bağlı olarak etkin olan faktörlerin tespit edilmesi, yeraltı suyu sisteminin anlaşılmasında, potansiyel erişilebilirliğinde ve sürdürülebilirliğinde kullanılan en önemli araçlardandır. Bu çalışma boyunca, CBS hücre temelli bir su bütçesi modeli olan mGROWA uzun dönemli yer altı suyu beslemesinin ve diğer su dengesiyle ilgili büyüklüklerin tahmin edilmesinde kullanılmıştır. Su dengesiyle ilgili büyüklükler hidro-iklimsel veriler, arazi kullanımı, zemin yapısı, jeoloji ve topoğrafya gibi havza karakterlerine bağlıdırlar. Çalışma Türkiye'nin Akdeniz havzalarından birisi olan 11000 km^2 alana sahip Ergene Nehri su toplama havzasında gerçekleştirilmiştir.

Simülasyonlar 1991-2010 yılları arasındaki 20 yıllık dönem için ve 100 m'lik bir uzamsal çözünürlükle yapılmıştır. Taban akımı indislerine (BFI) dayalı hidrograf ayırma teknikleri, havzanın toplam akışının yeraltı suyu beslemesi ve direkt akış bölgesi olarak ikiye ayrılmasında kullanılmıştır. Bu ayrıştırmada jeoloji ve yeraltı

suyu derinliği gibi özellikler etkendir. Model, 10 alt-havzada yer alan uzun dönemli günlük kayıtlarla doğrulanmıştır. Sonrasında, Pearson korelasyon yöntemi ve birincil bileşen analizi (PCA) de dahil olmak üzere bazı istatistiksel araçlar havzanın yeraltı suyu beslemesi üzerindeki etken parametrelerin değerlendirilmesinde kullanılmıştır. Yeraltı suyu beslemesinin periyodik değişkenliğinin resmedilmesi amacıyla simülasyon sonuçları olarak elde edilen yeraltı suyu besleme değerleri uzun dönemli yıllık ortalama ve aylık ortalama şeklinde gösterilmişlerdir.

mGROWA uzamsal ve zamansal yeraltı suyu beslemesi değişkenliğini tahmin etmek konusunda yüksek bir doğrulukla başarılı olmuştur, ancak hidrolik basınç değerlerini tahmin etmemektedir. Modeli geliştirmek amacıyla bölgesel bir yüzey suyu akış modeli olan MODFLOW kullanılarak bu model mGROWA'ya entegre edilmiştir. mGROWA'dan elde edilen yeraltı suyu besleme değerleri MODFLOW'a kararlı durum için girdi olarak, MODFLOW'dan elde edilen yeraltı suyu derinlik değerleri ise mGROWA için girdi olarak kullanılmıştır. Bu ikili eşleşmede iterasyon, kabul edilebilir bir yeraltı suyu seviyesi elde edilince sonlanmaktadır.

Model doğrulama aşaması ve istatistiksel analiz, simülasyon sonuçlarıyla ölçülmüş değerler arasında %20'den daha büyük bir farkın ve herhangi bir tutarsızlığın bulunmadığını göstermiştir. PCA analizi besleme değişkenliğinin daha çok, önem sırasıyla; bitkisel arazi tipi, zemin yapısı ve iklimsel değişkenlerden etkilendiğini göstermiştir. Elde edilen sonuçlar bölgede yeraltı suyu sistemlerinin mevcut durumlarının sayısal olarak değerlendirilmesinde ve su kaynakları yönetimi politikalarının geliştirilmesinde kullanılabilir. Ayrıca, çalışma besleme değerlerini yukarı havza sınırında girdi olarak kullanılmasıyla su akış modellerinde iki farklı yöntemin eşleşmeli olarak kullanılmasının avantajlarına dikkat çekmektedir.

Anahtar kelimeler: Ergene su toplama havzası, Besleme, Su bütçesi bileşenleri, Su toplama havzası karakteristikleri, Birincil bileşen analizi

1

Introduction

1.1 Literature Review

Groundwater reservoir is an important source of water for nearly 50 % of the earth's population for different purposes such as in the domestic activities use, power generation, and irrigation practices [1]. The groundwater can be considered as a renewable water resource for giving assistance to the agricultural, industrial, environmental, and domestic needs which nowadays present an important increase in their demands [2]. The determination of recharge is necessary in order to address some of the key study priorities in the groundwater reservoirs and estimate its continuous access possibility even though other parameters must be considered, e.g. social, economic and hydrogeological information [3]. However, the recharge component in water balance quantities remains the least understood quantity generally caused by its extensive spatial and temporal variability and require more attention for direct measurement [4]. The research on groundwater recharge in a river basin or at a regional scale is very important to provide insight into the quantitative status of the groundwater reservoir, thus the groundwater resources management.

The existing studies related the groundwater in the Ergene River basin has only put attention on quality, not the quantitative status of the groundwater [5], [6]. The spatially differentiated water balance together with recharge within this catchment has not been studied and satisfactorily understood. However, the Ergene catchment, in the northwestern part of Turkey, is considered as an important source of the freshwater. The Ergene drainage area provides assistance to the economies of the area in providing the domestic water to the people living in the area, approximately equals to 1.150.000, in satisfying the industrial needs which are about 2500 textile factories, supplying the irrigation water for the agrıcultural lands of approximately

73% of the total area of the Ergene river basin, and also keep the environmental sustainability of the ecosystem within the investigated area [7]. Groundwater is of great importance as the main source of a direct water supply system and important for the irrigation for the land of the Ergene basin. To expand the Ergene catchment methodology of sustainable groundwater resources management, the recharge together with other water balance components must be quantified in spatial and temporal resolution, there is a need to broadly ascertain and well understand them over the study area. Groundwater recharge refers to as deep infiltration of water from the rainfall or river that percolates from the earth to unsaturated zone of soil namely vadose zone of the soil, then replenishes acquirer, and the recharge quantitative analysis remains important in the management of groundwater.

In last years, a lot of researches in the hydrogeology, mainly took attention in the determination of base flow, as portion contribution of groundwater discharged into the river [8], [9] and some methods were used for this objective including the recursive digital filter approach [8], smoothed minima base flow separation techniques, approach of graphics, chemical budget techniques and also the conductivity mass budget approach [9]. Some other numerous techniques were also applied to determine the groundwater recharge including direct measurement approaches, such as seepage meters and tracer methods. Nevertheless, the field measurements methods showed their limitation in terms of high cost [10], and are mostly influenced by the analysis of errors and the irregularity patterns in spatial [11]. The water balance including the recharge was recently simulated by using computer-based models, which depend on soil–water balance approach and they are well-known by their high accuracy. However, their simulated results are of limited estimates especially in the lack of model calibration and verification caused by the significant uncertainties presented in input data.

The spatially distributed groundwater recharge levels are paramount input data of regional sub-surface water flow models, especially concerning a reasonable and precise determination of sub-surface water dynamics and quantities. At catchment or regional scale, the sub-surface water flow models, the spatial and temporal patterns are unable to be determined accurately by trial and error approach

throughout the adjustment of the model within the investigated area. Nevertheless, this may be done by taking into account the hydrogeological procedures and apply the water budget modeling approach to describe and simulate the upper boundary recharge to the groundwater flow models. The analysis of the influence of natural and anthropogenic drivers of dynamics at the catchment scale for a long period of time necessitates a combination of awareness and modeling ability throughout hydrological information and processes, and computer potential. Models integration aims to expand the model control range in order to incorporate a new aspect of the operations with the purpose of figuring out progressively. The fundamental aim of coupling models is to link disciplines and connect separated knowledge among them for reinforcing their abilities to severely assess the interactions issues between environment an human activities along with the dynamics scenarios analysis [12].

Groundwater flow models are known as very helpful tools for understanding the groundwater systems of a given region, applicable for groundwater resources management, and in its future exploitation planning. Last decades, different studies have focused on the developments of subsurface water simulation models. For instance, Groundwater modeling system GMS, designed by the united states department of defense, and it supports the MODFLOW 2000 code, Visual MODFLOW, FEFLOW, Groundwater Vistas, and SWIFT. The use of MODFLOW, which is a modular three-dimensional finite-difference groundwater model of united states geological survey, in the representation and estimation of the response of groundwater systems, has become greater over the last decades. The model can generate the influence of wells, rivers, drains, head-dependent boundaries, recharge, and evapotranspiration and their codes are named packages used to model the hydrological systems. A number of stand-alone programs, in last years, were able to interface together with MODFLOW through the data files in many studies, for instance, the effective transport program PMPATH, the solute transport model MT3D, MT3DMS, and PEST for parameter estimation.

The water budget model mGROWA is well used for large scale water balance components simulation including the groundwater recharge [13]. The development

of the model allows the calculations with high resolution of the recharge and this the main objective of mGROWA. This grid-based spatially distributed water balance model (mGROWA) and modular three-dimensional finite-difference groundwater flow model MODFLOW [14] are proven to be applied for simulating the hydrological responses. Nevertheless, mGROWA and MODFLOW differently symbolize a building structure, (e.g. regional discretization and hydrological response modeling) and are respectively restricted to their modeling world, each presenting strengths and weaknesses while simulating hydrological responses and applying computational resources [15].

MODFLOW model is well-proven to be applied for assessment of the groundwater system which is frequently quasi-steady state and consequently requires spatially distributed groundwater recharge in the long period as upper boundary input data. Therefore, mGROWA, which generates accurate long-term groundwater recharge depending on climatic data, land-use types, soil groups, topography, and geology of the investigated area, could be applied in integration with MODFLOW for the aim of assessing the sub-surface water dynamics and groundwater reservoir. This will enhance the modeling of the influence of long-term stressors e.g., climate and land-use change [16], [17], [18], groundwater contaminant transport assessment, crop-specific irrigation demand estimation, and applied as the decision support system for water resources management.

MODFLOW has become nowadays the most useful simulating tool in the researches about the assessment of the groundwater flow within an aquifer system. The various graphical user interfaces (GUIs) have been designed in order to make easy the work of modeling using MODFLOW model with the purpose of production of a model definition of input and output files and for the visualization of the results and interpretation of outputs of the model [19]. The graphical user interface mainly possesses an interactive environment where the user develops simulation cells insert input data such as hydraulic properties and boundary conditions, execute the simulation and perform the post process of the obtained results. However, the different graphical user interface is designed with varying complexity and sophistication levels [19]. Recently, scripting MODFLOW model in Python has

become popular and Python permits in the insert and applies the modeling in its environment. It has the advantages in the development of the model input data files execution of the simulation and read and draw outputs of the model. The importance of using Python in groundwater flow remains in existence of packages to ease the simulation development process, together with packages used for plotting the model outputs, controlling array, making a maximization, and the assessment of data.

1.2 Objective of the Thesis

The main objective of this thesis is to develop a new approach by coupling the mGROWA and MODFLOW models in order to assess the groundwater recharge at a regional study by considering a case study of Ergene river basin. The thesis specific purposes are split into two objectives (1) to develop a method for determining spatially distributed water budget components including groundwater recharge that can assist to some of the key study priorities in groundwater and to show the importance of the method for regional scale; and (2) to couple mGROWA with MODFLOW models and apply it to Ergene catchment to improve the model results for groundwater recharge and hydraulic heads assessments.

The novelty of this study is first that a distributed water budget model such as mGROWA was applied to the entire Ergene river basin for the first time, and this will enable to provide a detailed groundwater resource information necessary for water resources management in the investigated area. Secondary, due to the limitation of mGROWA ability to provide details on groundwater dynamics, and also to determine the groundwater table levels, which is an important data in estimation of recharge in wetlands dependent zone or shallow areas, the coupling of mGROWA and MODFLOW was necessary and done for the first time in other to improve the two model details results.

This study generally developed a new approach that strongly relies on the impact of soils groups, land-use types, topography, and climatic conditions in order to calculate spatially distributed recharge and generate at the same time the sub-surface water flow dynamics by coupling mGROWA and MODFLOW models. The accurate estimate of recharge at the regional scale is the leading variable required

for exploring the recharge-discharge systems along with providing the authenticity in sub-surface water flow models calibration and validation. The groundwater recharge and dynamics are a prerequisite to the sustainable sub-surface water quantity and quality management.

1.3 Hypothesis

The hypothesis of this study is defined as mGROWA model generates no valid contradictory behaviors on water balance quantities and the coupling mGROWA and MODFLOW models generate all observed behavior of groundwater dynamics (for instance hydraulic heads).

The mGROWA model is a grid-based distributed hydrological water budget model and will be applied in order to simulate the water budget components: actual evapotranspiration, total runoff, direct runoff and groundwater recharge at Ergene River basin. mGROWA simulations will be performed in daily time steps for the hydrological reference period of 20 years from 1991-2010 and in a spatial resolution of 100 by 100 m. Simulated groundwater recharge rates will be presented as long-term annual averages and as long-term monthly values in order to indicate the seasonal fluctuation of groundwater recharge rates.

The most important mGROWA output will be groundwater recharge levels which will be used as the upper boundary condition of MODFLOW. Iterative mGROWA MODFLOW applications will be done in order to improve model results relating to groundwater dynamics (Figure 1.1). In the dependent wetlands areas, to estimate the evapotranspiration and recharge, the position of the water table plays the important role in the calculation, the mGROWA model, in this study is iteratively coupled with the groundwater flow model MODFLOW which is capable to generate the groundwater table level within the catchment as input data in mGROWA. In coupling the mGROWA returns the groundwater water recharge to MODFLOW. In this study, the calculated groundwater recharge in the investigated area as the output of the mGROWA is integrated into a groundwater flow model (MODFLOW) as upper boundary layer in order to determine groundwater dynamics e.g. the hydraulic heads distribution as shown in Figure 1.1. The outputs of this approach

are tested and validated by comparing the recorded and calculated hydraulics heads.

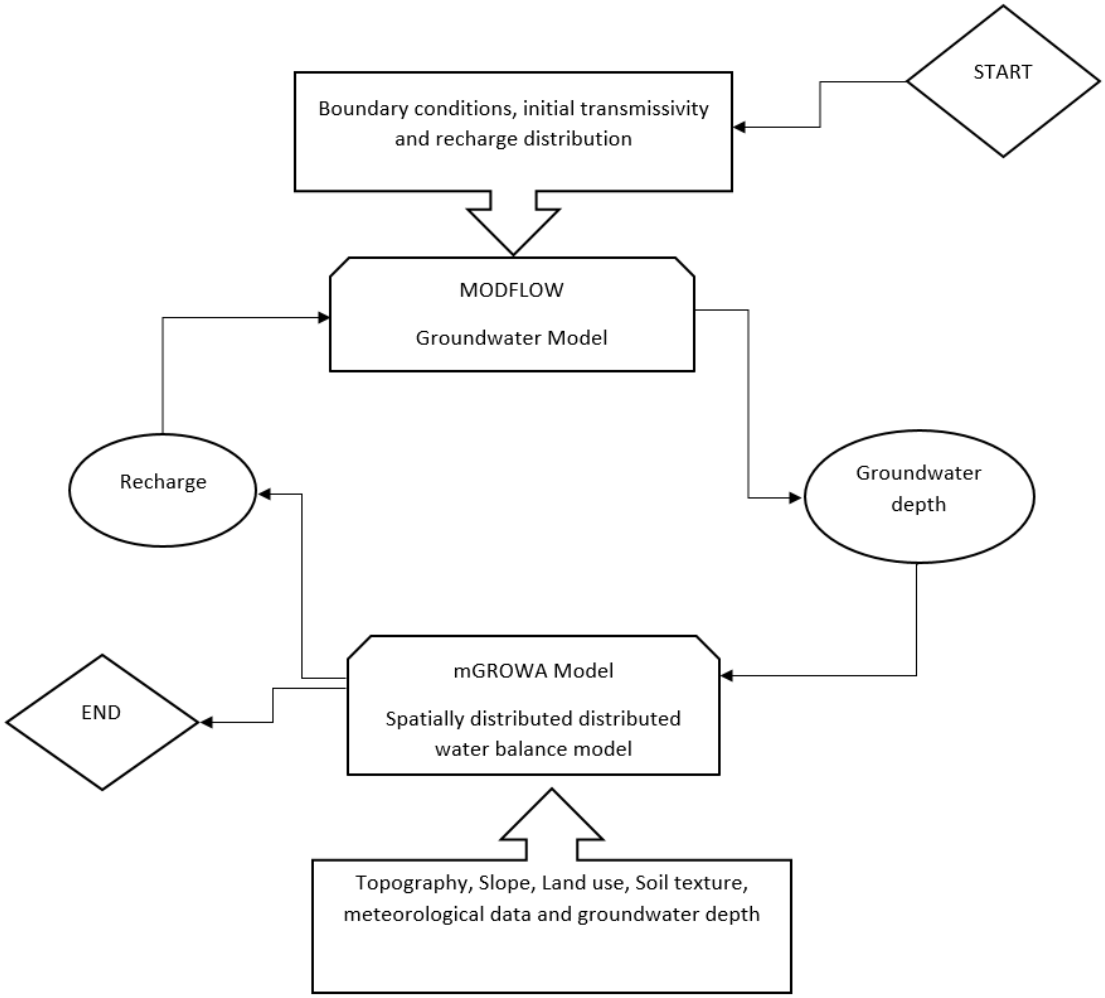

Figure 1. 1 Schematic Diagram of the Iterative Process Between mGROWA and MODFLOW Models

2

General Review

2.1 Introduction to Modelling Groundwater Recharge Process

Accurate spatial and temporal characterization of groundwater recharge is fundamental for effective water resources management. However, surface water bodies and groundwater system have been always in dynamic interaction. Due to the connection between groundwater and surface water, their interaction mainly happens when a part of groundwater flows to the surface water body, e.g. rivers or when some amount of water surface infiltrate and replenish an aquifer as recharge [20]. A recharge is commonly referring to as the hydrologic process where water flows downward from the surface water body and pass the water table to groundwater reservoir. This process generally takes place in the unsaturated zone under the plant roots zone where there is excess soil water and is commonly referring to as a flux to the water table level. However, all the excess water in the unsaturated soil does not necessarily get to the groundwater due to ability properties of storing in the unsaturated zone, also when groundwater system is not able to accommodate further recharge. For instance, the infiltrated water may be stopped by impervious or semi-pervious rocks and flow laterally in the soil [21]. The recharge in shallow aquifers might also lead to local seepage by establishing an increase in the level of the water table; also the groundwater reservoir may subsequently be withdrawn by plant evapotranspiration [21].

Different methods may be used to estimate the recharge. The most applied methods are direct measurement by using lysimeters, tracer methods, and stream gauging techniques [22]. A lysimeter can be defined as a device used in the site, possessing a weighable soil column where the water coming to and leaving from this device are calculated and storage change can be detected. The lysimeter approaches may be also applied to estimate the evaporation as it can be able to estimate other water

budget elements. However, these direct approaches are sensitive to the errors in measurement and spatial change pattern, and highly expensive [11]. Groundwater models are also applied to determine recharge in case of all other elements of the hydrologic water cycle are given with high accuracy. However, as hydraulic properties of the aquifer are also largely unreliable, the recharge is usually roughly determined as a lumped fitting parameter along with other uncertain variables throughout the calibration [23]. Accordingly, it can be said with confidence that an advanced calibration can be reached given that the observed rates of recharge are inputted into the groundwater.

2.1.1 Water or Soil Moisture Budgets Techniques

In the soil moisture budget approach, for determination of groundwater recharge, when the soil water content equals or arrives at the field capacity, the soil starts draining. Therefore, it is required to determine the soil water content conditions for the duration of a year in order to analyze the critical conditions of the soil. Against this background, there is a need for clarification of appropriate characteristics of the soil along with the ability of the plants to extract water from the soil and transpire it. In the case where there are no plants cover in the investigated area or bare soil, only evaporation is taken into an account. The evaporation of such bare soil can be very significant in some locations such as in the semi-arid areas in order to explain the water content status in the soil when the dry season ends and in temperate climates where in the winter seasons the groundwater recharge is observed and the evaporation is considered as a lost water from the soil. Mostly, evapotranspiration happens at a lower amount than their potential amount because of plant stress coming from the restricted availability of water content existing in the soil. In the water balance approach, the input is the difference between daily precipitation and interception and runoff in order words infiltration. The equation below shows the water budget.

$$Q_r = P - R - ET_a - \Delta S \qquad (2.1)$$

Where $Q_r$denotes recharge [L], P stands for the precipitation [L], R represents runoff [L], ET_a stands for actual evapotranspiration [L] and ΔS shows the storage change in the soil [L].

In the recharge determination, the design of the conceptual model (Figure 2.1) is a key step. It can be designed at the starting of the recharge assessment and examined as additional information that gives new insights to the hydrological system [24]. Soil moisture balances present the main elements of any conceptual model in hydrology, giving a joint in groundwater recharge together with other processes in the water cycle.

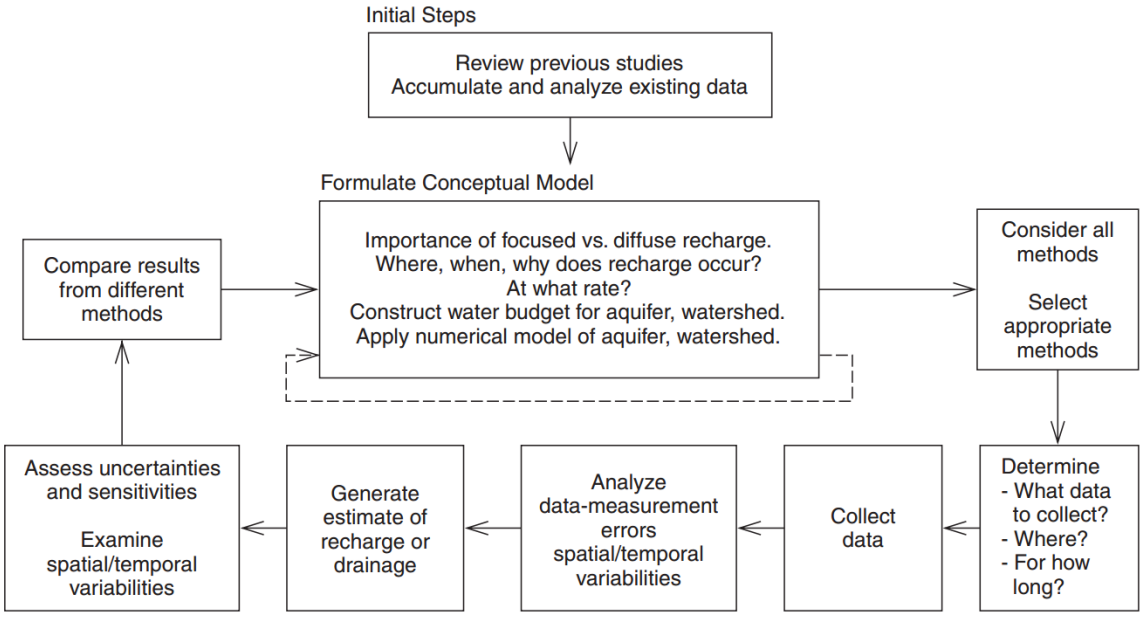

Figure 2. 1 The Iterative Process for Designing a Conceptual Model of Groundwater Recharge Processes

2.1.2 Spatial and Temporal Variability in Recharge

Generally, the groundwater recharge levels spatially change either in systematic or random patterns over an investigated area. The climatic data, land-use change and geology play the principal role in systematic patterns of a recharge. The higher precipitation occurs in the area where the more recharge rates occur. The random parameter in spatially distributed groundwater recharge may be presented as a local-scale alteration in space that may be assigned, for instance, to various diversity

in permeability in soil types and land cover changes e.g. vegetation. The groundwater recharge can be also changed in time. The recharge variability is affected by seasonal trends and trends that are happening in long periods of years. The groundwater recharge rates may be also affected by alteration in time of land-use changes e.g. vegetation. The significance of spatially and temporally distributed area change in groundwater recharge have to be taken into account with the overview of the aims of the study. In the groundwater resources assessment, the change in recharge may not be critical when a mean amount of groundwater recharge has to be estimated for the whole aquifer. For analyzing the aquifer vulnerability to contamination, the distributed area change in recharge becomes significant, thus, techniques to produce point estimates of groundwater recharge can be suitable. In the last decades, the design of the groundwater flow models have taken into account the assumption of considering a recharge as non-variable in time. Nowadays, the groundwater flow model applications frequently permit a recharge to change during a long time, however, a recharge is taken as non-variable for years.

Many studies around the world for spatially distributed groundwater recharge were done and some literature of them were summarized and presented in the section below:

Kunkel and Wendland (2002) in [25] applied the GROWA98 model for an area distributed water budget assessment in Elbe catchment. In this study, the water balance components were estimated depending on regional site conditions such as the precipitation, temperature, land cover, soil groups, geology, and topography. They presented a methodology of total runoff separation by applying baseflow indices in unconsolidated and hard rocks by considering geology and groundwater depths. This study has permitted the applications of the models for instance for the determination of diffuse nutrients existing in groundwater.

Bogena et al. (2005) in [26] focused on the assessment of the uncertainties in the modeling of the recharge for various scales. In this research, the grid-based water balance model GROWA was applied to assess the influences of various sorts of uncertainties on the simulated recharge due to the uncertainties existing in the input data. In this study, the area differentiated input errors were estimated in

topography attribute by applying Monte Carlo approach. The authors discussed the uncertainties existing in the GROWA outputs for various scales.

Karpuzcu et al. (2008) in [27] conducted a study on three Turkish catchments with the main objective of assessing the water pollution in these investigated areas. The water balance model GROWA was used in order to produce water budget components such as runoff, evapotranspiration, and recharge based on soil, land, topography, geological and climatic data of the interest areas. GROWA model has proven its capability in simulating the recharge in Turkish catchments.

Herrmann et al. (2009) in [28] studied the regional groundwater recharge by applying GROWA in Germany in the Lower Rhine lignite mining area. The aims of this study were to generate the groundwater recharge rates and provide a comparative assessment of the results of the groundwater model Rurscholle and two groundwater recharge different datasets and finally to provide a methodology for the validation of GROWA model outputs where the modeled hydraulic heads together with the recorded data from the wells were used. This research showed the benefit of applying a coupled methodology and the techniques for groundwater recharge calibrating and validation for regional studies.

Panagopoulos et al. (2015) in [29] discussed the results of the area distributed water budget model in the case study of Pinios catchment located in Greece. The GROWA model was applied for this purpose and has shown the successful applicability in the groundwater resources management in this interesting area which is a part of the Mediterranean basin, regardless the climatic information, soil and land parameters together with geological characteristics for which the model was developed and tested.

Herrmann et al. (2015) [13] developed a new model mGROWA for simulating the components of water budget including the recharge at a large scale. The mGROWA is grid-based water balance model which determines, at the regional scale, the recharge as long term yearly mean and also the temporal monthly recharge with the purpose of showing the seasonal fluctuations. The in- and out fluxes of each individual grid cell of the model are calculated separately without considering lateral water or energy fluxes. The outputs of this model were used for assessment

of the use of groundwater in the Federal State of North Rhine Westphalia in Germany.

Tetzlaff et al. (2015) in [30] investigated the area distributed groundwater recharge taking a case study of Slovenia in the line of Europe water legislation. For this purpose, the spatially differentiated water budget model GROWA was applied in order to provide an accurate water budget components including the recharge. In this study, it was found that the groundwater resource display huge regional and seasonal patterns. The outputs of the study were used for water resources management by decision makers of Slovenia.

Zomlot et al. (2015) in [31] studied the area distributed of recharge together with the base flow and their influencing parameters in Brussels, Flanders, and Wallonia in Belgium by using the spatially distributed water budget model named WetSpass to determine the long-term recharge. The WetSpass is classified as a quasi-steady state model to estimates the water and energy transfer among the soil, plants, and atmosphere. The model produces the spatial distribution of water balance components such as runoff, evapotranspiration, and groundwater recharge on a large scale. During this study, the influencing factors controlling recharge and base flow were examined.

Ehlers et al. (2016) in [18] focused on the sensitivity of-of recharge estimated by a grid-based water budget model mGROWA considering the soil and land use characteristics changes and climate change in the Mediterranean catchment. The research assessed the climate change influence on recharge by taking a case study of Riu Mannu basin which located in Sardinia. The study also analyzed the impact of changes in the crop coefficient together with various soil structure differentiation in a catchment on modeled recharge. The research was appropriate to possess involvement in water security in the basin and the results provided by this research was an extremely important direction for decision makers in the water resources management sector.

Herrmann et al. (2016) in their study [32] about modeling the future recharge by considering the climate change models in the Mediterranean basin in the Thau basin located in France. This study combined the recorded climate information together

with the combination of global and regional circulation models and executed in the water budget grid-based model mGROWA in order to determine the current and the future recharge for the investigated case study. The outputs have shown that there is no trend of reduction in recharge and soil characteristics taken in the maps and synthetic aperture radar convey to the good model outputs.

Hermann et al. (2016) in [33] conducted the research about the influence of climate change to the required irrigation and water resources specifically the groundwater resource and the investigation happened in the catchment of Hamburg located in Germany. In this study, the required irrigation and recharge ratio was analyzed in order to detect the influence of climate change on the groundwater resource vulnerability. Against this background, the water balance model mGROWA was applied by taking into account of the modeled recharge rates and the required field plant-specific irrigation. The outputs of this research showed the significant role of area distributed parameters in simulating recharge and base flow.

Cheo et al. (2017) in [34] applied water balance model GROWA in the Far- North region located in Cameroon with the aim of simulating the area distributed groundwater recharge through precipitation in order to provide information related to the sustainable groundwater resources management. It was summed up that GROWA model outputs provide a reliable groundwater recharge in the interested area through precipitation.

2.2 Groundwater Flow Models

In the century of 19th, the researchers worldwide had initiated the basic development of the groundwater water flow models for its quantitative description. Hegen and Poiseuille in 1839 and 1840 respectively in [35] and [36], were first to provide the techniques and equations to handle some issues with a viscous flow in the capillary pipes. In 1958, the scientist Henry Darcy in [37] developed the approach to estimate water motion in a porous medium, this has been used as Darcy Law. A big number of models nowadays use this law in order to analyze the groundwater flow, not only in the models but also in some experimental studies, the Darcy law has been used. Since the groundwater is the fundamental source of fresh water which do sustain the different life aspects of planet earth, numerous studies

have put their focus on surface and groundwater interactions to handle different hydrological, geological and environmental issues caused by this interaction.

The study of the groundwater reservoir within the aquifer is complex due to the issues of accessibility of the data, but also the financial problem as some studies requires experimental studies which are costly, difficulties in allocating the boundary conditions for the investigated area, even less expertise in the assessment of groundwater, etc. Due to the complexity of analyzing the groundwater at a large scale, there is a need for using models. Several groundwater models were developed to analyze the issues of groundwater. For instance, Groundwater modeling system GMS [38], designed by the united states department of defense, and it supports the MODFLOW 2000 code, Visual MODFLOW [14], FEFLOW [38], Groundwater Vistas, and SWIFT.

Normally, understanding the process of a complex physical process, there is a need for the development of models for simplifying the process. This is the same for interpreting the groundwater system, a groundwater model may be taken into account as an important, accurate and valuable estimating tool for subsurface management and planning for future exploitation. The models are nowadays so applicable in order to simulate the behavior groundwater flow [39]. Besides, groundwater models are considered as a powerful tool, as they determine the groundwater heads for complex hydrogeological conditions [40]. The groundwater models are split into two categories [41], where the first one includes models used for determining the head distribution of under certain conditions, for instance, in the study of the hydrological alteration under agriculture activities such as irrigation or in water supply in groundwater abstraction. The second category deals with the solute transport models, which are mainly applied to simulate the solute concentration influenced by dispersion, advection and chemicals reactions. However, these models can be grouped into two classes namely physical and mathematical models. It is stated that the physical models are developed in the laboratory environment by applying the porous medium such soil (silt, sand, and gravel) to determine the heads and directions of flow [40]. Whereas the mathematical models are mainly relying on mathematical partial differential

equations of groundwater flow. The analytical or numerical techniques can be applied to provide the answers of this partial equations, thus their names are mathematical groundwater models. The mathematical structure is applied to decrease the complexity of the geometry of the domain for delivering a quick response. These models are dependent on physical characteristics of an investigated area such as climate data, land use data, soil data, geology topography, and the boundary conditions, to achieve this objective they use different approaches including the finite difference and finite element techniques [40].

2.2.1 Physical Models

The experimental models are being for analyzing the water flow and transport process in the soil, thus the physical models are developed in the laboratories environment. SandBox Model is mostly known as a physical one and has got expertise in simulating groundwater flow and transport processes. Many experimental setups were performed to analyze the processes of the variable density flow of underground water flow in a saturated medium in the objective of applying the validation of the output of numerical models. Thus, SandBox models enable to get the data necessary for performing the benchmark examples [42]. Besides, they may be applied to analyze the contaminant in groundwater water and remediation under various site conditions. Nevertheless, a number of important dissimilarities between the small size of the experimental model compared to the real observations on the site. Thus their results should be verified if used with the observed ones [42].

2.2.2 Mathematical Models

Various groundwater flow models are categorized as mathematical models and have been applied in application from the 18 century. The basic approach of mathematical models is to analyze the behavior of the groundwater reservoir system and constitute by expressions including partial differential formulas. Generally, the mathematical models are categorized as deterministic and stochastic models [42]. In the deterministic ones, it takes into account the principle in which the occurrence of considered input events reaches a certain determinable result. In the stochastic approaches, there is an advance assumption of uncertainties in input

data, and regarding this, the model observes the uncertainties. The deterministic models are greatly applied compared to the stochastic approaches, despite the fact that the intended trend, in the study to establish the adoption of stochastic approaches, exists. Inflow issues, to solve the partial differential equations, there is a need for knowing the initial conditions, and boundary conditions, in order to numerically solve it [42].

Numerical methods are very useful to solve some realistic site cases, especially for regional groundwater flow studies. In the last decades, the numerical models were attracting the attention of researchers in their design and they become suıtable for dealing the complex issues, with the high speed in processing by computers. These numerical models presented the interests in modeling the multidimensional and complex physical systems, modeling the temporal and spatial distributions of different program results, enabling the use of boundaries conditions, matching the input information spatial variability and both steady and transient states. Thus these models are good for solving the issues of real groundwater flow at different scales. As a matter of fact, the design of groundwater flow models for a mathematical method by governing equation together with the related boundaries states would be much difficult than developing an analytical model approach. The computer code is needed for solving the differential equations, and these equations are presented by a number of algebraic equations which must be decoded by simultaneously as many methods were developed to analyze these numerical models [42].

In the groundwater flow issue, the hydraulic heads are the approximates responses of these models at a given point in time and space domain. Here, a number of algebraic formulas with regard to discrete piezometric heads, an environment of the model, take a place of partial differential equations at given locations. In solving the water-related issues, numerical approaches for many combinations of diffusion-advection issues were used. In most cases, the groundwater issues can be analyzed by pure diffusion equation whereas the solute transport may be described by diffusion-advection methods.

The section below presents the literature about the use of groundwater model worldwide: Khalaf and Abdalla (2014) in [43] applied Groundwater modeling

system for multi-aquifer systems of Nubian aquifer system located in Weste of Africa with aim of studying the issues related to dewatering and increasing in depths of groundwater table whether in shallow or deep aquifer. The results of the study were used to analyze the optimal pumping rate for various modeling temporal references.

Qiu et al. (2015) in [44] applied the groundwater modeling system model GMS in order to assess the groundwater system and the water resources in the study area namely Jilin catchment located in China. In this study, it was proven that the groundwater recharge presented the most sensitive parameter in the developed model. It was concluded, in this study, that a numerical model such as GMS can be applied in the interested area in order to produce efficient results that can be used in the investigated area groundwater resources management and sustainability.

Rahnama and Zamzam (2013) in [45] studied on modeling the groundwater in quantity and quality using mathematical models with help of groundwater flow model MODFLOW together with MT3DMS in the case study namely Rafsanjan aquifer. Through the results of the study, ıt was suggested that the use of water resources in the investigated area have to be reduced and stop the flow provided by agriculture wells.

Guzman et al. (2015) in [15] developed a new approach of integrating Soil Water Assessment Tool well known in surface water studies and groundwater flow model namely MODFLOW in order to simulate the dynamic interaction between surface and groundwater. The outputs of this developed integration displayed the similarity in modeled and observed discharge and groundwater levels and it was concluded that this linkage can be applied for modeling dynamic interaction between the domain of surface and groundwater water systems.

Bailey et al. (2016) in [46] focused on studying spatial and temporal patterns interactions of surface and groundwater domains at large scale. The study applied a coupled approach of Soil Water Assessment Tool and groundwater flow model MODFLOW in the Sprague catchment located in the USA in order to examine the interaction between surface and groundwater and later on apply this information in the water resources management and water rights in the investigated area. The

outputs of this study also had shown the potential places from the aquifer to rivers with mass loading of heavy nutrients.

Qadir et al. (2016) in [47] conducted research about a 3-D conceptualization and modeling groundwater flow in Dera Ismail Khan basin located in Pakistan. The study applied the groundwater flow model Visual MODFLOW for the long-term hydrological period in order to examine the present status and future groundwater levels in the investigated area. The modeled results showed incremental drawdowns during the considered simulated temporal duration.

Bakker et al. (2016) in [19] have presented a new technique for groundwater model by designing a Python package named FloPy that can build model input files, execute and post-processing of the results of the MODFLOW model. The application of this groundwater flow model in the environment of the python ease the data exploration, and possible model evaluations which may be easier for a graphical user interface.

3

Materials and Methods

3.1 Study Area Description

This study was conducted in Ergene river basin which is located in the middle of the Thrace region, at the part of north-west of the Republic of Turkey. This investigated area is bordered by north Marmara river basin, Meriç river basin and the country of Bulgaria, and situated between the latitude coordinates of 466.000 and 602.000 m and the longitude coordinates of 4.510.000 and 4.660.000 m as shown in Figure 3.1. The Ergene river basin covers 1.4 % of the Republic of Turkey and possesses an area of approximately 11,000 km^2. The topography in the digital elevation map shows that the minimum and maximum elevations in the Ergene river basin reach respectively 2.4 m and 1,021 m above the sea level as shown in Figure 3.1. The main river of Ergene drainage area runs from the West-side in the Istranca Mountains to the East side of the catchment with the length of 265 km with the average annual discharge of 28.7 m^3/s. The River of Ergene and its affluent streams are of great importance source of the water in the north-western side of the Republic of Turkey. It assists the economies of the area as a the main source of the water in supplying the municipal domestic water for approximately around 1,150,000 habitats and the industrial water needs for approximately around 2,500 textiles factories located in this area, the agricultural water needed by crops in irrigation, noted that the agricultural lands mainly control the basin with approximately an area of 73% of the whole Ergene river basin and maintaining the sustainability of the ecosystem life in this region.

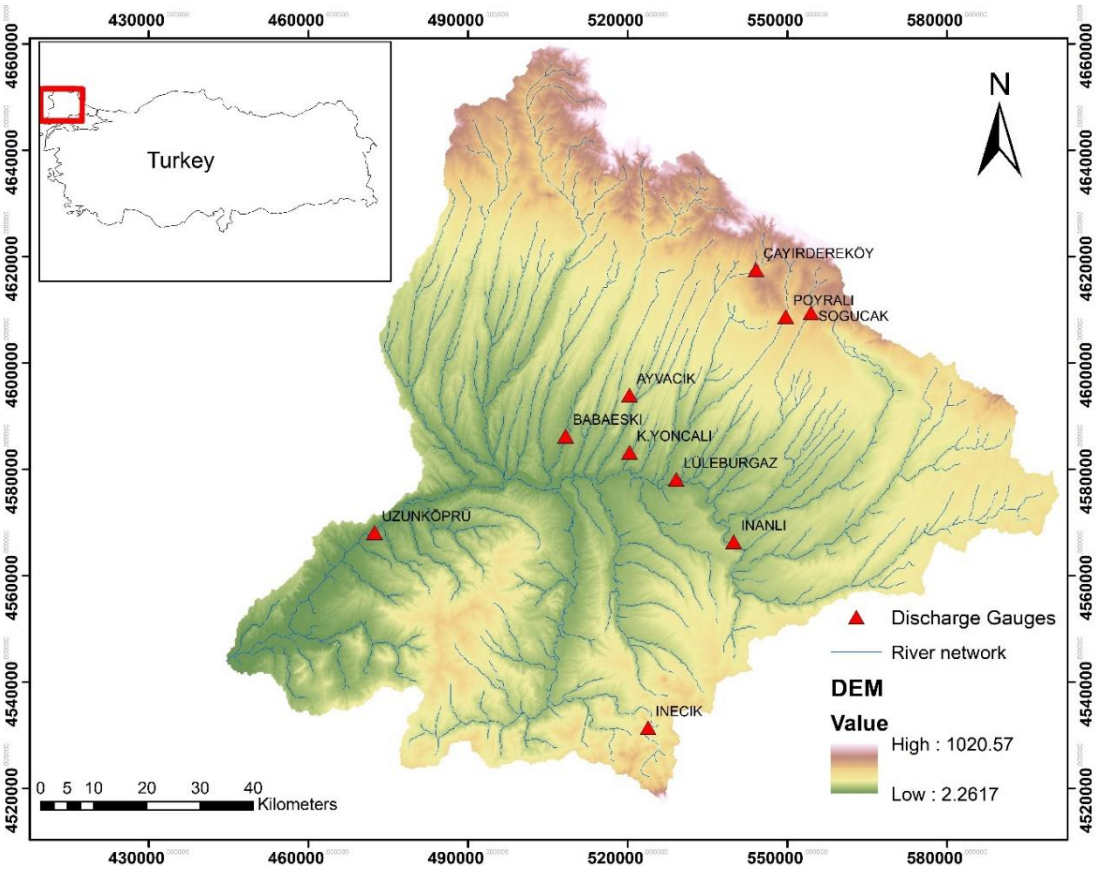

Figure 3. 1 Ergene Catchment Geographic Context and Available Gauging Stations

3.2 Water Balance Modeling Based on mGROWA Model

A grid-based hydrological water balance model mGROWA was designed the application of regional or catchment scale, for spatially highly resolved long-term estimation of water budget components including direct runoff, evapotranspiration and groundwater recharge[13]. Regarding the classification of models by Becher and Serban (1990) in [48], it is categorized as a grid-based hydrological water budget model. The development of mGROWA goes around the flow of ideas of conceptual models where the representation of the hydrological operation uses the fundamental laws of physics. However, this model at a certain level, it has an empiricism approach. In addition, the mGROWA approach is extremely dependent to the basis of the data which is mostly area covered by the regional information for groundwater resources management and the need of having spatially highly resolved water quantities patterns, for instance for 100 m resolution or lesser, which is appropriate for the execution of sustainable groundwater resources

management. mGROWA, in its first run, estimates physically the soils moisture dynamics, capillary rise, from the groundwater to the root zone, total runoff and actual evapotranspiration in daily time.

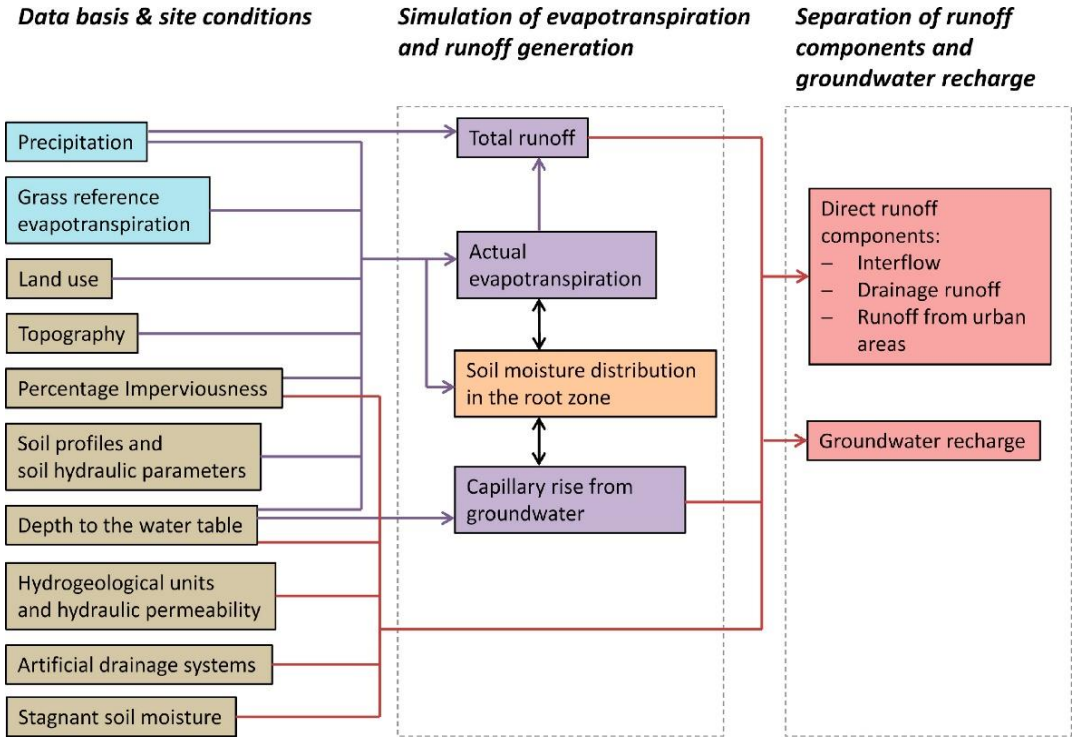

Figure 3. 2 mGROWA Model Input Data and Its Simulation Scheme

Figure 3.2 shows the general modeling scheme realized in mGROWA. The left column lists the spatial data basis mandatory for performing simulations. The middle column shows the main water balance quantities simulated by the programme Mgrowap. The separation of runoff components and groundwater recharge is based on results produced by Mgrowap and is performed by the programme Mgrowa Runoff Separation.

The water budget quantities for each discrete grid cell and the vertical flux are determined by applying the water budget formula in Equation 3.1.

$$\frac{ds}{dt} = p + q_{cr} - et_a - q_t \qquad (3.1)$$

Where s denotes the storage level that can be stated as the soil moisture (mm/day), p presents the precipitation in a grid cell (mm/day), q_{cr} stands for the capillary rise from the groundwater, eta denotes the actual evapotranspiration (mm/day)

estimated by using equation 3.2, and q_t shows the total runoff in the grid cell (mm/day).

The actual evapotranspiration depends on grass reference evapotranspiration (et_0), crop coefficient (K_{LN}), relief function depending on slope and aspect ($f(\beta,\gamma)$)and a function of soil water content (s) as denoted in equation 3.2, f (β, ϫ) was obtained by applying the equation 3.3.

$$et_a = et_0 . K_{LN} . f(\beta,\gamma) . f(s) \quad (3.2)$$

In the high elevation of topography, the actual evapotranspiration rates are also affected by topographic factors such as slope and aspect. This impact is considered in the form of a correction factor given by equation 3.3.

$$f(\beta,\gamma) = \gamma[1.605 \cdot 10^{-2} \cdot \sin(\beta - 90) - 2.5 \cdot 10^{-4}] + 1 \quad (3.3)$$

Figure 3.3 shows the dependency of the correction factor on relief factors such as aspect and slope. It is shown that the actual evapotranspiration on southerly exposed slopes prevails or dominates that on northern slopes.

As a result, for instance, a 16 % higher evapotranspiration rate is determined for southerly exposed slopes for a slope inclination of 10° compass direction than flat land. When it comes to the northerly exposed slopes for the slope inclination of 10° compass direction, against this background, the rate of evapotranspiration is determined to be equal to 84 % of the evapotranspiration of flat area. These dissimilarities in evapotranspiration raise with increasing slope inclination. Because of the additive correlation between precipitation and actual evapotranspiration in the simulation of the total runoff rates, it can cause a change of the runoff rates for determined considerations.

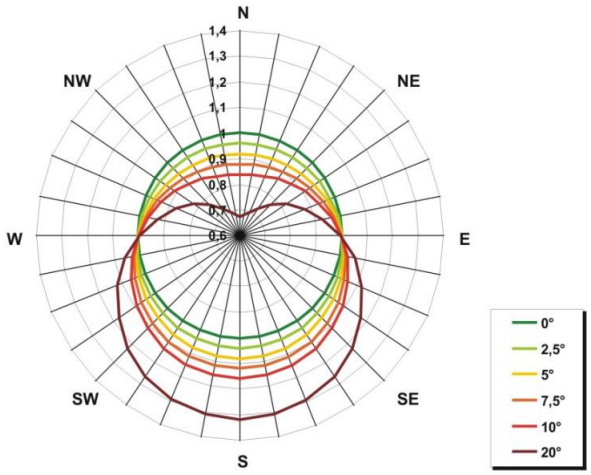

Figure 3. 3 Function Values of Topography

Depending on the site parameters and conditions e.g. vegetation covered land, impervious covered land, and free water, the storage function can be determined. Equation 3.4 represents the Disse function which is the inter-dependent function of actual evapotranspiration and varies in the range [0,1]. When the soil water content diminishes to the permanent wilting point, the Disse-function turns to zero thus the real evapotranspiration does. When the water content in the soil increase up to field capacity level, the Disse function displays 1 and thus the real evapotranspiration is maximum.

$$f(\theta) = \frac{1-e^{-r\frac{\theta-\theta_{pwp}}{\theta_a}}}{1+e^{-r\frac{\theta-\theta_{pwp}}{\theta_a}-2\cdot e^{-r}}} \tag{3.4}$$

where θ represents the actual soil water content, e stands for the Euler number, r shows vegetation or plant-specific factor, θa represents the plant's available soil water content at field capacity, θ_{pwp} soil water moisture at the permanent wilting point.

In the land located in impervious surface, e.g. in urban areas, the storage function is determined by applying the equation 3.5 and the storage function equals to 1 for the water body areas as enough quantity of the water is accessible for the evaporation action.

$$f(s) = \begin{cases} 1, & s \geq et_0 . K_{LN} . f(\beta, \gamma) \\ 0, & s = 0 \\ \frac{s}{et_0 . K_{LN} . f(\beta, \gamma)}, & 0 < s < et_0 . K_{LN} . f(\beta, \gamma) \end{cases} \quad (3.5)$$

The water storage capacity of 1 mm over an impervious grid located in urban areas [49] is considered in mGROWA and if daily precipitation goes beyond the 1 mm, the excess of precipitation becomes the direct runoff. Consequently, the more impervious sites exist in the investigated area, the more direct runoff is generated.

In the second run of the simulation, mGROWA split up empirically the total runoff into direct runoff and groundwater recharge and the outputs of the model are presented in monthly time steps as it was proved that the groundwater management does not need a higher temporal resolution[13]. The separation approach applied the concept of a base flow index (BFI) as described in Kunkel and Wendland, (2002) in [25](Equation 3.6).

$$q_t = BFI . q_t + (1 - BFI) . q_t = q_r + q_{d,} \quad (3.6)$$

Where q_d shows direct runoff and q_r denotes the groundwater recharge.

Figure 3.4 presents the concepts of BFI that are used in distributed water balance model mGROWA for determining the groundwater recharge in the investigated area. The impervious area, such as urban areas, generates a total runoff which equals to direct runoff as presented in Figure 3.4. Under this impervious area, there is no account of the recharge due to the imperviousness of cover of the land, there is even no penetration of the water counted in these areas. In the previous areas, such as in the vegetation land cover, or the dependent wetland zones, the groundwater table level plays an important role in the hydrograph separation. In a shallow zone, the net groundwater recharge is estimated due to the impact of the capillary rise occurring in such kind of area. In the area that the impact of capillary rise is not taken into account, the rock types of investigated area dominate the recharge. Regarding the types of rocks of an aquifer, the base flow index is determined [13].

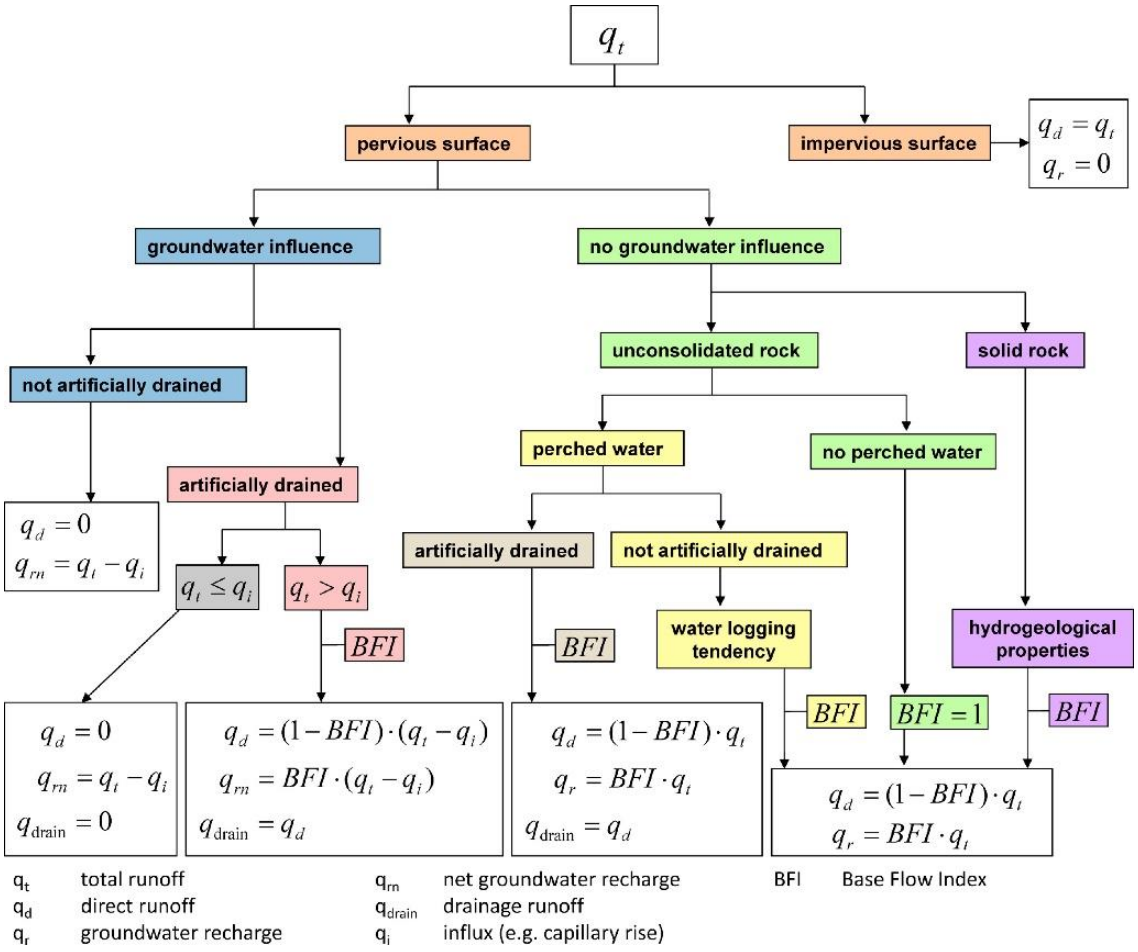

Figure 3. 4 Base Flow Index Method for Total Runoff-Separation in mGROWA [13]

3.2.1 Computation of Daily Climate Drivers

Two categories of climatic input data have to be prepared for the mGROWA-simulation. First, station-based daily time series of p and et_0 in order to derive the time behaviour and second, regionalised monthly sums of p and et_0 in a grid format in order to input a precise water and energy budget. There are mainly two reasons for the use of the monthly budget in grid format in the end. (1) The number of interpolations to perform increases significantly if they are performed on a daily basis and thus the runtime of the pre-processing of the simulation and eventually the occupied disk space. (2) The regionalisation of station-based monthly sums of p and et_0 lead to a more reliable spatial distribution compared to a regionalisation on a daily basis because of the short-term spatial heterogeneity of these quantities. Finally, the modeller is able to use regionalisation techniques which are suited for the specific conditions in the area under consideration.

The programme *Mgrowap* repeats the sorting of the two internal lists of *p*- and et_0-stations concerning the distance of stations to the grid cell being processed in ascending order. Each grid cell is encompassed by four quadrants in the mathematical meaning. For each of these quadrants the programme determines the nearest *p*- and et_0-stations that have daily values for the month being computed available. Based on these four stations (in the best case), the programme computes so-called merged daily sums for the days belonging to the corresponding month by using the inverse distance weighting method [50]. If in any quadrant no suitable station could be found, the number of stations is reduced, respectively. The merged daily sums are then used as weights for the calculation of daily values based on the gridded monthly sums by using the following equations 3.7 and 3.8:

$$p_i = p_g \cdot \frac{p_{st,i}}{\sum_{i=1}^{t} p_{st,i}} \tag{3.7}$$

$$et_{0,i} = et_{0,g} \cdot \frac{et_{0,st,i}}{\sum_{i=1}^{t} et_{0,st,i}} \tag{3.8}$$

i - index of the days in a month, *g* - grid-based monthly value, *t* - the number of days in that month, *st* - merged station-based daily value. By using this approach, the simulation results finally base on the water and energy budget originating from the monthly grids and have obtained their climate-induced time behavior from the daily station-based time-series.

3.2.2 Method for Base Flow Determination

In the Ergene river basin, the only 10 streamflow gauging stations were identified to possess data and their hydrographs represented the data since the hydrological year of 1991 to 2010.

The ArcGIS tools were used to delineate the sub-basins based on the availability of gauging stations, and the river grid map and topographic data from the Ergene digital elevation model(DEM). The daily mean data of total runoff was analyzed at selected gauging stations for the calibration and verification of the mGROWA model results analysis as shown in figure 3.6. The selected 10 discharge stations constitute areas in the catchment in the range from 50 to 1094 km^2, these sub-catchments

present a large change in characteristics related to climatological data, geological information, and site soil parameters. The recorded mean long-term total runoffs have been used to test the validity of the estimated mean long-term total runoff. In the numerous number of literature, it has been proven that the groundwater recharge may solely indirectly be estimated from the observed discharge by adopting relevant hydrograph separation methods.

For the determination of BFI values, in the first step, the recorded runoff was used to estimate the base flow indices values within the selected sub-basins. For this purpose, the runoff data were assessed, however, it was found that the most basins of Ergene are greatly affected by activities of water management such as irrigations, dams and other reservoirs, thus the necessity of using a large scale has to be taken into account for this purpose. The basin related base flow indices (BFI_{basin}) were estimated according to the equation 3.9.

$$BFI_{basin} = Q_G/MQ \quad (3.9)$$

Where MQ stands for Mean annual discharge in m^3/s, and Q_G means groundwater discharge in m^3/s.

The base-flow in the interested sub-basins was separated from the total observed discharge by applying the method known as monthly low water flow rates (MoLR) [51]. Wundt (1958) in [52] showed that, regarding the unconsolidated aquifers, for long term series of years, for instance, more than 10 years, the mean monthly low water flow values present the accurate estimates of groundwater recharge of the investigated area. This approach is known as Monthly Mean Low water discharge for a prolonged long period of years (MoMLR). Regarding the impervious zone such as hard rock aquifer, the MoLR-values are not accurate compared to the mean groundwater recharge, as the MoLR possesses also valuable quantities of direct runoff, such as direct runoff and interflow, whıch is also taken into account by the MoMLR method. Thus, Kille (1970) in [53] and Demuth (1993) in [54] generated a useful hydrograph separation method for the consolidated zones, to allow a decrease of MoMLR values in the interflow component as shown in figure 3.5. MoMLR-method is presented in equation 3.10. Then, the MoMLRr-value were generated by the use of concept the slope m, the number of MoLR values n and the axis intercept y0 as shown in figure 3.5 and expressed in equation 3.11

$$Q_G \approx MoMLR = \sum_i^n MoLR_i/n \quad (3.10)$$

$$MoMLR_r = m \cdot \frac{n}{2} + y_0 \quad (3.11)$$

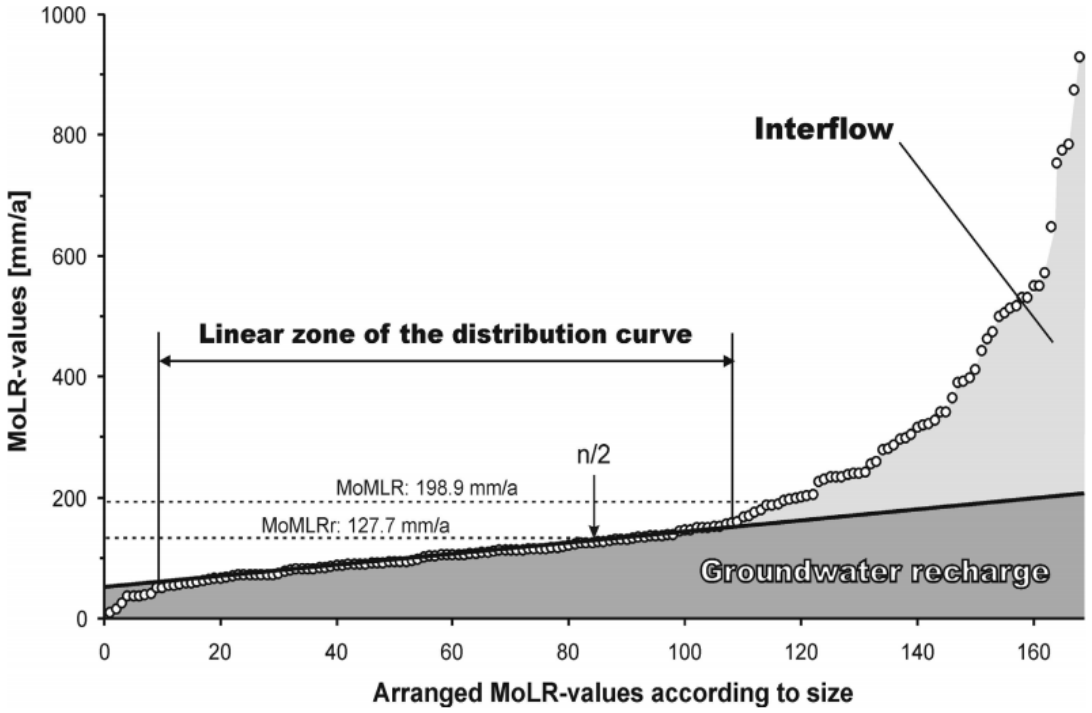

Figure 3. 5 Separating the Interflow Component from Groundwater Recharge in Consolidated Rock Areas(MoMLRr-method)

3.2.3 Attribution of Area-Differentiated BFI Values in mGROWA

In the unconsolidated rock regions, the mGROWA model uses the BFI values from the literature, as it was proven by my studies such as [55] and [56] to reach to the realistic groundwater recharge values. BFI are presented in table 3.1. For the solid rock regions, as the effect of geological subsoil conditions by far predominates that of soil characteristics by Kunkel and Wendland(1988) in [55], the influence of geology in determining the river flow fractions, and they established the hydraulic conductivity classes and their corresponding BFI values generated by calibration (Table 3.2).

Table 3. 1 BFI-values of the Unconsolidated Rock Areas According to Dörhöfer & Josopait (1980) [*56*], Hennings (2000) [*57*] and Wessolek & Facklam (1997) [*49*]

Degree of sealing	Groundwater depth	Water logging tendency	Slope	Baseflow indices
	> 2 m	No water logging	< 1 %	1
	1.3 – 2 m	1 (very low)	1 – 3.5 %	0.9
I (10 – 45 %)				0.82
			3.5 – 7 %	0.67
			7 – 10 %	0.59
	0.8 – 1.3 m	2 (low)	10 – 13 %	0.5
	0.4 – 0.8 m	3 – 4 (medium – high)	13 – 15 %	0.44
	< 0.4 m	5 (very high)	> 15 %	0.4
II (45 – 75 %)				0.33
III (75 – 90 %)				0.28
IV (>90 %)				0.2

Table 3. 2 The Classification of the Hydrogeological Properties of the Hard Rocks in North Rhine-Westphalia and the Associated BFI-Values Obtained by Calibration

Hydrogeological class	Hydraulic conductivity	k_S-value	Baseflow Indices
I	very high	$> 10^{-2}$ m/sec	0.9
II	high	$> 10^{-3} – 10^{-2}$ m/sec	0.6
III	medium	$> 10^{-4} – 10^{-3}$ m/sec	0.57
IV	moderate	$> 10^{-5} – 10^{-4}$ m/sec	0.3
V	low	$> 10^{-7} – 10^{-5}$ m/sec	0.29
VI	very low	$> 10^{-9} – 10^{-7}$ m/sec	0.18
VII	extremely low	$< 10^{-9}$ m/sec	0.12

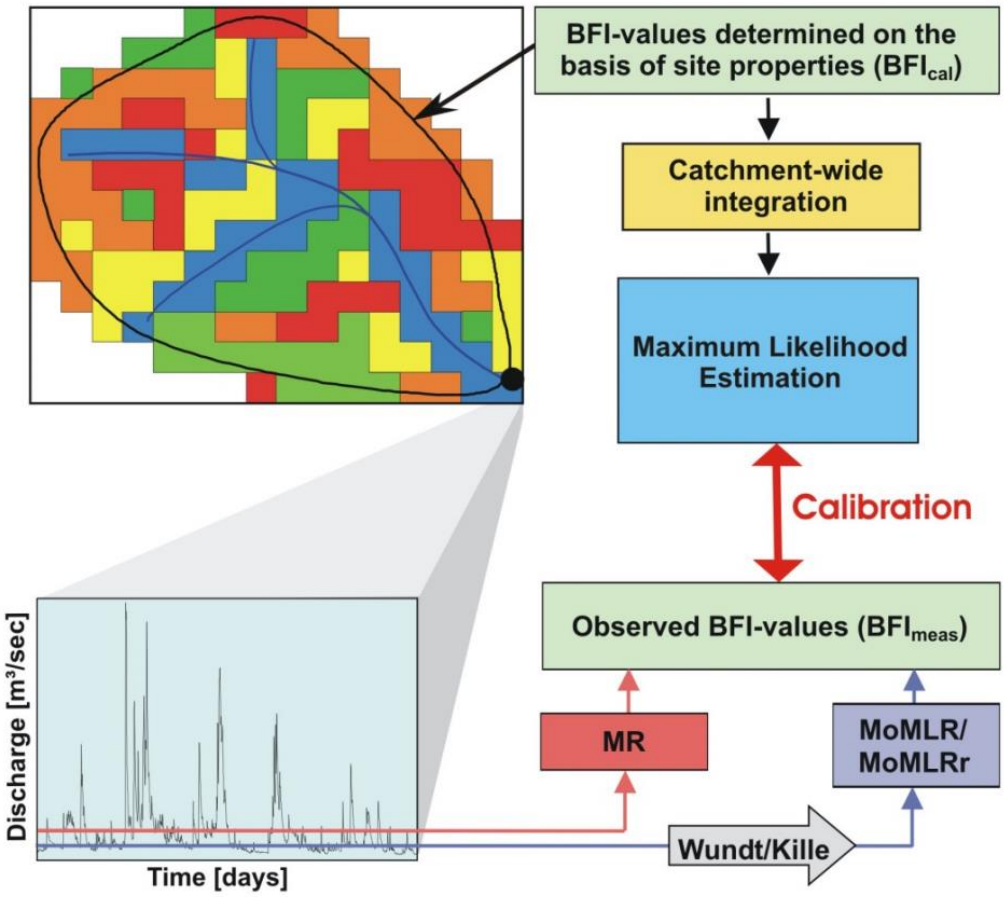

Figure 3. 6 Procedure in the mGROWA Model for BFI Calibration

The calibration is performed in a catchment-area-related manner. For this purpose, the relative area fractions (ai) of the individual site parameters in each region under investigation were multiplied by the respective (BFIi), added up and compared with the base flow indices observed (BFImeas). As expressed in equation 3.12 below:

$$BFI_{meas} = MoMLR(r)/MR \quad \xleftrightarrow{compared\ \ with} \quad BFI_{cal} = \sum_{i=1}^{n} BFI_i \cdot a_i \tag{3.12}$$

where MR denotes the measured long-term average total runoff.

The base flow indices varied in a continuous iteration process (depending on the properties of rock types) by maximum likelihood method, until the sum of the square deviations between calculated and measured base flow fractions, assumes the lowest value, as shown in the equation 3.13.

$$\sum_{j=1}^{n}(BFI_{meas} - BFI_{cal,j})^2 = Min \tag{3.13}$$

3.2.4 Validation of mGROWA Models Results

The validation of mGROWA model, in the investigated area, was performed by comparing the observed and estimated water budget components of Ergene river basin by applying the Nash-Sutcliffe index techniques[58] to spatially analyzing the differences in estimated recharge and total runoff with observed hydrographs in sub-basins having the sufficient discharges recorded data.

The Nash-Sutcliffe index, commonly known as the efficiency index noted as E_f has been widely used and possibly considered as a valid statistic indicator for analyzing the goodness of fit of a model [59]. The efficient index E_f can change with the interval of $-\infty$ and 1. The acceptable interval relies on the interval of 0 - 1, if a negative occurs, this shows a nonconformity in the development of the hydrological models, where the value of 1 reveals a perfect performance. The other concept for this efficient index was presented by Herrmann et al. (2015) in [13] for applying simultaneously this efficient for the all selected discharge stations within the basin together with their related drainage areas by using the Equation 3.14.

$$E_f = 1 - \frac{\sum_{i=1}^{n}(A_i.(Q_{observed,i} - Q_{simulated,i})^2)}{\sum_{i=1}^{n}(A_i.(Q_{observed,i} - Q_{observed,\ A_V})^2)}, \tag{3.14}$$

Where $Q_{observed}$ denotes the recorded discharge per unit of area, $Q_{simulated}$ stands for the related modeled discharge, $Q_{observed,Av}$ represents the observed overall discharge per unit of all considered sub-basins, A stands for the specific basin area and i is the sub-basin indicator.

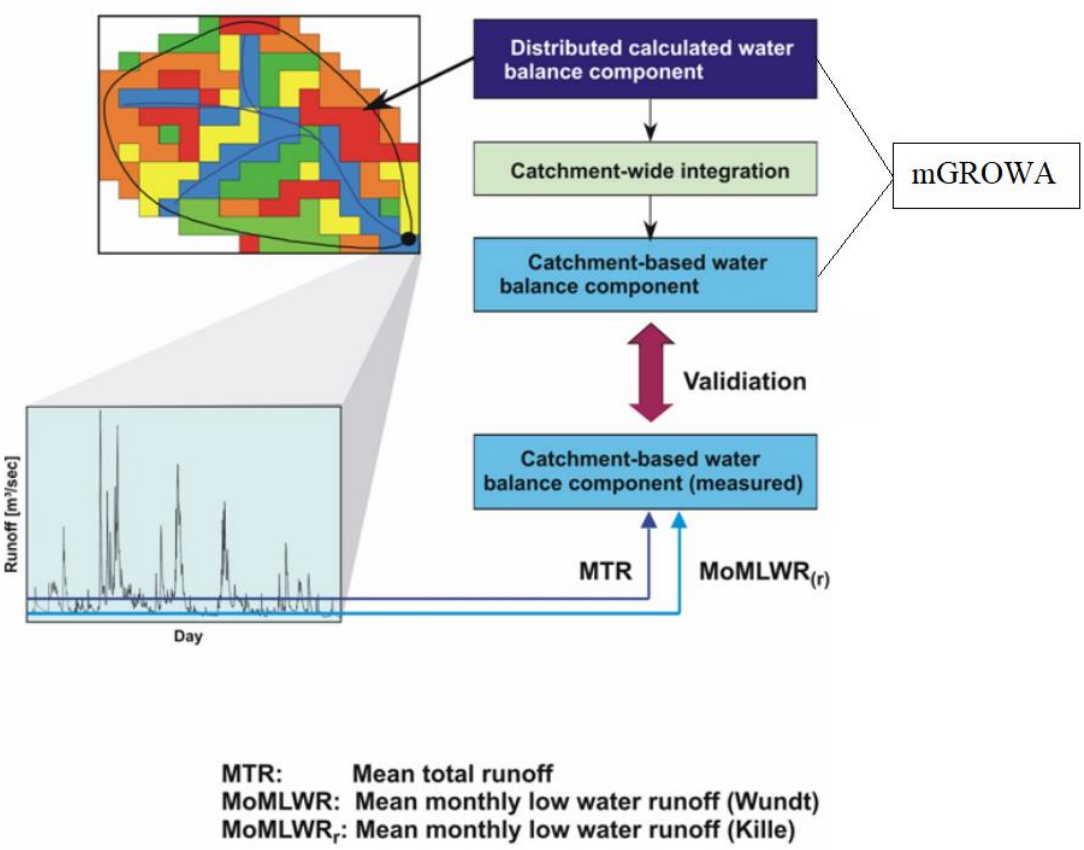

Figure 3. 7 Procedures for Validating the Simulated Water Balances by mGROWA Model

Figure 3.7 presents the procedure for mGROWA model validation. First of all, a blending of the gauge-related catchment areas with the total runoff levels calculated by the GROWA model in an area differentiated manner is performed. The individual values of the grid cells are then integrated over the respective catchment areas and compared with the measured runoff levels. The attention was considered here that the same reference period is used for both the calculation and the gauge through-flow values. If a satisfactory agreement is achieved for a sufficiently large number of catchment areas, it was assumed that representative information has been obtained with the underlying model.

3.3 Principal Component Analysis

During this research, a multivariate approach known as Principal Component Analysis (PCA) was used by means of the software called the XL-STAT. The principal component analysis is defined as of the multivariate statistical tools applied to

perform an assessment of data tables which possess the recorded data from surveying and quantitative inter-correlated dependent variables. The aim of the tools was to convert the data table into a new generated orthogonal and without correlation inset of parameters known as principal components (PC), which can be useful to withdraw the important information from the data. PCA squeeze the data by saving only the most significant information in it, making easy meaningful, and investigating the structure data with its configuration [60]. In this research, the PCA helped to decrease redundancy in the database but also to provide the controlling factors that present the high variance in recharge, therefore the variables mostly contributing to the spatial pattern or change in recharge of Ergene river basin. A varimax rotation technique has been done for rising the variation between the factors for each component [61].

In the use of PCA, the standardization concept of the original variables eliminates the impact of calculation units, returning the data dimensionless, as shown in equation 3.15.

$$Z_i = (X_i - \mu)/\sigma \tag{3.15}$$

Herein Zi stands the standardized variable i, μ presents the mean, σ means the standard deviation of the set of available data, and X_i denotes the original variable i.

The PCA technique breaks down the original matrix presented as X into two factors namely factor scores and factor loading matrices, as expressed in equation 3.16.

$$X = TP' + E \tag{3.16}$$

Herein, the X is the standardized matrix of variables, T (I observations of J variables) matches to the matrix J PCs; P' stands for the original transpose where E denotes the residual matrix.

3.3.1 Procedures for PCA

Firstly, the Pearson product moment correlation coefficient was determined and used to show the strengths of correlations among the recharge and drainage area characteristics [62]. The matrix of correlated parameters with catchment area was

calculated, then the linear relationship between the Ergene river basin characteristics was done by determining the Pearson correlation among the characteristics, these correlations rely on the range of -1 and1. The significance of the correlation is given by the high coefficient, the positive and negative signs show the similarity and the reverse in the direction respectively among the characteristics of the drainage area [63].

Secondly, parameters which were found meaningfully correlated with the recharge had been assessed with the principal component analysis method. In the presentation of components, the first one possesses the information of a high portion of the variance in the original data. The eigenvalue of the principal components was calculated and the PCs possessing an eigenvalue higher than 1 with a factor loading greater than 0.7 was taken into account as the variables that influence mostly the spatial patterns of recharge [9], [31]. Regarding the PCA, the highly weighted variable in PCs has been estimated regarding the status of correlation values and their sums [62]. This technique has decreased the number of variables and generate a small dataset that presenting a high control of the recharge in the Ergene river basin.

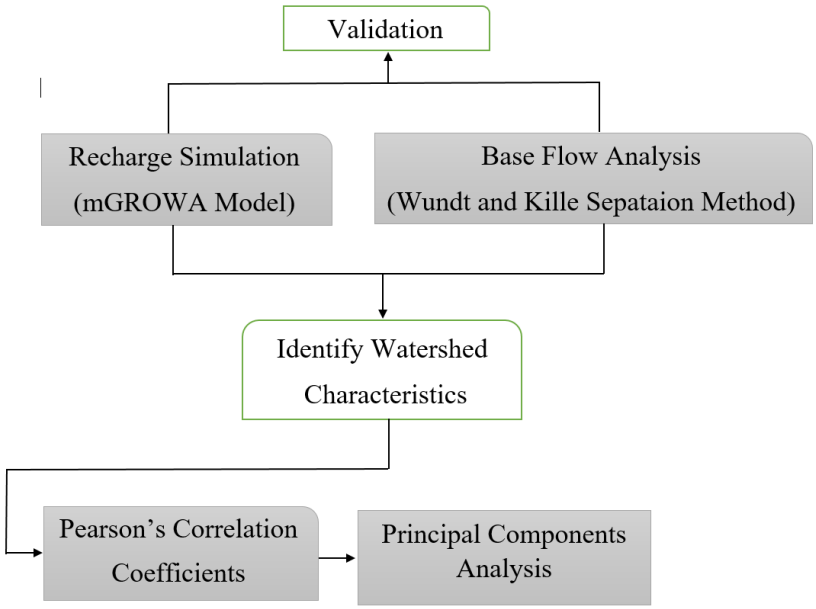

Figure 3. 8 The Overview of the Methodology for Assessing the Recharge and its Controlling Factors

The overview of the approach used to deal with the first objective consists of mGROWA model application to determine different water balance quantities including recharge. Against this background, the spatial distribution was determined as a dependent function for different attributes including relief, soil groups, land use type, and hydro-climatic characteristics. Then the Wundt and Kille separation approach were used to estimating the base flow. The recharge obtained from the mGROWA model and base flow were compared. Next XL-STAT software was used to detect the influencing characteristics affecting the recharge. Then, PCA was applied to reduce the dimensions of the data and to detect the data with high variance together with the recharge.

3.4 Groundwater flow modeling

In this study, a subsurface water model known as MODFLOW was applied in the python environment to simulate groundwater flow dynamics in the study area. MODFLOW is a remarkably adaptable three-dimensional model which generates groundwater conditions and flow dynamics through the confined or/and unconfined aquifer [14]. It is characterized as a finite-difference model. MODFLOW incorporate the approaches to determining the flow from external stresses e.g. wells, drains river beds, areal recharge, head boundaries, and evapotranspiration. The equation 3.17 exhibit the three-dimensional groundwater flow formula operated in sub-surface water model (MODFLOW). The formula was obtained by expending the conservation of mass concept applied on a control volume of an investigated area.

$$S_s \frac{\partial h}{\partial t} = \frac{\partial}{\partial x}\left[K_{xx} \frac{\partial h}{\partial x}\right] + \frac{\partial}{\partial y}\left[K_{yy} \frac{\partial h}{\partial y}\right] + \frac{\partial}{\partial z}\left[K_{zz} \frac{\partial h}{\partial z}\right] - W \qquad (3.17)$$

Where K_{xx}, K_{yy}, and K_{zz} are function of space stand for hydraulic conductivity in x, y and z directions respectively with units of $[LT^{-1}]$; h denotes the potentiometric head[L]; W is a function of space and time and expresses the water source and /or sinks $[L^3T^{-1}]$; S_s stands for the specific storage$[L^{-1}]$, and t denotes the time[T]. Figure 3.9 shows the database and all steps of groundwater modeling procedures that were taken into account during this study.

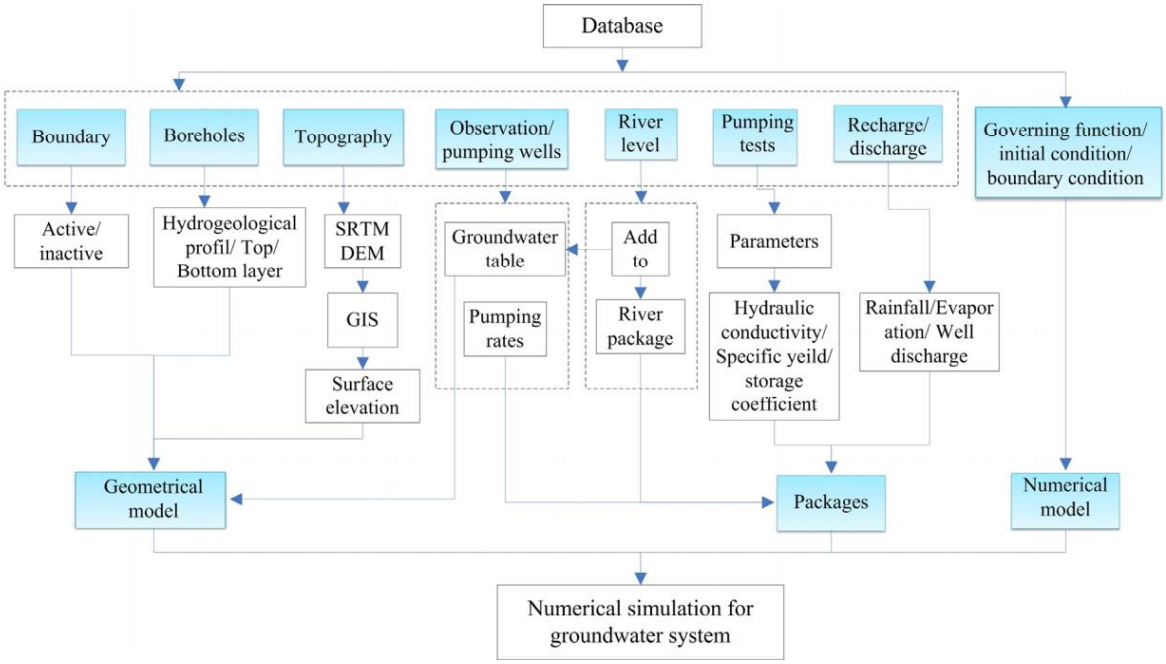

Figure 3. 9 Procedure for Data Processing and Groundwater Modeling Studies

The solution to equation 3.17 is attained when applying approximation of block centered finite-difference. Together with the boundary information and initial conditions, equation 3.17 presents the transient flow existing in the heterogeneous and anisotropic medium given that the principal axes of hydraulic conductivity are aligned with the coordinate directions. In this study, we considered a steady state condition, thus the right term of the equation 3.17 is not considered. MODFLOW packages are the basic package (BAS), Block-centered flow package (BCF), Horizontal flow barrier package (HBF), and source term packages, which can be head dependent or head independent packages. The head dependent packages include the river package (RIV), drainage package (DRN), general head boundary package (GHB), and evapotranspiration package (ETV). The head independent packages are the well package (WEL) and recharge package (RCH).

3.5 Coupling Methodology

In the coupling mGROWA and MODFLOW models, one model runs then after the second model runs with the interrupted transmission of input data. The most important mGROWA outputs were the groundwater recharge rates which was used as the upper boundary condition of the MODFLOW model. Iterative mGROWA-

MODFLOW applications will be done in order to improve model results relating to groundwater dynamics. A grid-based water balance model mGROWA model is applied to the investigated area to determine the spatial and temporal water balance quantities including surface runoff, actual evapotranspiration, and groundwater recharge. As in the dependent wetlands areas, to estimate the evapotranspiration and recharge, the position of the water table plays the important role in calculation, the mGROWA model, in this study is iteratively coupled with the groundwater flow model MODFLOW which is capable to generate the groundwater table level within the catchment as input data in mGROWA. which in coupling the mGROWA returns the groundwater water recharge to MODFLOW. The stabilization of results was verified manually and it was done by checking the differences between the current and the previous modeled results the iterations were stopped. The coupling was done python environment by considering the following steps:

1. Build a running MODFLOW model that has the desired input parameters and initial conditions including the groundwater recharge,
2. Run MODFLOW for one-time step,
3. Use the FloPy HeadFile class to read the binary heads file created by MODFLOW. Read these heads, and then write them out to a file that can be read by mGROWA model,
4. Run the mGROWA model,
5. Read the recharge results from the mGROWA model and then write them to the MODFLOW recharge package,
6. Go back to step 1 and repeat for the next stress period.

3.5.1 Import Libraries in Python Environment

This study necessitates Python core libraries such as Scipy libraries (stands for a Python-based ecosystem of open-source software for mathematics, science, and engineering) such as numpy (to deal with an N-dimensional array object) and matplotlib (used to plot library for the Python), and the Flopy library. For the management and data extraction from raster files, the GDAL library was used. The MODFLOW and FloPy utility packages were imported where the aliases were also provided as bf for utilities. During this study, the FloPy package is

composed of some python scripts to run MODFLOW, MT3D, SEAWAT, and other MODFLOW-related groundwater programs. The os is a python package applied to provide access to operating system dependent functionality for instance to open files.

3.5.2 Generate a MODFLOW Model Object

The second step is to generate a MODFLOW model object which is saved in a Python variable named as the model. The set up of the model name and working directory is provided. In this study, based on regarding the complexity existing in the geometry and layers thickness and elevations, the Newton solver was applied to this model in order to find the solutions of the finite difference equations in every step of a MODFLOW-NWT stress period in Python environment. Linmeth stands for as a flag that shows that can be applied by matrix solver, and in this code, the number 2 shows that XMD is applied in the simulation. For increasing the MODFLOW model performance, specifically in non-linear issues, the Newton linearization approach can be applied and has been integrated in MODFLOW 2005 as NWT solver package to resolve the non-linear linear formulas. The NWT solver package is mostly used for assessing the common issues related to unconfined aquifers and the interaction between the surface and groundwater. Furthermore, for a wide range of hydraulic conductivities existing in the rocks type of an investigated area, the MODFLOW presents the difficulties for solving a matrix that gathers together all of the numerical discretization equations and obtaining the solutions. Thus, χMD solver package, which is relying on a preconditioned gradient sort matrix solver, can be applied to increase the performance of the model. The preconditioning procedure allows different levels of incomplete (lower-upper) LU decomposition and arranging of unknowns. The maxiterout here stands for the maximum number of iterations to be allowed for the solution of the nonlinear problem for this model.

3.5.3 Working with Raster Files

The GDAL library was necessary to work with the raster such as digital elevation model DEM and boundary conditions in order to have the geo-transformation parameters. The raster should have the same working grid cell resolution. The

information from the raster can be read by means of Numpy arrays and as input to the top of the model (Figure 3. 10)

```
In [1]:
import flopy
import os
import flopy.utils.binaryfile as bf
import numpy as np
from osgeo import gdal
import matplotlib.pyplot as plt

In [2]:
modelname = "model1"
modelpath = "../Model/"
#Modflow Nwt
mf1 = flopy.modflow.Modflow(modelname, exe_name="../Exe/MODFLOW-NWT_64.exe", version="mfnwt",model_ws=modelpath)
nwt = flopy.modflow.ModflowNwt(mf1 ,maxiterout=150,linmeth=2)

In [3]:
#Raster paths
demPath ="../Rst/ergenedem.tif"
bcPath = "../Rst/ergenebc1.tif"

#Open files
demDs =gdal.Open(demPath)
bcDs = gdal.Open(bcPath)
geot = bcDs.GetGeoTransform() #Xmin, deltax, ?, ymax, ?, delta y

geot

Out[3]: (444512.0, 100.0, 0.0, 4659841.9544333685, 0.0, -100.0)

In [4]:
# Get data as arrays
demData = demDs.GetRasterBand(1).ReadAsArray()
bcData = bcDs.GetRasterBand(1).ReadAsArray()

# Get statistics
stats = demDs.GetRasterBand(1).GetStatistics(0,1)
stats

Out[4]: [3.0, 1009.0, 164.05608310275, 116.29508206644]
```

Figure 3. 10 Importation of the Libraries, the Creation of the Object and Reading Raster file in Python

1. Spatial Discretization

The discretization of Ergene catchment model was indicated by the MODFLOW discretization file called DIS. The geology of Egene river basin reveals that it is mainly composed of four main layers such as alluvium layer, aquiclude, aquifer, and an aquitard. The geometry of each layer was prepared by ArcGIS tools and imported in the python. In the discretization, the first input data was the model object created in the previous code. The column and row number and dimension for the Ergene river basin model come from the imported raster attributes.

2. Description of groundwater flow packages for the MODFLOW model

To specify if the grid cells are active or inactive with the purpose of making the conductance of inactive cells to be zero. The so-named boundary array IBOUND which a terminology of the MODFLOW model was applied. IBOUND can be used as an indicator of the boundary variable in the investigated area. Only one value can be attributed to every model cell. Generally, IBOUND numbers are read a layer at a

time. In three dimension the value of IBOUND can be expressed as presented in the below statement:

If IBOUND (J, I, K) < 0, means cell J, I, K possesses constant head.

If IBOUND (J, I, K) = 0, means cell J, I, K is inactive.

If IBOUND (J, I, K) > 0, means cell J, I, K is active and means heads will be determined.

In this study, the basic package(BAS) are used to describe the active cells where there is a need to compute the heads and the IBOUND array was used for this purpose. NumPy package was applied to firstly initialize existing arrays characterized by code 1. HNOFLO variable is MODFLOW terminology which stands for the value of the head to be assigned to all inactive grid cells in the modeling. As the head existing in the no-flow cell or inactive grid cell are considered as unwanted heads in the model simulations, it will not influence model output, thus to be used in the indication of inactive grid cells in case of the head results are printed.

NRCHOP is MODFLOW terminology and in this model stands for one of the option code of recharge. In the investigated area, the recharge fluxes were expressed in the layer variable by a presentative number assigned for every vertical column. Against this background, the groundwater recharge was assigned to the cell for every column thus the option code shows the grid cell is assigned to recharge. The code 1 presents that the recharge is only assigned to the of the grid layer, the code 2 means that the vertical distribution of recharge is identified in the layer variable, and the code 3 reveals that the groundwater recharge is assigned to the highest active grid cell in every vertical column (figure 3.11).

```
#Boundaries for Dis = Create discretization object, spatial/temporal discretization
ztop = demData
zbot = [Layer1, Layer2, Layer3, Layer4]
nlay = 4
nrow = demDs.RasterYSize
ncol = demDs.RasterXSize
delr = geot[1]
delc = abs(geot[5])
```

```
dis = flopy.modflow.ModflowDis(mf1, nlay,nrow,ncol,delr=delr,delc=delc,top=ztop,botm=zbot,itmuni=1)
```

```
# Variables for the BAS package
iboundData = np.zeros(demData.shape, dtype=np.int32)
iboundData[crData > 0 ] = 1
bas = flopy.modflow.ModflowBas(mf1,ibound=iboundData,strt=ztop, hnoflo=-2.0E+020)
```

```
# Array of hydraulic heads per layer
hk = [1E-4, 1E-5, 1E-7, 1E-8, 1E-9]

# Add UPW package to the MODFLOW model
upw = flopy.modflow.ModflowUpw(mf1, laytyp = [1,1,1,1,0], hk = hk)
```

```
#Add the recharge package (RCH) to the MODFLOW model
rch_data = rechargeData
rch = flopy.modflow.ModflowRch(mf1, nrchop=3, rech =rch_data)
```

```
#Add the evapotranspiration package (EVT) to the MODFLOW model
evtr = evtr_data
evt = flopy.modflow.ModflowEvt(mf1,nevtop=1,surf=ztop,evtr=evtr_data, exdp=0.5)
```

Figure 3. 11 Discretization and Defining Flow Packages in Python Script

For this model, the sorts of results that MODFLOW prints to a result file are identified by the output control (OC) package of the MODFLOW model. For this context, the balance outputs are written and heads are stored thus no arguments are required (figure 3. 12).

```
#Add the drain package (DRN) to the MODFLOW model
river = np.zeros(demData.shape, dtype=np.int32)
river[crData == 3 ] = 1
list = []
for i in range(river.shape[0]):
    for q in range(river.shape[1]):
        if river[i,q] == 1:
            list.append([0,i,q,ztop[i,q],0.001]) #layer,row,column,elevation(float),conductanceee
rivDrn = {0:list}

drn = flopy.modflow.ModflowDrn(mf1, stress_period_data=rivDrn)
```

```
# Add OC package to the MODFLOW model
oc = flopy.modflow.ModflowOc(mf1) #ihedfm= 1, iddnfm=1
```

Figure 3. 12 The River Package and Output Control Package Definition in Python Script

At the end of the model, the MODFLOW input files were written and saved, these files including eight files of the Ergene river basin model and then the generated model was executed (figure 3.13).

```
#Write input files -> write file with extensions
mf1.write_input()

#run model -> gives the solution
mf1.run_model()
```

Figure 3. 13 Code for Writing MODFLOW Input Files and Running the Model

3.6 Input Data

3.6.1 Hydro-Climatic Data

Table 3. 3 Datasets for mGROWA Model

	Data base	Scale/spatial resolutions	Data source
Climate data	Precipitation (1970 to 2014) Temperature (1970 to 2014)	100x100 m	General Directorate of State Hydraulic Works (DSI)
Soil data	Main soil groups	1/25,000	National soil database by General Directorate of State Hydraulic Works (DSI)
	The depth of the groundwater table, Perching water influence Root depth, effective field capacity Capillary rise from the groundwater table	Derived based on pedo-transfer functions	National soil database by General Directorate of State Hydraulic Works (DSI) and fields studies
Land cover	Land use types Percentage imperviousness	1/25,000	National soil database by General Directorate of State Hydraulic Works (DSI)
Hydrogeology	Geological map	1/500,000	General Directorate of State Hydraulic Works (DSI) and fields studies
Relief	Digital elevation model SRTM Ground surface slope Ground surface exposition	30x30 m	SRTM/X-SAR by National imaging and mapping agency
Runoff		Station data Monthly and daily resolution	General Directorate of State Hydraulic Works (DSI) and fields studies

Table 3.3 presents the prepared dataset that was used in mGROWA model to simulate the water balance components in the Ergene catchment.

The available climatic information in Ergene river basin was collected from 41 stations and climatic data were used, in this research, in water balance components simulation. All the data were collected from the Turkish General Directorate of State Hydraulic Works (DSI) and specifically, the collected data includes daily precipitation and extreme temperature data. The grass reference evapotranspiration rates were estimated by applying Hargreaves approach [64] where the input data was the minimum and maximum temperature Tmin and Tmax respectively, and average temperature (daily temperature) and extraterrestrial radiation as shown in the equation 3.18.

$$ET_0 = 0.408 * K_H Ra * (T_{max} - T_{min})^{eH} * \left(\frac{T_{max}-T_{min}}{2} + K_T\right) \quad (3.18)$$

Where K_H, K_T and eH coefficients should be adjusted depending on the region of application.

The Hargreaves method was decided to be an appropriate and accurate approach by the Food and Agriculture Organization (FAO) for determining the grass reference evapotranspiration in case study presenting the issues of climatic data availability such as relative humidity, net solar radiation, wind velocity etc [64]. Nevertheless, for humid regions, this approach needs calibration [65]. For Turkey as well, there was a need for calibration in order to estimate the grass references evapotranspiration, the study of Cobaner et al (2017) in [66] provided the calibration of Hargreaves in Turkey, and modified it, this modification suggests the use of coefficient K_H =0.00419, K_T=17.8, and eH=0.2342. Then by means of GIS, the datasets were generated as digital datasets for the period of 1991-2010 as shown in Figures 3.14 and 3.15 in the form of grids pattern.

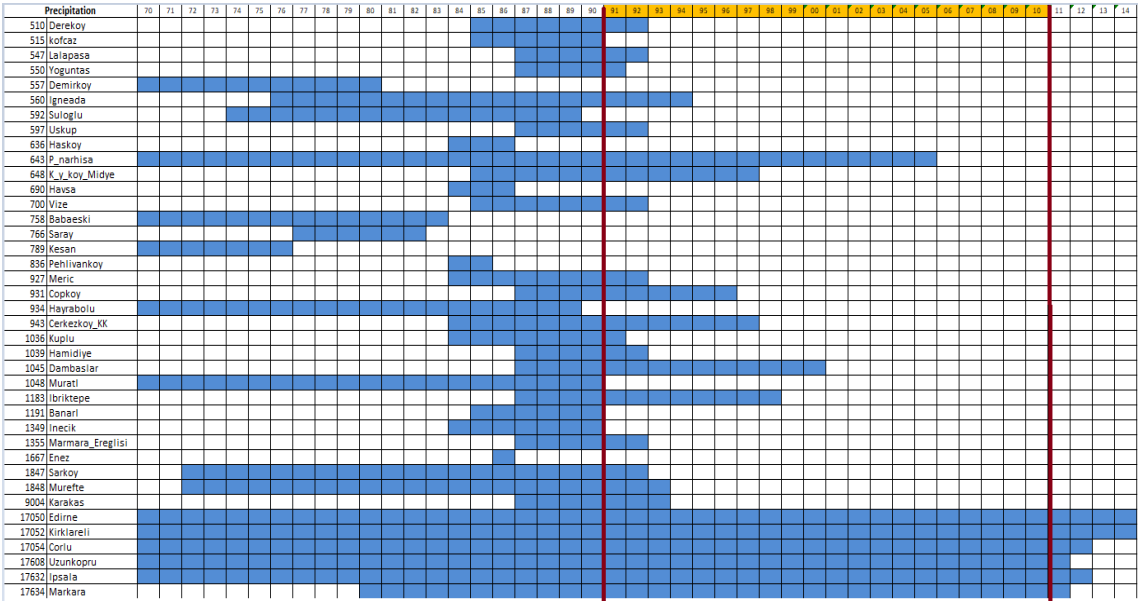

Figure 3. 14 Daily Precipitation Data Availability and the Period for the Modeling

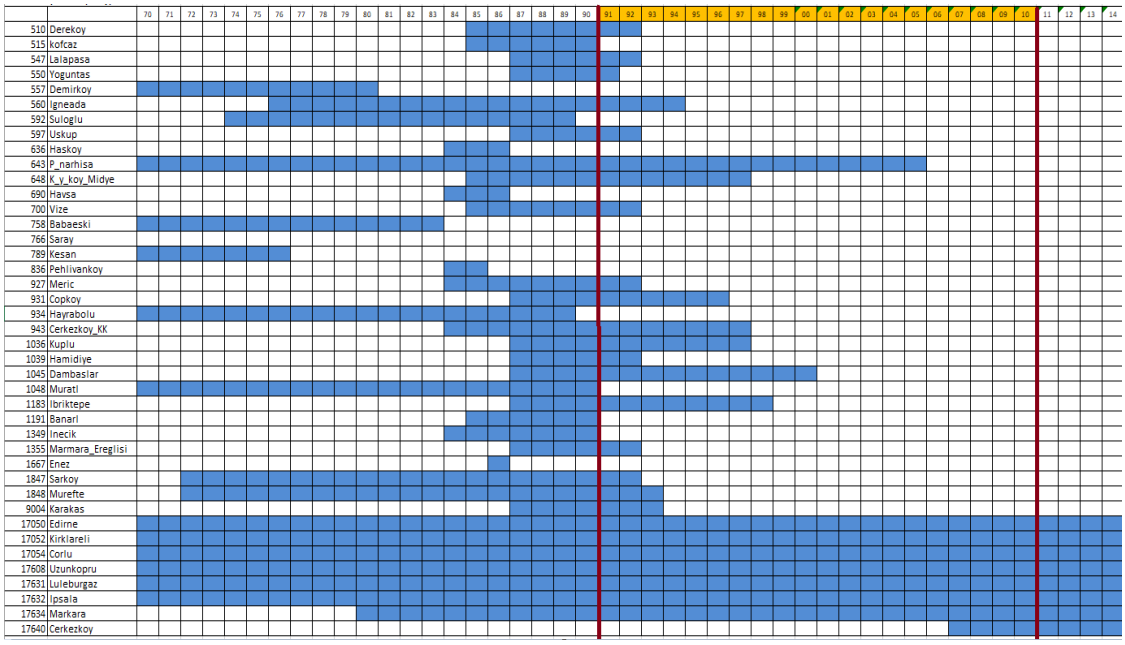

Figure 3. 15 Daily Temperature Data Availability and the Period for the Modeling

In figure 3.14 and 3.15, it can be seen that most of the stations' data do not cover the whole years between 1970 and 2014. There are 41 climate stations that have the precipitation and temperature data. Only 5 stations and 6 stations for precipitation and temperature respectively, can provide the data for the whole period 1970 – 2014 as presented in Table 3.4 and Figure 3.16. Therefore, after evaluation of the

climatic databases, the period of 20 years (1991-2010) was selected as the modeling period of the Ergene catchment.

Table 3. 4 Selected Stations According to the Continuous Availability of Data for the 1991-2010 Period

Precipitation	**Temperature**
17050Edirne	17050 Edirne
17052Kırklareli	17052 Kırklareli
17054Çorlu	17054 Çorlu
17608 Uzunköprü	17608 Uzunköprü
17632 İpsala	17631 Lüleburgaz
17634Malkara	17632 İpsala
	17634 Malkara

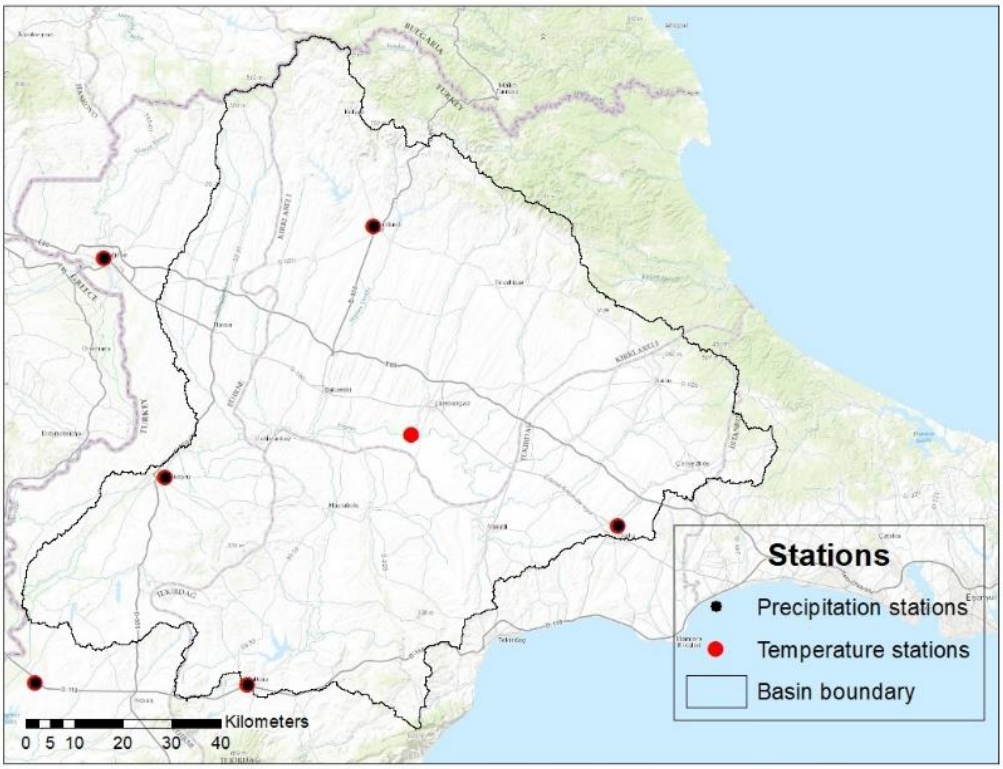

Figure 3. 16 The Location of Gauging Stations Used in Ergene Catchment

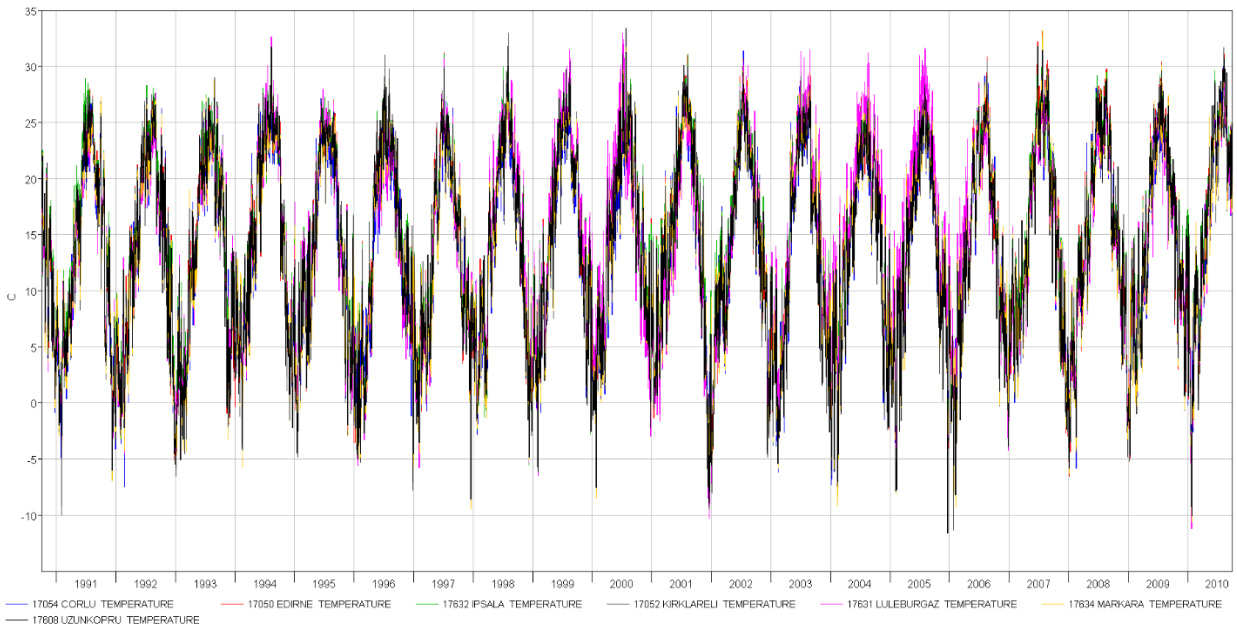

Figure 3. 17 Daily Average Temperature for Considered Stations in Ergene Catchment

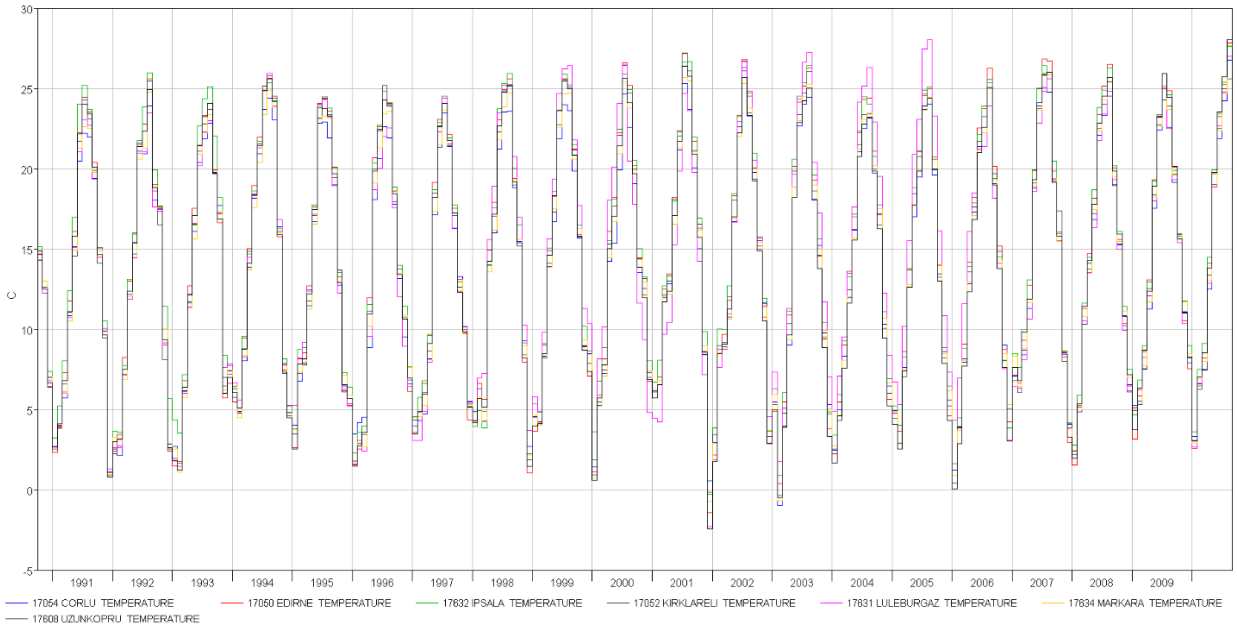

Figure 3. 18 Monthly Average Temperature for Considered Stations in Ergene Catchment

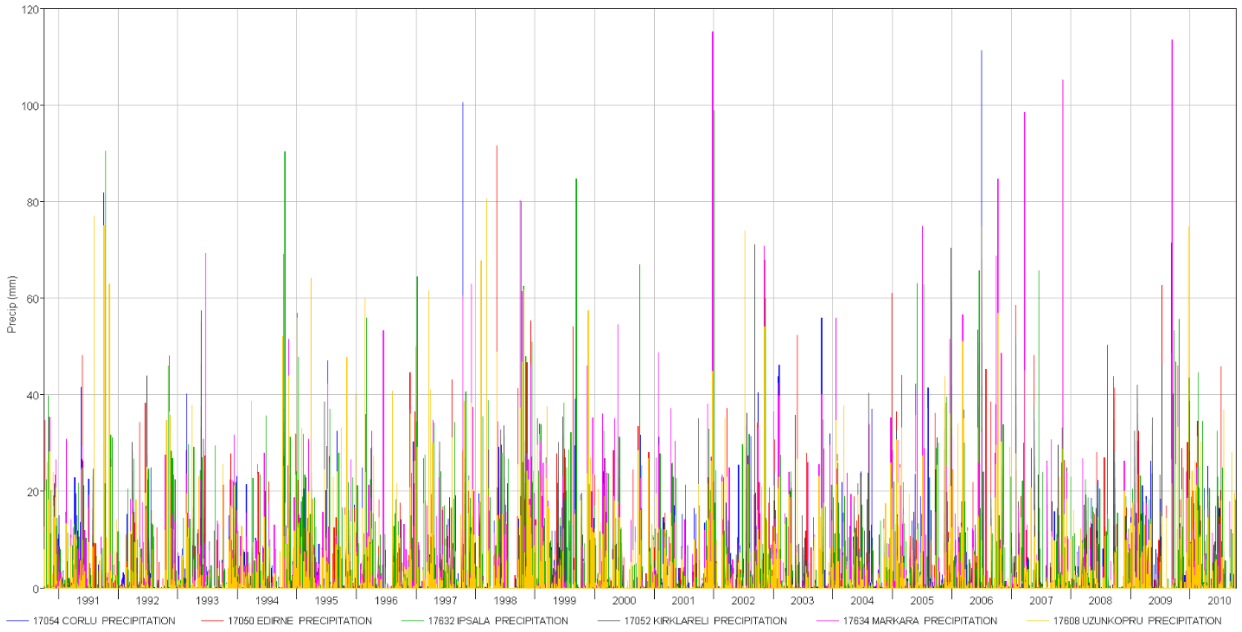

Figure 3. 19 Daily average Precipitation for Considered Stations in Ergene Catchment

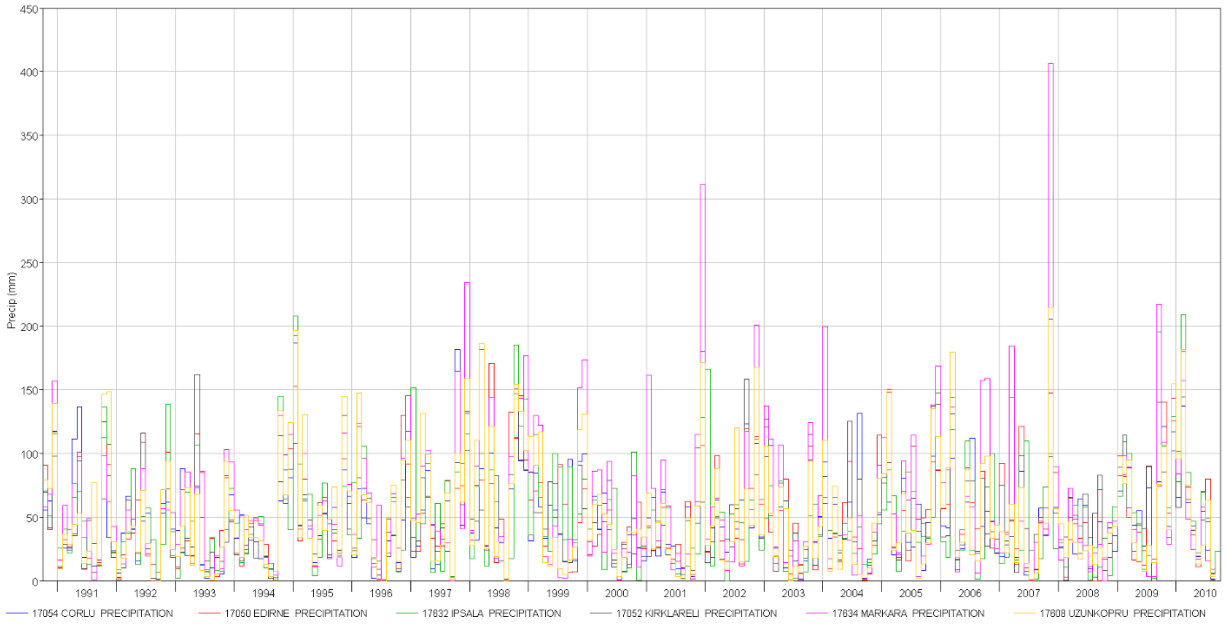

Figure 3. 20 Monthly Average Precipitation for Considered Stations in Ergene Catchment

Table 3. 5 Extracted Statistics about Climatic-Variables

Temperature Stations	Minimum		Average		maximum	
	Daily	Monthly	Daily	Monthly	Daily	Monthly
17050 Edirne	-10.5	-1.42	14.22	14.16	33.1	27.83
17052 Kirklareli	-11.35	-0.36	13.93	13.85	33.35	27.2
17054 Corlu	-10.35	-0.95	13.58	13.5	32.5	26.74
17608 Uzunkopru	-11.6	-2.42	13.83	13.76	31.8	28.08
17631 Luleburgaz	-11.2	-2.3	14.17	14.1	32.95	28.02
17632 Ipsala	-9.45	-0.27	14.65	14.57	31.95	27.61
17634 Markara	-10.6	-0.72	13.79	13.64	33.25	27.64
Precipitation Stations	**Minimum**		**Average**		**maximum**	
	Daily	**Monthly**	**Daily**	**Monthly**	**Daily**	**Monthly**
17050 Edirne	0	0	1.66	50.72	91.5	180.2
17052 Kirklareli	0	0	1.5	45.82	74.9	161.71
17054 Corlu	0	0	1.5	48.05	111.3	205.4
17608 Uzunkopru	0	0	1.72	52.35	105	214.45
17632 Ipsala	0	0	1.63	49.78	98.8	208.8
17634 Markara	0	0	2	61.11	115.1	406.4

Table 3.5 summarizes the descriptive statistics of the information data provided in figures 3.17,3.18, 3.19 and 3.20. It shows the average daily and monthly statistics (minimum, average and maximum) climatic data.

The Ergene river catchment is dominated by terrestrial climate, summers are hot and arid in the north, whereas the winters are cold. In the south part, it is characterized by a Mediterranean climate where the summers are hot and dry and winters are warm and rainy. During the year, January and February are the coldest months, with an average minimum temperature of 4 ^{0}C, whereas June and July are the hottest months, with an average maximum temperature of 20 ^{0}C (Figure 3.17 and 3.18). The average annual temperature of the Ergene river basin is around 13 ^{0}C. The mean annual long-term precipitation is about 590 mm, the highest precipitation amounts occur in November and the minimum in August. In the south, annual precipitation distribution increases from 650 mm/year to 730 mm/year, whereas in the northern part, the precipitation ranges from 600 mm/year to 900 mm/year. In the Ergene river basin, since 1991, the precipitation information has been collected and no remarkable trend was found in precipitation. The annual average evapotranspiration ranges from 450 to 950 mm/year.

The climatic data, precipitation, and grass reference evapotranspiration were needed to be generated in the format of American Standard Code Information Interchange(ASCII) grid cells for the resolution of 100 m. For this purpose, the ArcGIS tools were used, and the inverse distance weighted method was adopted for interpolation of climatic data for the case study [67]. This approach has helped to generate the distribution of precipitation and grass reference over the Ergene river catchment. Over a period of 1991-2010, the long-term precipitation and grass reference evapotranspiration of Ergene river basin was found to be approximately 591.29 ± 66.9 mm/ year and 1035.26 ± 34.46 mm/year respectively. As the standard deviation counts more, the spatial variability of the precipitation and grass reference evapotranspiration is high over the basin. The next task was to settle the spatially distributed precipitation and grass evapotranspiration to be used as input data in the mGROWA model, then the daily climatic data were accumulated into the monthly data in mm, and their grids were generated to be used as a model as input data.

Discharge data in the Ergene river basin was needed for calibration and validation of the mGROWA model results. Data were collected, processed and made available by DSI. For the first step, the daily runoff data database for selected gauging stations was established, the stations cover the 44% of Ergene river basin. The selection of the gauging stations was done on basis of the availability of the continuous time series recorded data, where for this study, the span of 20 (1990-2010) hydrological years were taken into an account. The 10 stations were selected with the area from 20 to 2794 km^2, which are greatly showing differences in terms of climatological, geological and soils data. The mean long term runoff data helped to validate the simulated total runoff by mGROWA. For the groundwater recharge rates, as the results of the model, were adjusted and verified by using the baseflow from the separation hydrographs by Wundt and Kille method [52], [53]. Table 3.6 shows the gauging stations selected and their coverage areas.

Table 3. 6 Gauging Stations used for the Validation of the mGROWA Model Results for the Long-term Period 1991-2010

ID	Gauging station	Catchment area(km^2)	Observed Mean Annual Total Runoff (m^3/s/a year)
D01A008	Lüleburgaz	2794	109.5
D01A020	Inanlı	1415	72.9
D01A063	Ayvacık	25.8	4.5
D01A031	Soğucak	71.3	4.4
D01A039	Poyralı	69.4	5.7
E01A001	Babaeski	478.4	25.9
D01A065	Çayırdereköy	50.5	4.3
D01A052	K.Yoncalı	118.3	5.2
D01A013	Inecik	92.18	4.8
E01A005	Uzunköprü	10194.8	237.2

3.6.2 Topographic Data

The topography of an area can have a high influence on the regional water balance components. Primarily, the slope and aspect may impact the rates of actual evapotranspiration furthermore the slope helps as input data for estimating the base flow portion of river discharge. A distributed map for relief on 100x100 m of grid cells was generated by means of GIS tools as presented in Figure 3.21.

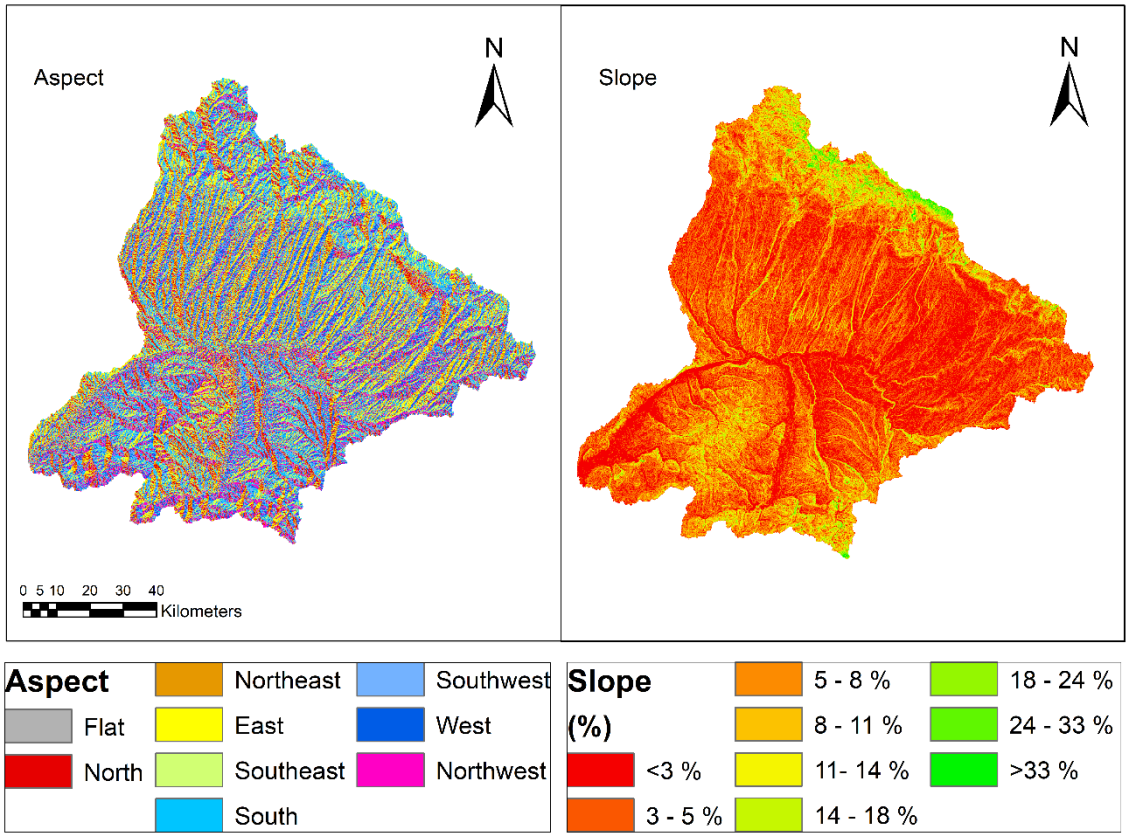

Figure 3. 21 Aspect and Slope Maps of the Ergene River Catchment

The slope and aspect datasets were derived from the digital elevation model and are presented in Figure 3.21. These datasets were used in formulating the rainfall-runoff relationship within the basin.

3.6.3 Landuse

For the calculation of vegetation actual evapotranspiration, the land use data was needed. The presentation of CORINE 2012 which stands for coordination of information on environment land covers was used in this study. This presentation possesses 44 classes, where 26 of them are presented in the Ergene river basin (Figure 3.22). As it can be seen, the high proportion of land use cover is composed by vegetation such as non-irrigated arable land with 211 CORINE presentation code which occupies approximately 54.9 % of the investigated area, the permanently irrigated land comes second with a Corine presentation code of 212 and covers an area of 8% of the catchment, thirdly, the land principally occupied by agriculture

covers an area of 7.1 % of the study area, then a 6.8% of the total area of Ergene basin is covered by transitional woodland-shrub, the other class such boar forest, pastures natural grasslands, rice fields and discontinuous urban land (112) cover an area of 6%, 3.9%, 3.2%, 2.6%, 1.7 % of the investigated area, respectively as shown in Table 3.7. The share of other categories exhibits low percentages (below 1%). For Ergene water balance components modeling, the information of imperviousness, rooting depth of plants and land-use-specific actual evapotranspiration factors were allocated to Ergene digital landscape model correspondingly.

Table 3. 7 Classes of CORINE Land Cover for Ergene River Basin

Landuse Categories	**Total area(km2)**	**Percentage of area(%)**
Continuous urban fabric	11.25604438	0.102134792
Industrial or commercial units	71.87197731	0.652150009
Road and Rail networks and associated land	16.81605205	0.152585039
Mineral extraction sites	25.73104596	0.233477671
Dump sites	3.025447711	0.027452226
Construction sites	4.539527242	0.04119064
Sport and Leisure facilities	0.135598701	0.001230392
Rice fields	294.0965197	2.668565067
Vineyards	2.049956045	0.018600836
Pastures	435.5440924	3.952028237
Land principally occupied by agriculture	786.6957913	7.138299051
Board leaved forest	656.5847895	5.957701352
coniferous forest	111.5690858	1.012352561
Mixed forest	65.21633963	0.591758263
Natural grasslands	359.2157988	3.259442626
Sclerophyllous vegetation	2.729198191	0.024764125
Transitional woodland-shrub	736.3867723	6.681806431
Sparsely vegetated areas	43.85892954	0.397965972
Burnt areas	0.708002226	0.006424252
Inland marches	2.377825852	0.021575852
water courses	0.137587343	0.001248436
water bodies	54.79066509	0.497158059
Discontinuous urban fabric	43.6608875	0.396168983
Discontinuous urban fabric	195.9622487	1.778116966
Non-irrigated arable land	6056.838171	54.95837482
Permanently irrigated land	905.6041487	8.217246496
Permanently irrigated land	5.450971523	0.049460878
Fruit trees and berry plantations	4.123233883	0.037413288
Fruit trees and berry plantations	3.66805748	0.033283121
Complex cultivation patterns	78.50727965	0.712357236
Complex cultivation patterns	41.62175094	0.377666321
TOTAL	11020.7738	100

mGROWA recognizes the land use of 4 classes, thus the CORINE land use cover was transformed into the vegetation land, urban land, water body surface and bare land as presented in table 3.8.

Table 3. 8 Land-Use Type used in mGROWA

Land type	Grid-cells number	Area(km²)	Percentage(%)
Vegetation land	996325.02	10589.896	96.09
Urban land	31947.30	339.56	3.08
Water body surface	5391.49	57.30	0.51
Bare land	3199.18	34.00	0.31
∑	1036861	11020.774	100

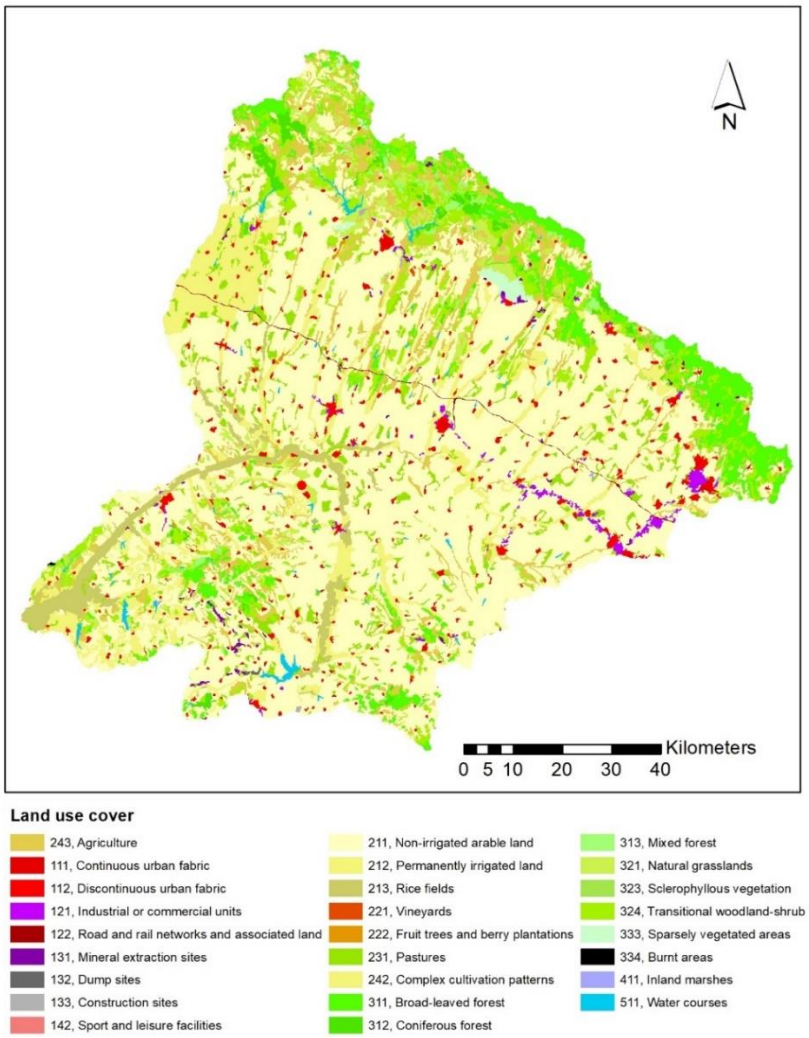

Figure 3. 22 Land Use Types of the Ergene River Catchment according to CORINE 2012

3.6.4 Soil Data

The water balance is particularly governed by pedological factors. In the study area, the evapotranspiration rate is controlled by the water stored in the soil, the so-called plant available soil water content. This soil hydrological parameter enters in the calculation of the water balance values. Information about the available field capacity, effective rooting depth and the capillary rise are required to derive this parameter. Some other soil parameters, e.g. depth of groundwater table are also important for separating the base flow fraction from the total runoff level. As it can be seen from Figure 3.23, the 8 soils type were found in the Ergene river basin. The brown forest soils without lime greatly control the northern part of this case study. Brown soils without lime and vertisol groups occur in the center of the case study.

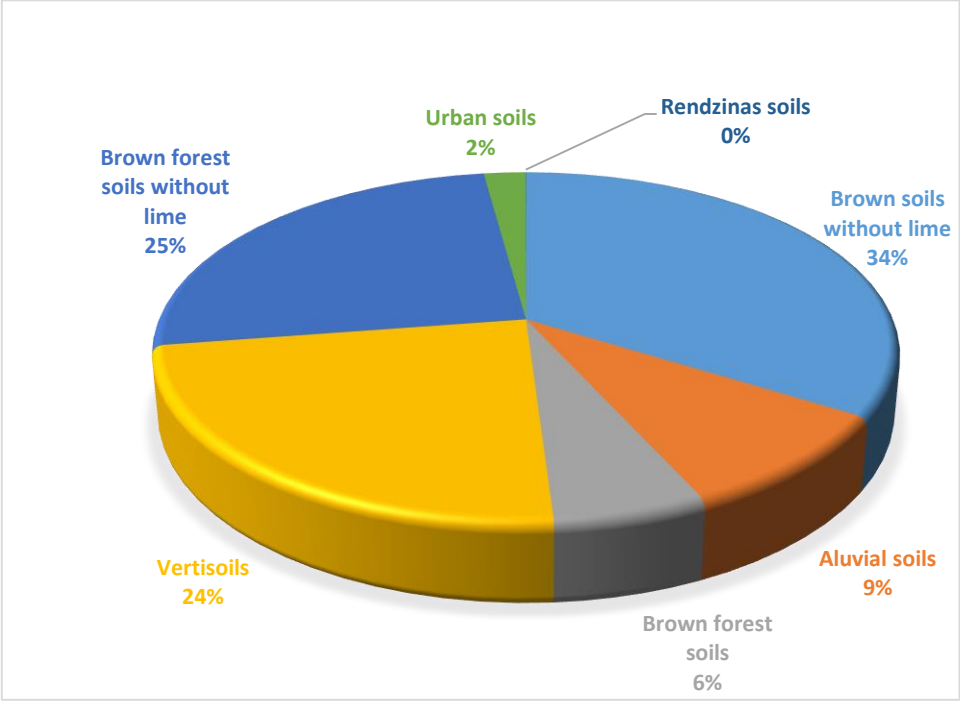

Figure 3. 23 Soil Groups in Ergene River Basin

The alluvial soils were found in the location of the river beds and the nearby areas whereas the brown forest soils with and/or without lime occurs in the south of the Ergene river basin. The small portion of urban soils was found dispatched with the case study area as well. In overall, the brown forest soils, brown forest soils without lime, vertisols greatly dominate the Ergene river basin with the portion of 33.8, 25.2 and 23.6 % respectively. The other soils groups are occurring in the investigated

area are in small proportion, for instance, alluvial soils, brown forest soils, urban soils, and rendzinas soil groups cover an area 9.2 %, 5.8 %, 2.1 %, and 0.02 % respectively as shown in Figure 3.23 and Figure 3.24. Pedotransfer functions were used to provide the parameterization of Ergene river basin soil profiles, and the parameters such as rooting depth, field capacity were provided in order to know the capacity of storage and release of water for different soils groups of Ergene river basin.

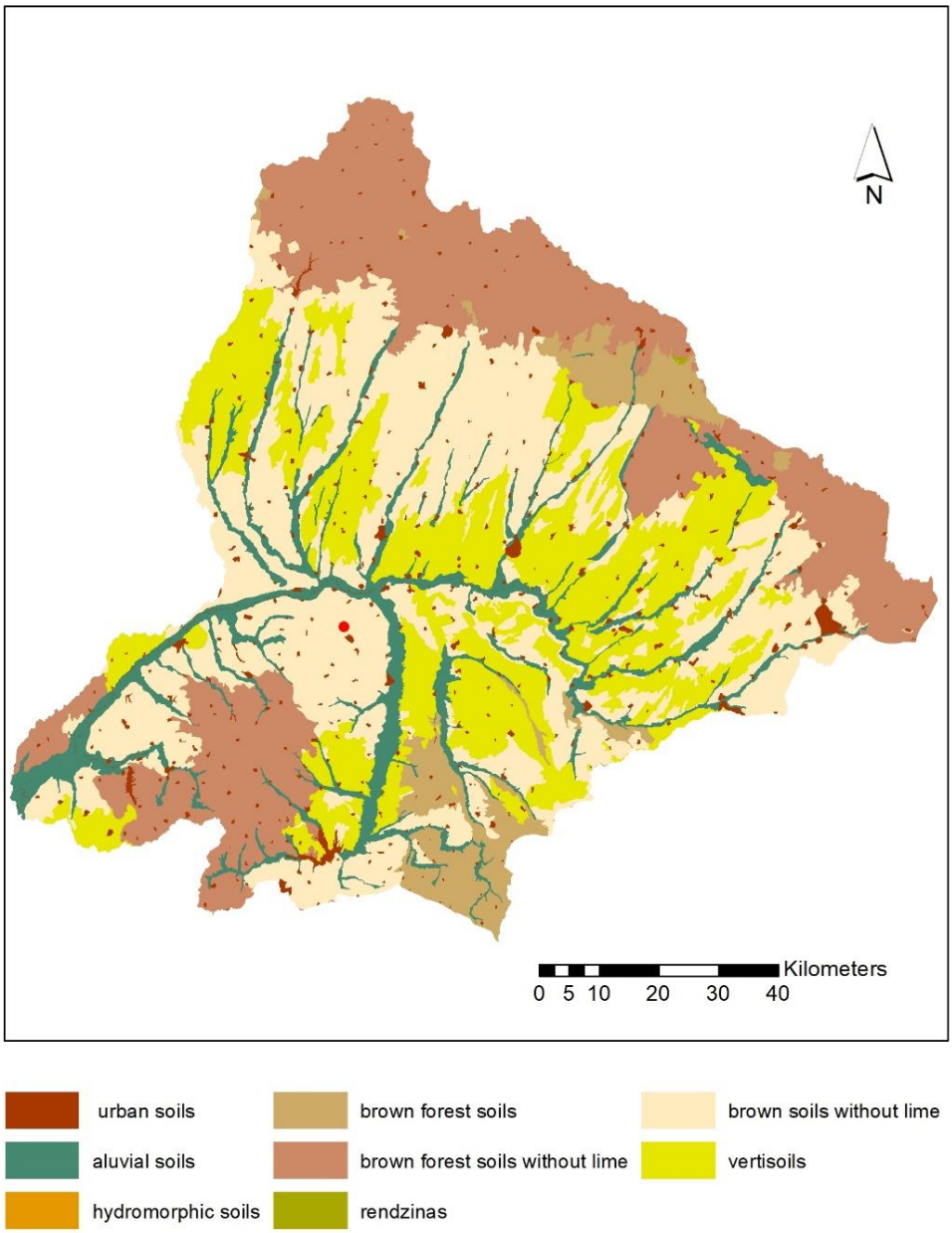

Figure 3. 24 Soil groups in the Ergene River Catchment

3.6.5 Geology

Hydrogeological information has given insight into groundwater flow through hard rocks and unconsolidated rocks and therefore, this information was used for spatial-related clarification of the runoff constituents. Within the framework of the data requirements of the mGROWA model, the geological units are important for the separation procedure for calculating groundwater recharge.

Figure 3.25 shows the geological units in the catchment of the Ergene River which was used in mGROWA for determination of groundwater recharge and Figure 3.26 shows different sections across the investigated area.

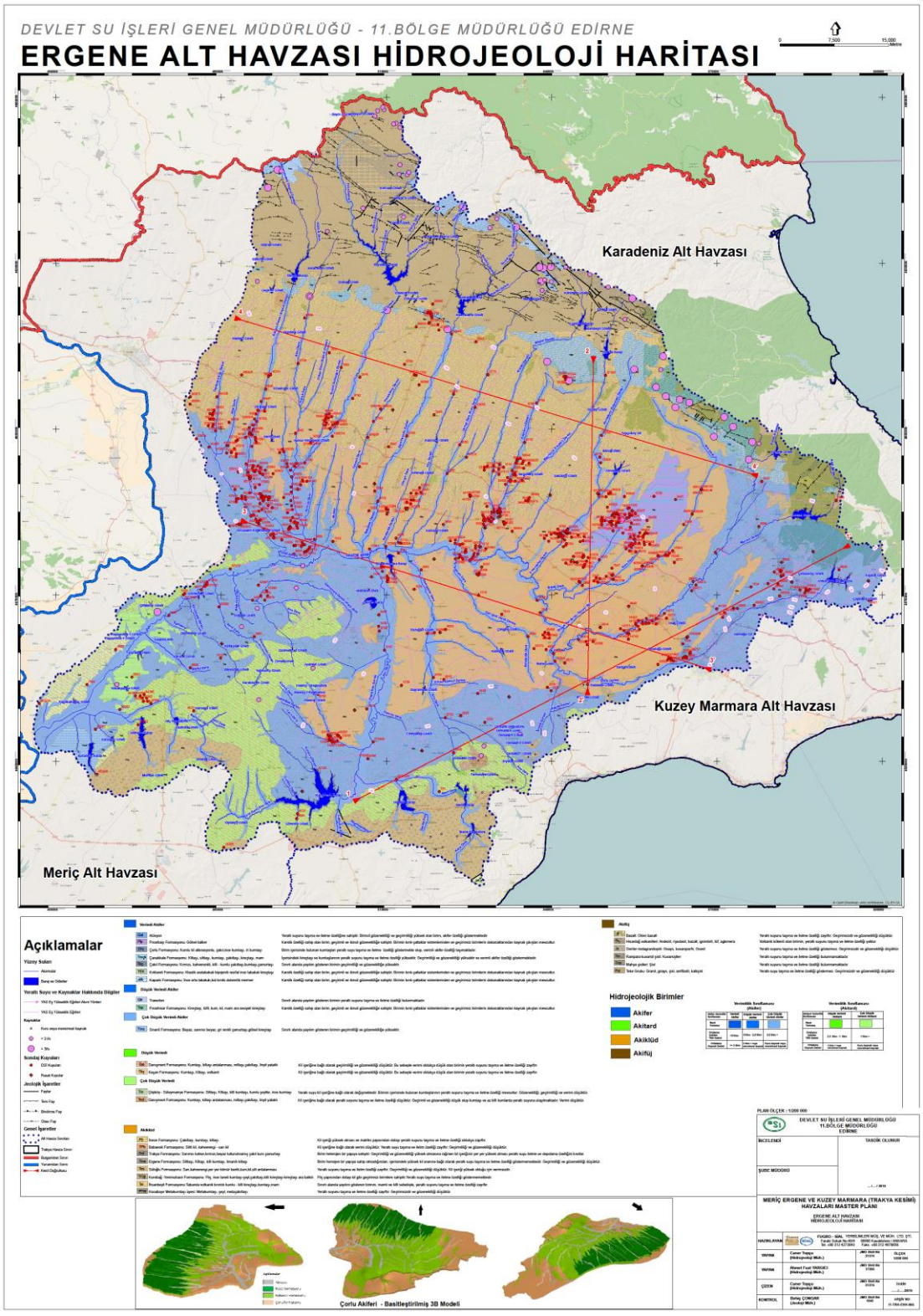

Figure 3. 25 Geological Map of the Ergene River Basin

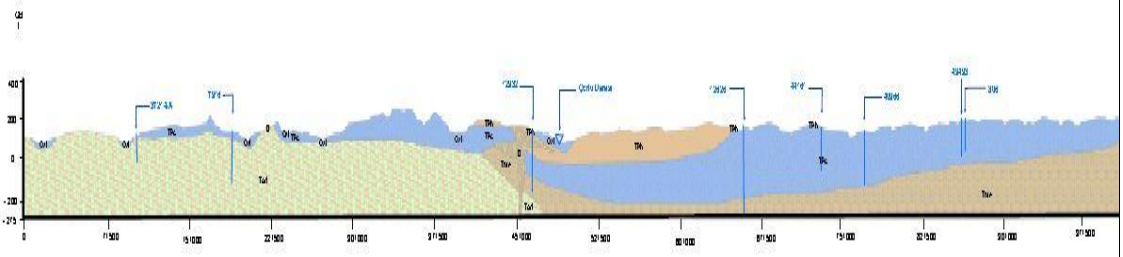

Section 1-1

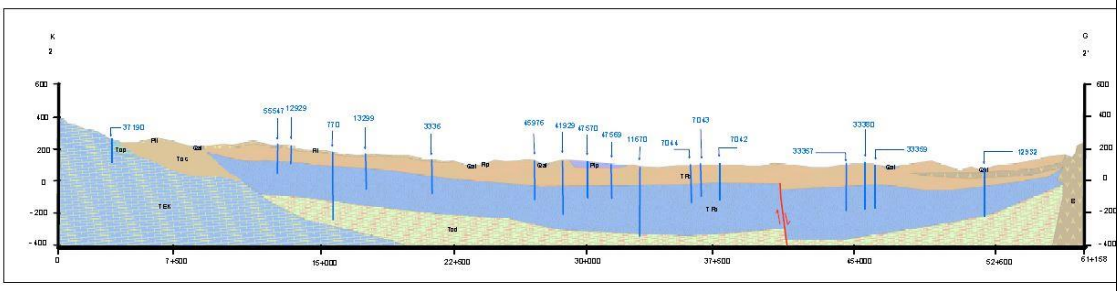

Section 2-2

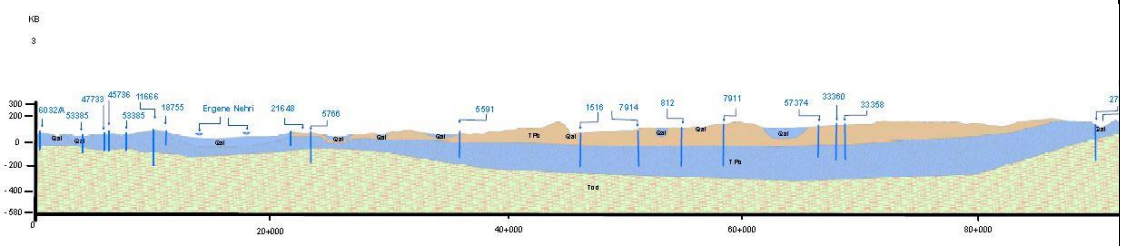

Section 3-3

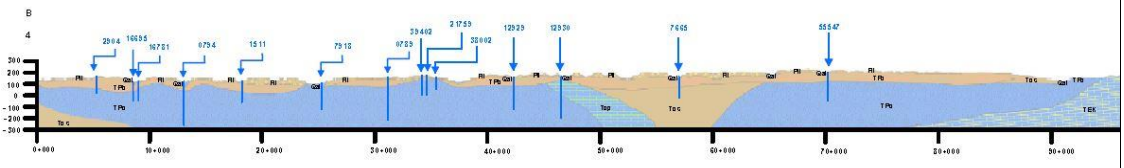

Section 4-4

Figure 3. 26 Section of Geological Units at Ergene River Basin

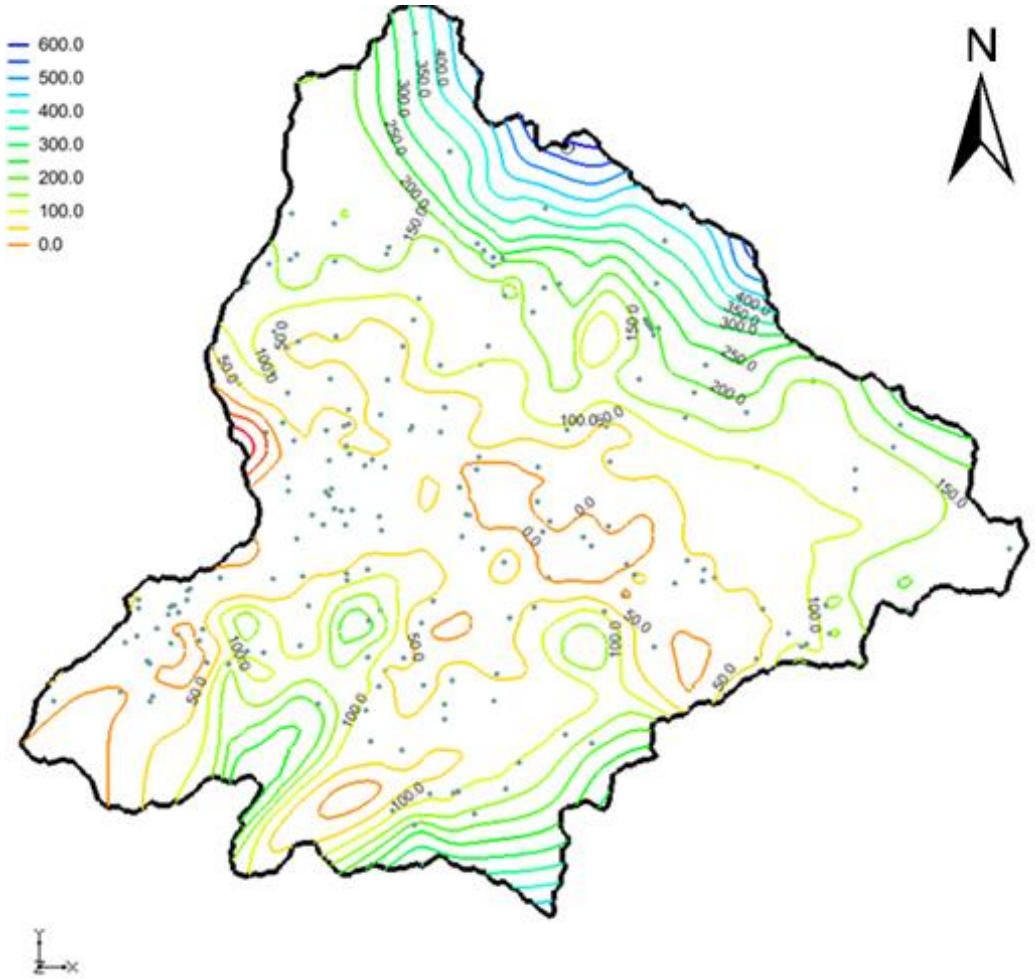

Figure 3. 27 The Recorded Groundwater Depth from Monitoring Wells in the Ergene River Catchment

As it can be seen in the Figure 3.27, the maximum measured groundwater elevation was observed in the north part of the investigated area in the range of 400 to 500 m of elevation whereas the minimum recorded levels were noticed by in the central and southern part of the study area.

Table 3. 9 Hydrogeological Classifications of the Rocks in Ergene River Basin

Low permeability - low water retention potential	**Low to high permeability, locally variable - low water retention potential**	**medium permeability low water retention potential**	**high permeability, low water retention potential**	**Low permeability-high water retention potential**	**High permeability- high to low water retention potential, locally variable**
Metamorphic rocks • Gneiss • Schist: Paleozoic -upper paleozoic • Phylite, Marble, Metabasic rocks- upper Paleozoic-triassic	• Marble, schist in places-mesozoic • Marble-schist Devonian • Metaclastic and metacarbonate rocks – upper crateceous • Clay, sand gravel, conglomerate-pliocene	• andesite • granite	• Crystallized lime-stone-paleozoic • Marble-middle triasssic-jurassic • Cherty marble-middle triassic-crateceous • Limestone-crate-ceous • Limestone yellow – tertiary • Lacustrine carbonate rocks-miocene • Lacustrine limestone, mam, shale-miocene • Basalt-pliocene-quarternary	• Marl, limestone,marly limestone – tertiary • Marl, marly limestone, limestone, tuffite – tertiary	• Conglomerate, sandstone – tertiary • Continental clastic rocks – miocene • Clastic and carbonate rocks-miocene • Alluvial fan, slope debris, moraine etc.-quaternary
Ultrabasic rocks • Peridotit – Mesozoic undifferentiated basic and ulrabasic rocks-mesozoic • Basal splite-upper cretaceous • Ophiolitic mélange – upper crateceoous • Ophiolitic series					
Pyroclastic rocks • Pyroclastic rocks – lower-middle miocene • Undifferentiated volcanic rocks – lower middle-miocene • Pyroclastic rocks, tuffite – Pliocene - quarternary					

In Ergene river basin, the principal lithological structure is composed of metamorphites and clastic rocks. The metamorphites are mainly grouped in gneiss, schist and marble rocks and are characterized by the long period of existence whereas the clastics are mainly of low age compared to the metamorphites and possess low permeability. Basalt rocks were seen in the southeastern part of the Ergene catchment in the form of holms. The tectonic lines were observed in the north and northeast. The quaternary rocks covered by alluvium composed by sand, gravel, and clay were found along riversides. Based on the geological information of the study area, the hydraulic properties of the geologic rock units were studied and summarized in Table 3.9 and Table 3.10.

Table 3. 10 The Range of Hydraulic Conductivity in Ergene River Basin

Layer	Layer Name	Matrial	Horizon K (m2/day)				Porosity	Aquifer Type
			Min	Max	perposed by pumpinging Tests	Given		
1	Aluvium	Soils and Rivers Aluvium	1	400	2-53	35	0.35	Free (Unconfined)
2	Aquiclude	clay and silt	0.01	1	-	0.05	0.35	Leaky
3	Aquifer	Sand and silt	1	400	0.3-41	Variable (0.3-41)	0.35	Semi-Confined
4	Aquitard	Silt and Clay	0.1	10	-	1	0.35	Semi-Confined

3.6.6 Stating Head

After generation of the grid with the resolution of 100 x100 m, for groundwater computation needs to suppose initial water surface that known as starting head. As a default starting head equal to the upper-level elevation of each layer surface as shown in Figure 3.28.

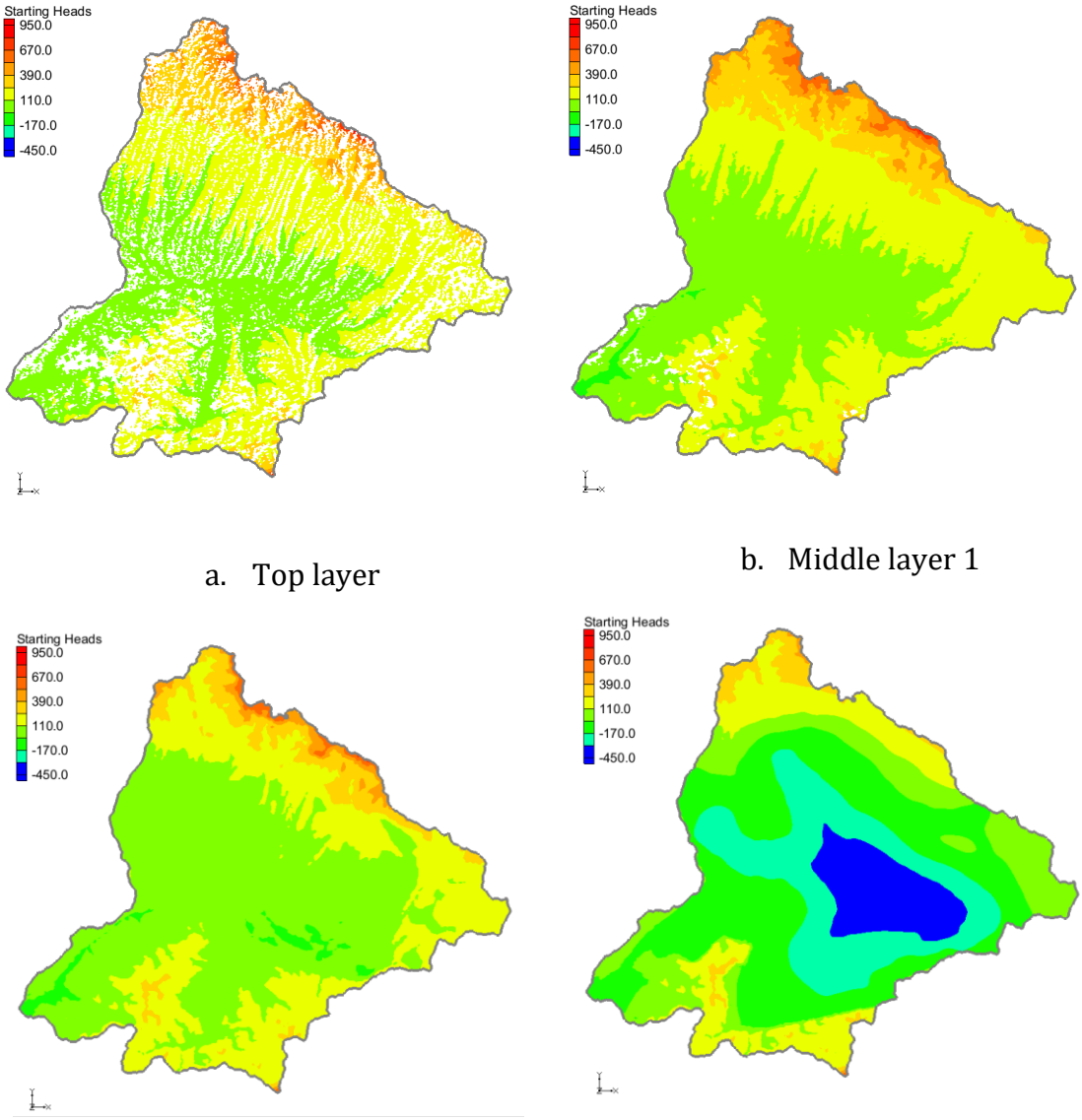

a. Top layer

b. Middle layer 1

c. Middle layer 2

d. Bottom layer

Figure 3. 28 Starting Head of Water Surface as the Initial Condition for Groundwater Modeling by MODFLOW

3.6.7 River and stream

Generally, river and streams are able to obtain or lose their water from or to groundwater reservoir. Rivers and streams are classified in MODFLOW as the head dependent boundary. Concerning the Ergene river basin soil properties, characterized by alluvium soils in plains, the potentiality of gaining of losing water referred to as conductance were determined for this case study. Rivers and streams

of the investigated area (figure 3.29) were categorized by their width where their conductance was calculated by applying the following relationships:

Darcy law for flow in media:

$$Q = k\frac{\Delta H}{L}A \tag{3.19}$$

Where Q = flow rate [L^3/T]

k = hydraulic conductivity [L/T]

A = gross cross-sectional area of flow [L^2].

ΔH = the head loss [L]

L = the length of flow [L]

The variable C= k*A/L given as geometry and hydraulic characteristics of the river and referred to as conductance [L^2/T]. The river bed thickness and area can be represented for rivers in the following form.

$$C = \frac{k}{t}lw \tag{3.20}$$

where:

t = the thickness of the material in the direction of flow [L]

lw = the cross-sectional area perpendicular to the flow direction [L^2].

Conductance per unit length should be entered as presented in equation 3.21:

$$C_{arc} = \frac{\frac{k}{t}lw}{L} = \frac{k}{t}\mathrm{w} \tag{3.21}$$

where:

C_{arc} = conductance per unit length [(L^2/T)/L] or [L/T]

t = the thickness of the material [L]

w = the width of the material along the length of the arc [L]

The computation of conductance for rivers and streams was performed by considering the hydraulic conductivity in the alluvium soils of 3.5 m^2/day and the calculated conductance is presented in Table 3.11. As it can be seen in table the unit

conductance of rivers for unit width of rivers is in the range of 53 to 315 m^2/day per meter.

Table 3. 11 The Conductance of the Streams in Ergene Catchment

Class	Numbers	River Width (m)			Length (Km)	Thickness (m)	Conductance (m2/day)	Conductance (m2/day/m)
		Min	Mean	Max				
1	79	10	15	20	656	1	34440000	53
2	33	20	25	30	532	2	23275000	44
3	35	30	40	50	450	2	31500000	70
4	24	50	75	100	302	3	26425000	88
5	14	100	150	200	86.1	3	15067500	175
6	19	200	270	350	98.5	3	31027500	315
Total	204				2124.6		161735000	

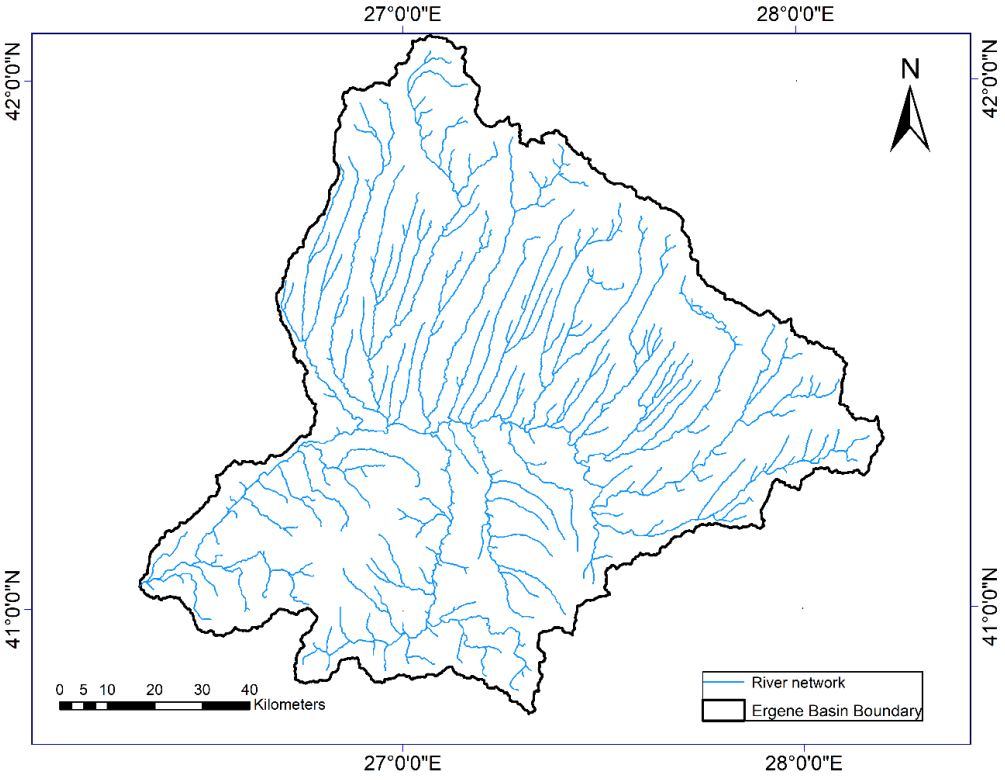

Figure 3. 29 The Streams in Ergene Catchment

3.6.8 Wells

In this investigated area, 1178 municipal wells, 1040 industry wells, and agriculture were recorded to be available (Figure 3.30). However many of them lacking the depth and discharge information. Thus 89 monitoring wells containing the all information related to discharge and water levels were used during this study for calibration.

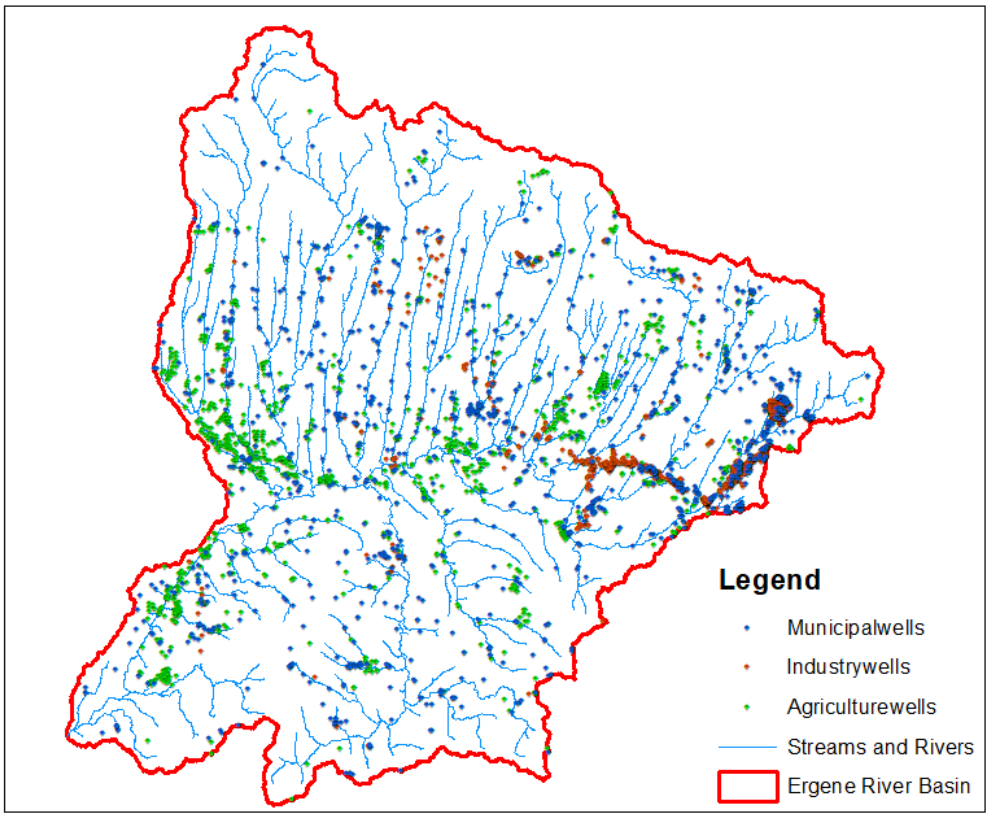

Figure 3. 30 The Location Wells and Usage in Ergene River Basin

3.6.9 Specified Boundary Flux

Generally, an aquifer can recharge or discharge naturally by its boundary formations and also an aquifer possesses an underground connection located out of the catchment boundary. In this situation, there is a linear or non-linear relationship between the flux into (or out of) groundwater and the head in the bound. During this research, the simplest connection between bounds of Ergene catchment and its groundwater was considered as a linear relationship. A reference head and conductance were computed for this relationship. When the head in the aquifer

nearby equals the reference head, the flux is zero. If the head in the aquifer nearby is less than the reference head, water enters the groundwater system through the general-head boundary. If the head in the aquifer is greater than the reference head, water leaves the groundwater system.

The conductance value (C) for the length of bound is calculated by the following relationship (equation 3.22):

$$C_{arc} = K * W * \frac{L}{D} \quad (3.22)$$

Where:

K is the average hydraulic conductivity.

W is the thickness of the saturated aquifer perpendicular to the flow direction.

L is the boundary length perpendicular to the flow direction.

D is the distance from the general head boundary to the model boundary.

4

Results and Discussions

4.1 Simulated Water Balance Components

After many iterations between mGROWA and MODFLOW models, the simulated outputs were stabilized and negligible variations were analyzed for the water balance quantities and hydraulics heads. In this section, the results of mGROWA model over the Ergene river basin are presented, including spatially water balance components for hydrological reference of 1991-2010. Figure 4.1 shows the simulated actual evapotranspiration expressed as actual evapotranspiration, total and direct runoff, and the groundwater recharge. The direct and total runoff produced by mGROWA were presented in the form of maps and represent the values generated for a grid cell of 100 m, thus the investigated area river flow values were not included.

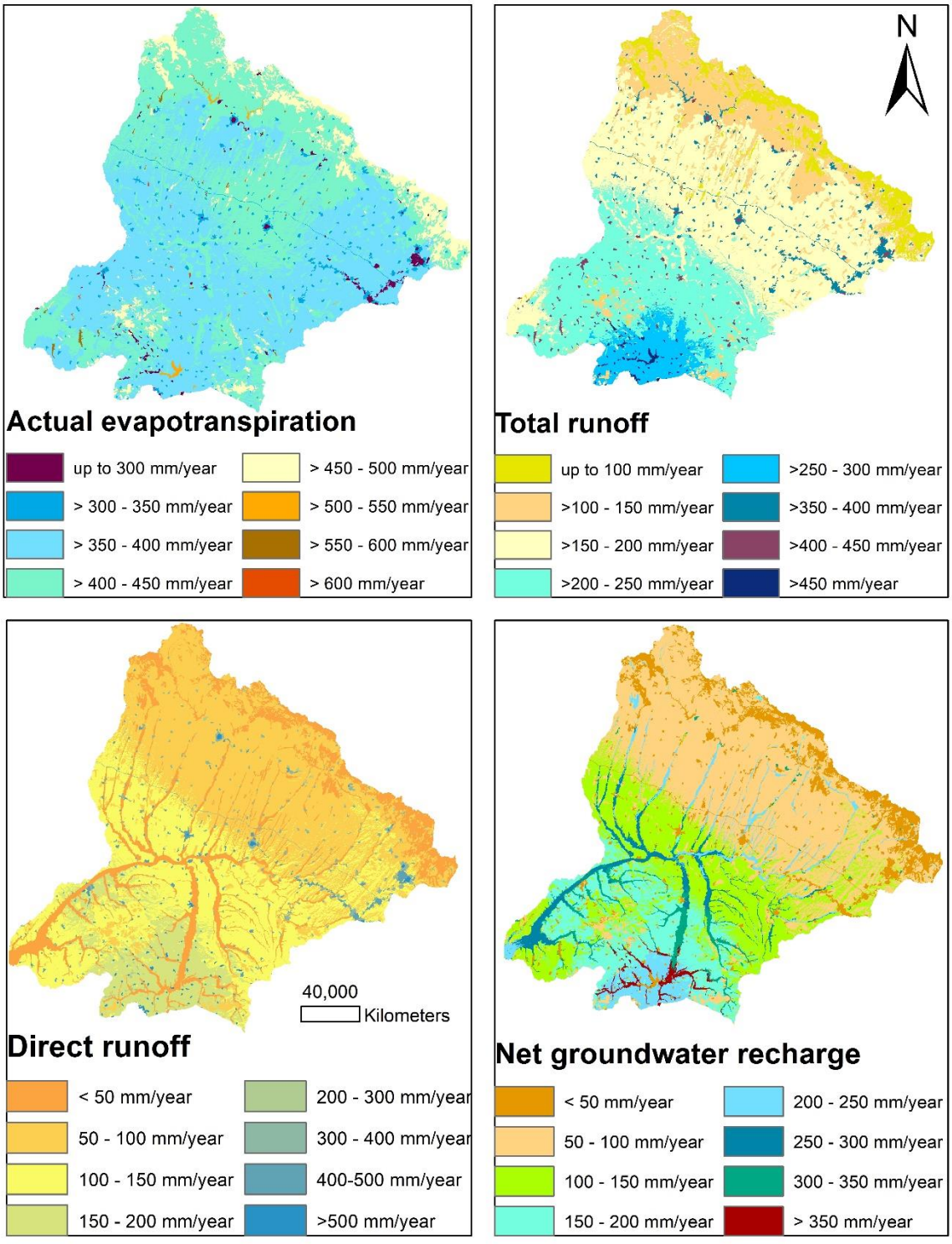

Figure 4. 1 Water Balance Components for Hydrological Reference of 1991-2010

Generally, the vegetation cover, soil texture and climate of the investigated area influence the actual evapotranspiration. In Figure 4.1, It is observed that the spatially differentiated actual evapotranspiration shows a large pattern in a

common way of land cover across the Ergene river basin. The lowest actual evapotranspiration under 300 mm/year can be noticed in the impervious zones located in urban areas. Large rates of actual evapotranspiration (400-450 mm/year) were observed in the highest topography located in the northern part of the study area where the land is characterized by the forest. In the land characterized by low elevation of topography, the actual evapotranspiration was also found to be affected by the land use groups, and it is noticed that in the non-irrigated arable land, which possesses a high portion in the investigated basin with 55%, the actual evapotranspiration changes in the range of 350-400 mm/year. Overall, it was found that the arithmetic average rates of the actual evapotranspiration within the Ergene river basin is 450 mm/year.

Concerning the total and direct runoffs as presented in Figure 4.1, due to the existence of large impervious area, the cell grids located in the urban zones show the large total runoff rates and direct runoff from 350 to 400 mm/year and 200 to 300 mm/year respectively. Regarding the simulated total runoff, it is steadily being reduced (under 150 mm/year) in the region of high topography existing in the north part of the study area because of the existence of large land forest that produces significantly the large ETa. Against this background, in the high altitude of the north-eastern zone of the study area, the total runoff rates become lower than 100 mm/year, and this continues up to the interval of 100-150 mm/year in the parts of north-west of the investigated area. The simulated direct runoff displays the same distributed area pattern as the total runoff and all of them are significantly affected by the land cover type. Overall, the arithmetic averaged for the total and direct runoffs were found to be 200 and 85 mm/ year in the Ergene river basin.

According to the generated long term recharge, as expressed in Figure 4.1, It can be noticed that the Ergene river basin may be categorized into 3 areas such as area characterized by high, moderate and low recharge levels with high dependencies of area related characteristics such as soil texture and structures, hydrogeology, the aquifer storage capacity together with the hydraulic conductivity of rocks. It can be observed that the impact of the hydrogeological characteristics plays the main role in the spatial pattern of the recharge. The highest rates of the groundwater recharge

up to 500 mm/ year was observed in the lowland of the Ergene basin catchment characterized by alluvial layer. This can be explained by the existence of high water penetration in an unconsolidated sand aquifer that is mainly composing these alluvial zones. The groundwater recharge in the range of 100 mm/year to 200 mm/year was simulated in the zone so-called moderate zone. The decreasing of the groundwater recharge rates was observed in the north part of the Ergene river basin, where it was found a recharge lesser than 50 mm/ year. For the investigated area, the simulated average recharge for 1991-2010 equals to 95 mm/year.

During this study, the monthly recharge for investigated hydrological reference (1991-2010) was also simulated. Figure 4.2 shows the outputs of the mGROWA model in the Ergene river basin for the average monthly groundwater recharge. It is noticed that the groundwater recharge levels take place from November to April in the investigated area, where the maximum rates were obtained in January. The diminishing of the recharge for this case study starts to occur in April and this is due to the starting of vegetation period.

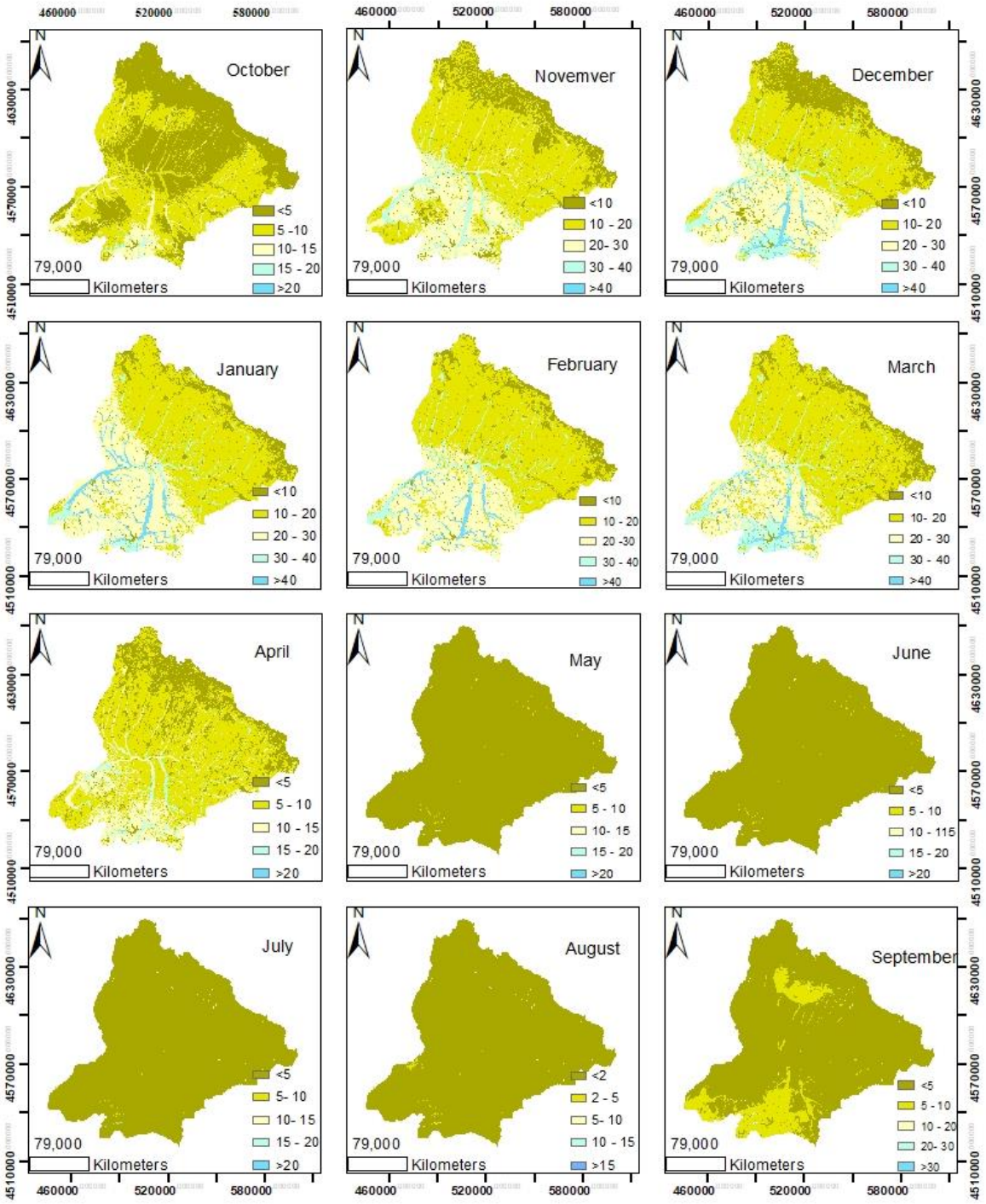

Figure 4. 2 The Average Long-term Monthly Net Groundwater Recharge (1991-2010)

For demonstrating the time behavior of the mGROWA model, the control points at different discharge station where the land is characterized by the vegetation were

presented. The Figures 4.3 to 4.9 show the computed some daily water budget quantities for selected grid cell corresponding to the mentioned stations for the hydrologic reference of 2002. The year of 2002 was taken randomly in order to show the balance values. The climatic input data for the mGROWA model are precipitation and grass reference evapotranspiration. These variables are presented in the first 2 lines of Figures 4.3 to 4.9. In general, the grass reference evapotranspiration reveals the seasonal ups and downs, and are very useful in the estimation of the actual evapotranspiration (Eta). The Eta, as presented in row number 3, comes after this cycling with the irregularity of periods where soil water content is close to the permanent wilting point as revealed in the row number 6 of the Figures 4.3 to 4.9. This divergence has strongly pronounced the end of May and end of September 2002 as shown in row number 4 of Figures 4.3 to 4.9, and this is caused by the drought.

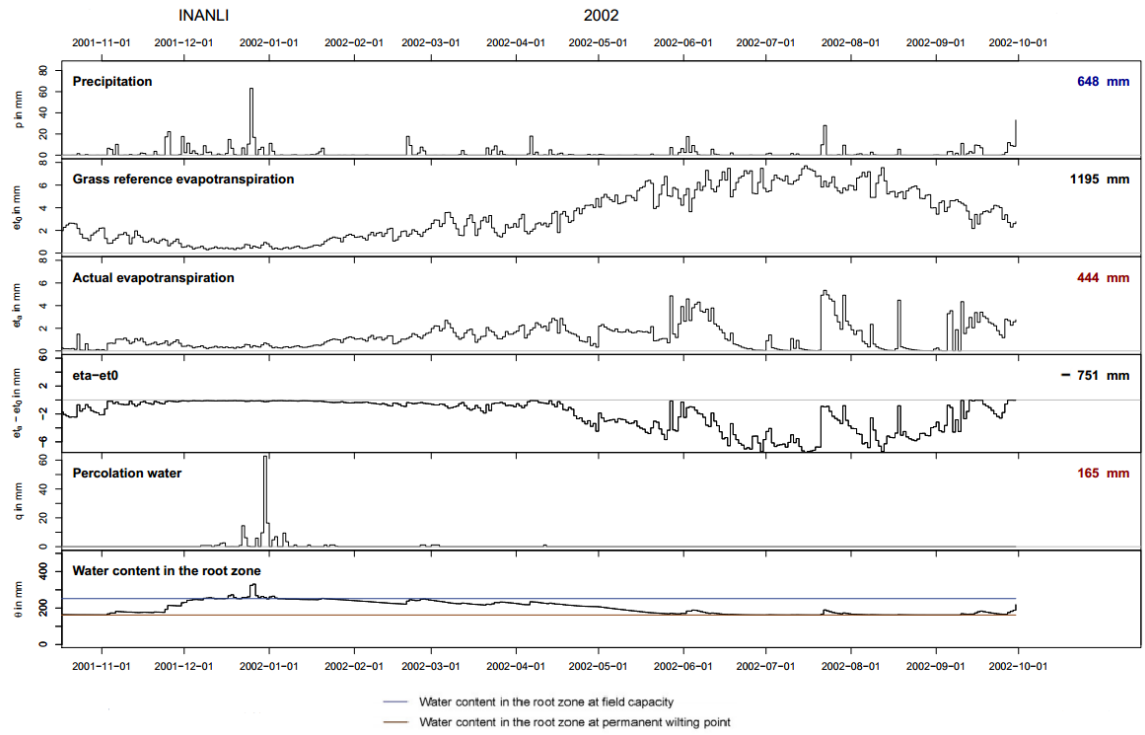

Figure 4. 3 The Temporal Simulated Water Balance for Example of the Hydrologic Year 2002 for an Individual Grid Cell at INANLI Station

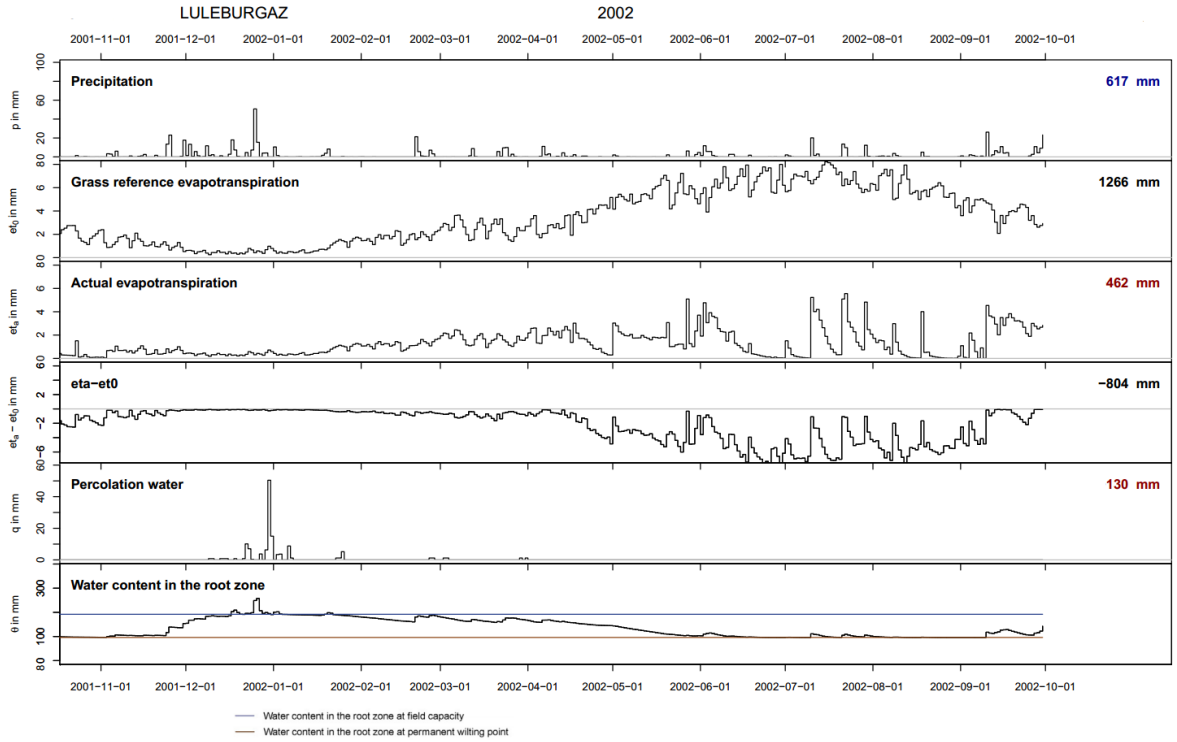

Figure 4. 4 The Temporal Simulated Water Balance for Example of the Hydrologic Year 2002 for an Individual Grid Cell at Luleburgaz Station

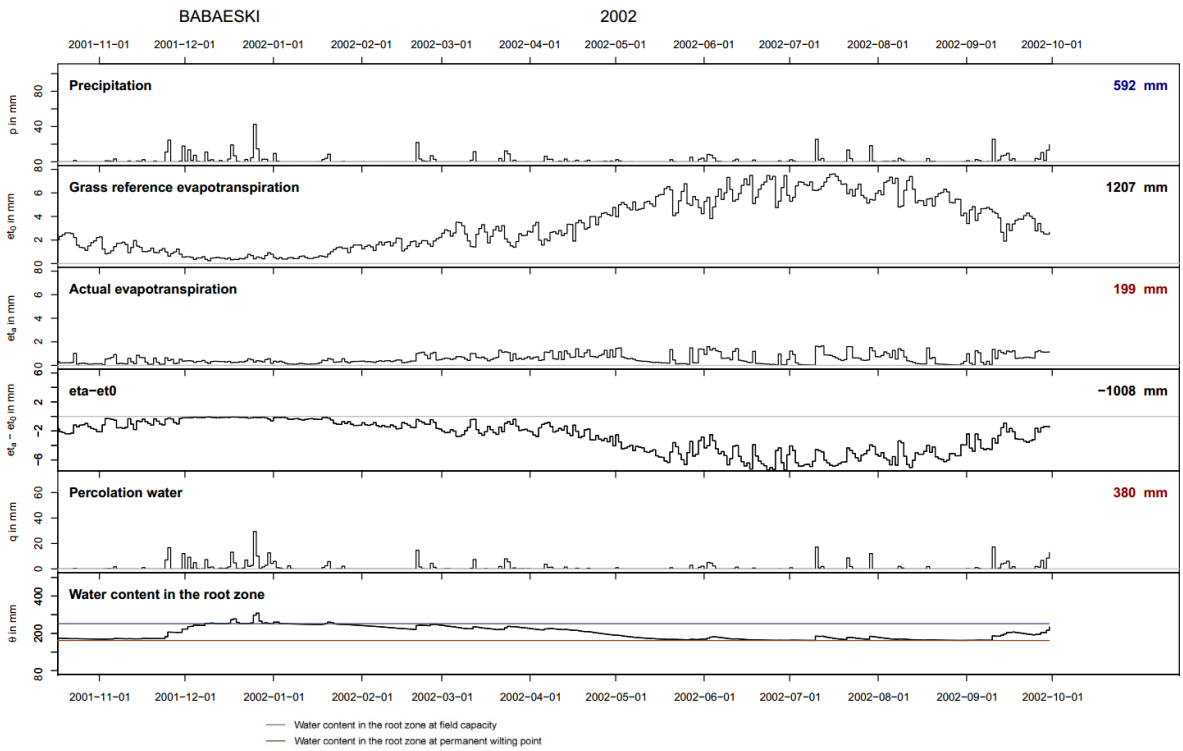

Figure 4. 5 The Temporal Simulated Water Balance for Example of the Hydrologic Year 2002 for an Individual Grid Cell at Babaeski Station

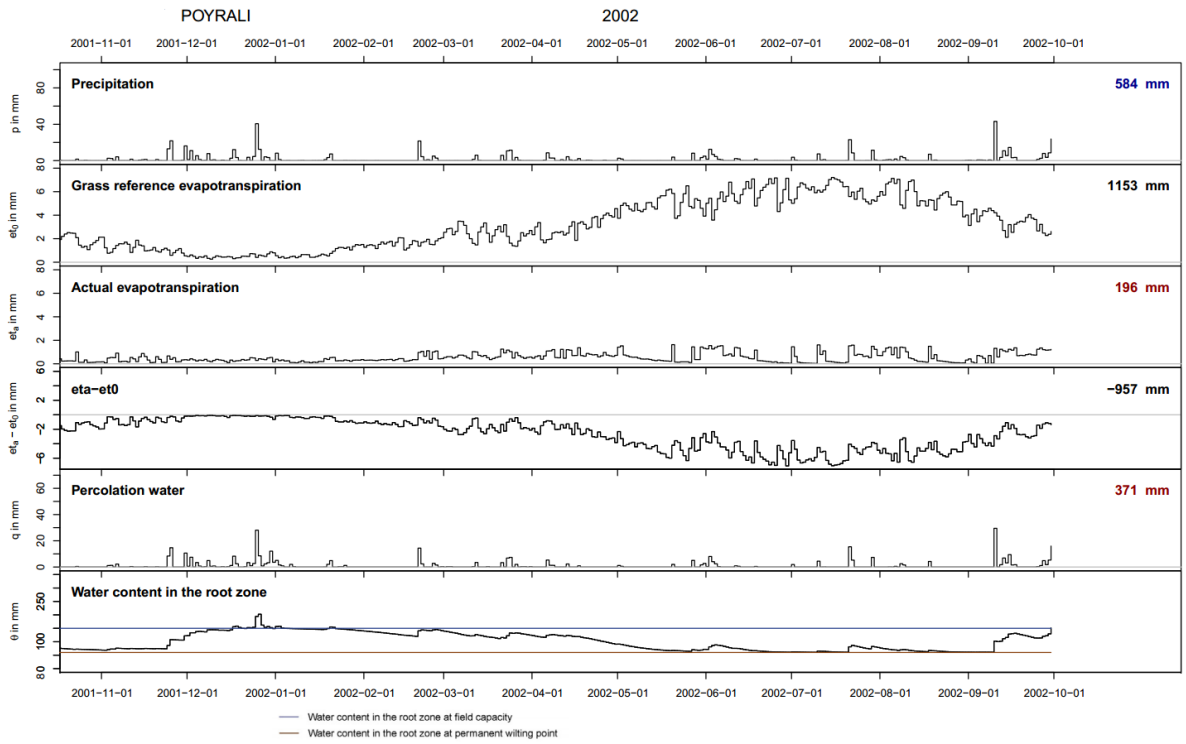

Figure 4. 6 The Temporal Simulated Water Balance for Example of the Hydrologic Year 2002 for an Individual Grid Cell at Poyralı Station

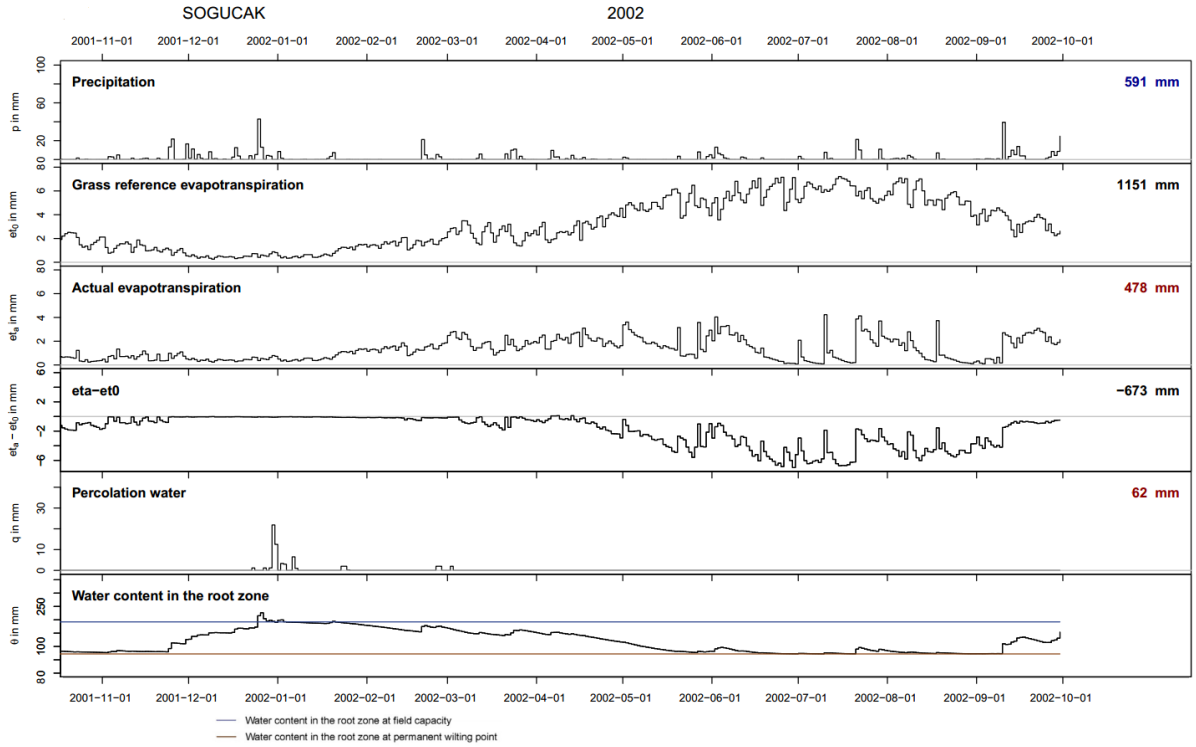

Figure 4. 7 The Temporal Simulated Water Balance for Example of the Hydrologic Year 2002 for an Individual Grid Cell at Soğucak Station

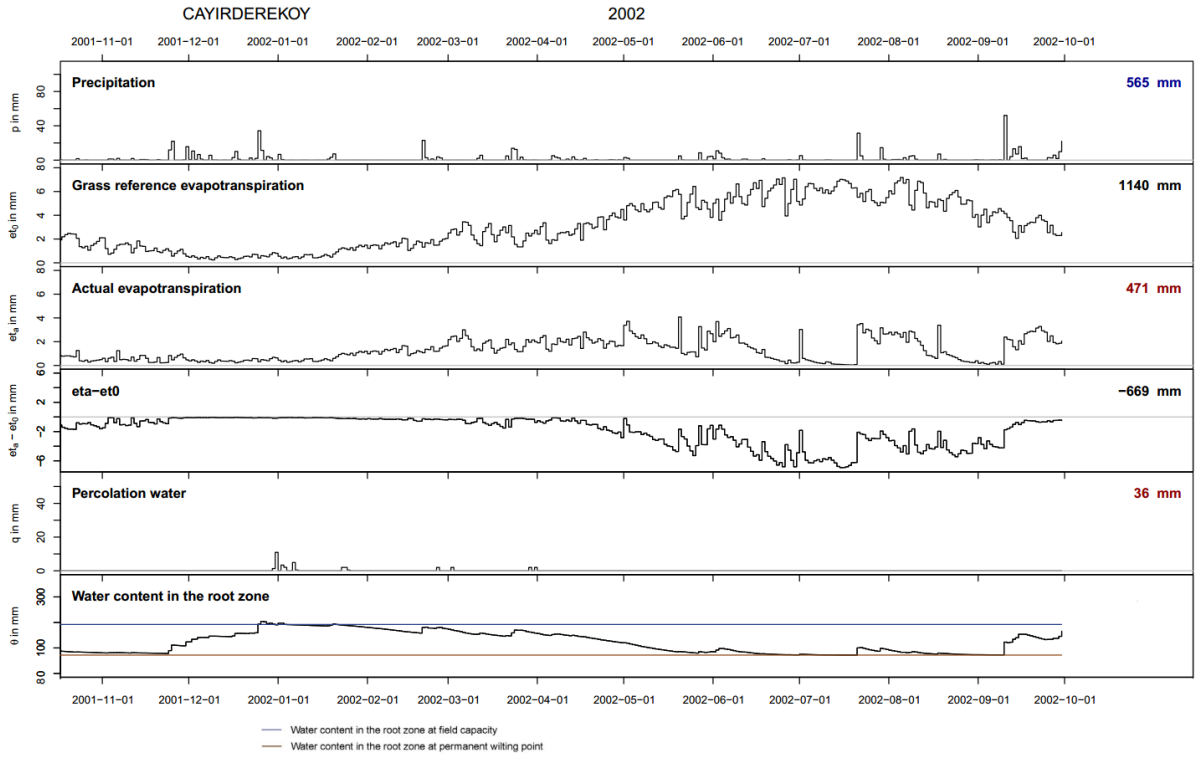

Figure 4. 8 The Temporal Simulated Water Balance for Example of the Hydrologic Year 2002 for an Individual Grid Cell at Cayırderekoy Station

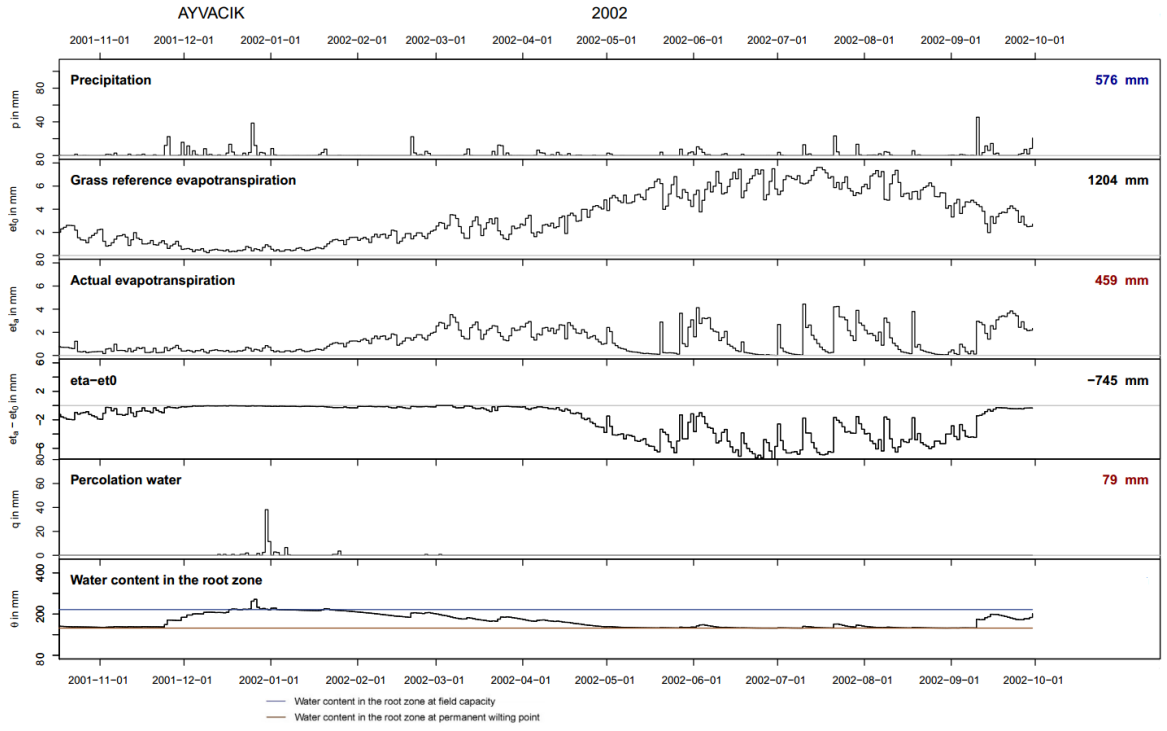

Figure 4. 9 The Temporal Simulated Water Balance for Example of the Hydrologic Year 2002 for an Individual Grid Cell at Ayvacık Station

During this study, the annual water balance components including real evapotranspiration, runoff, together with recharge rates were exhibited in the function of available Corine 2012 land use types together with soils groups in the study area (Figure 4.10 and 4.11). The related coverage zone area within Ergene river basin was also exhibited. As it can be seen in Figure 4.10, the simulated recharge exhibits a high variation based on the given Corine 2012 land cover. It can be observed that the artificial zone areas that are in terms of code such as 111, 112, 121, and 122 which stands for continuous-discontinuous urban fabric and Industrials zone areas, possess a very small rate of recharge because of the presence of great rate of imperviousness of abovementioned land covers. Therefore, they displayed great runoff rates.

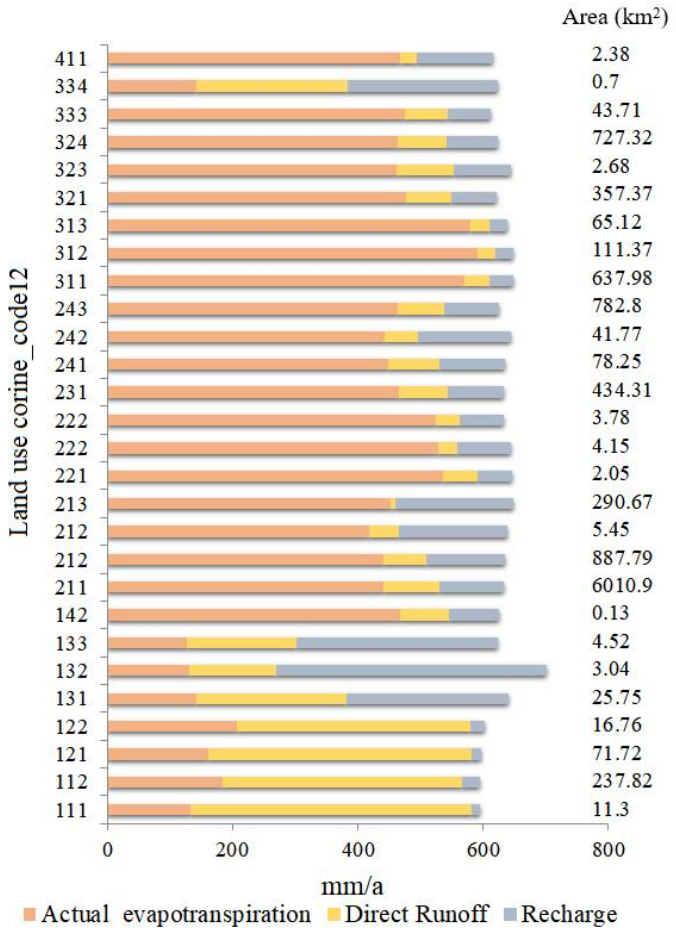

Figure 4. 10 Average Annual Rates of Water Balance Components Based on CORINE Land Cover

In the investigated area, 3 % of the total area is composed of the artificial grid cells (urban land) scattered in different places. The land cover of codes 131, 132 and 133 displayed the great rates of recharge and the code related land cover are mineral extraction sites, dump sites, and constructions sites, respectively and they possess only 0.3 % of the total area of the investigated area. The above-mentioned land cover classes for mineral extraction sites, dump sites, and constructions sites influence natural hydrogeology quite profoundly, where in this area characterized by this land cover, the permeability of the rocks can rise up to hundreds of times [68], [69].

On the sides of the agricultural grid cells represented by the Corine 2012 codes: 211, 212, 213, 221, 222, 231, 242 and 243, it can be noticed that the real evapotranspiration controls other water budget components in the study area, and this becomes the same for land covers such as the forest and semi-natural cells represented by the Corine 2012 codes of 311, 312, 313, 321, 323, 324 and 334. It was observed that such land-use covers exhibıted a medium average of groundwater recharge rates. However, the exception is noticed in land cover characterized by bunt grid cell with Corine code of 334, in this type of land cover, the recharge was found to be 240 mm/year which is greater than areal evapotranspiration. It is also observed in figure 4.11 that simulated recharge is a relying-variable on the soil classes of the Ergene river basin with great influence existing in grid cells characterized by the alluvial soils.

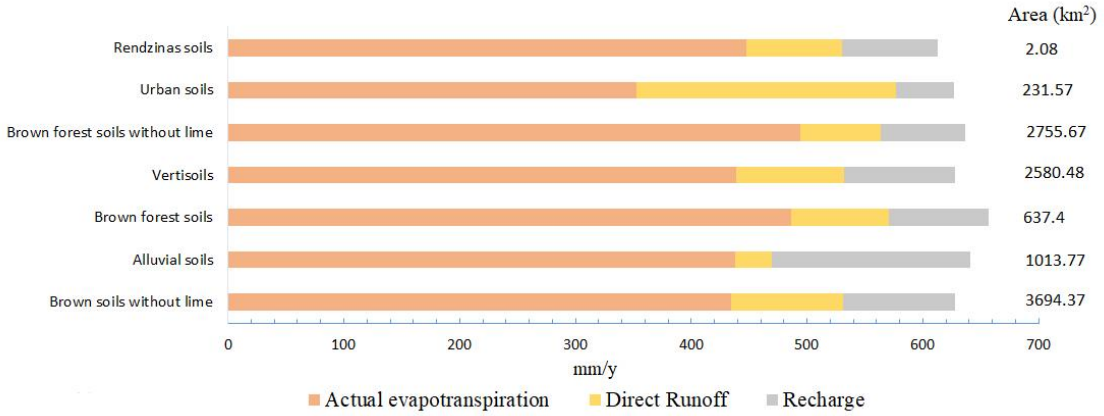

Figure 4. 11 Average Annual Rates of Water Balance Components Based on Soil Groups

The alluvial soil is characterized by a great capacity of the water conductivity where the penetration of the water becomes easier through this type of soil, and this penetrated water replenishes the groundwater aquifer. In the urban soil, it was noticed that it possesses a very small rate of recharge equals to 50.3 mm/year. Urban soil type may be characterized as anthropic soils, mainly resulting from human activities.

Figure 4.12 shows the base flow statistics resulted in the approach applied in this study namely Wundt and Kille hydrograph separation approach. The great media in the Ergene river basin is observed in sub-catchments: Soğucak, Çayirderekoy, Ayvacık, and Poyralı displayed respectively the base flow of 90.4, 77, 73.5 and 49 mm/year. These subbasins are located in the north part of the investigated area where the area described by high relief (slope and elevation). The topography influence greatly the groundwater recharge and the base flow, the increase in the topography for instance, the gradient slope augments the level of groundwater transmission within the catchment [70]. The basins such as Luleburgaz, Babaeski, and Inanlı exhibited respectively the small median in simulated values of the base flow: 33, 37, and 38 mm/year. They are found in the zone characterized by the average slope grid cells and average elevation. These small values of base flow can be explained by the related existing land use type characterized by the agricultural land with possession area of 73% of the total area of the investigated area which is frequently irrigated from the groundwater. A part composed by the urban grid cell zones can affect negatively the base flow because of the alteration in natural system ability of the surface and underground to drain the water. Thus, the surface and groundwater interaction can be disturbed and deteriorated [71]. In the investigated area, it may be concluded that the basins parameters such as relief, land cover and the surface and groundwater interaction control the interconnection between the groundwater recharge and base flow.

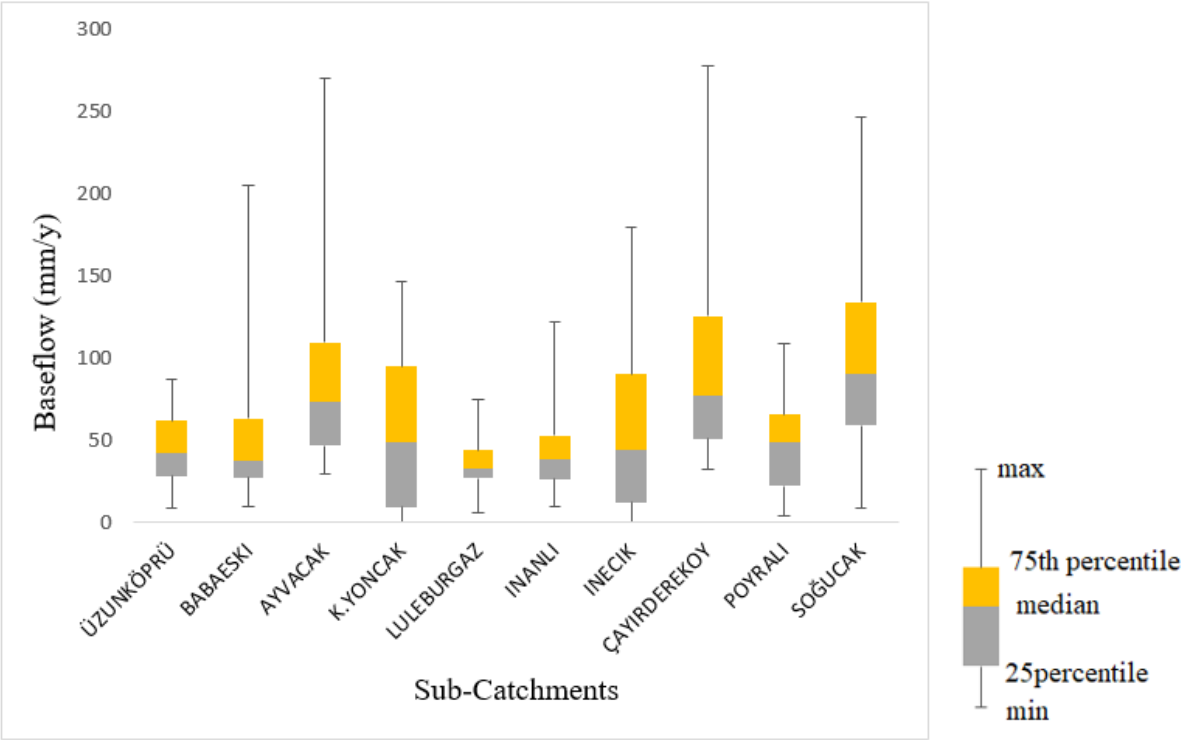

Figure 4. 12 Descriptive Statistics of Base Flow in Different Considered Sub-basins

4.2 mGROWA Model Evaluation

As mGROWA model is not a runoff concentration model, thus, its validation cannot be based on the comparison between the daily modeled and recorded water budget values [13]. Nevertheless, the valuation of the results of the model can be performed by balancing the long-term recorded and calculated total runoffs and groundwater recharge values. Against this background, Figure 4.13 presents the validation of the mGROWA model and a 45-degree plot line was presented to show the comparison among the simulated runoffs and recharge together with their corresponding recorded values. The comparison of the balance quantity was done for the hydrological reference horizon of 1991-2010. In this study, a quantitative statistic namely Nash-Sutcliff (E_f) was applied in order to indicate the performance of the model, and it can be seen in Figure 4.13 that a value of 0.94 was achieved for total runoff and this value shows a very good performance. For the groundwater recharge simulation, Nash-Sutcliff (E_f) was found to be 0.76, when the baseflow from hydrographic separation method was compared with the simulated recharge. The

Moriasi et al. (2007) in [72] showed that when the coefficient of Nash-Sutcliffe becomes higher than 0.75 and 0.65, this reveals the very good and good achievement in the modeling, respectively, in case of considering a single basin. As can be observed, the deviations between observed and simulated total runoff and groundwater recharge for almost all sub-basins taken into account is under ± 20%. Except only 3 sub-basins displayed the differences in the observations and simulations values which are greater than 20%. Generally, the inaccuracy existing in the modeled and recorded quantities can be explained by some discrepancy scale of an empirical model [51]. In addition, in the investigated area, there are some water management activities such as dams, irrigation, wells that can lead to the negative or positive alteration of the water system.

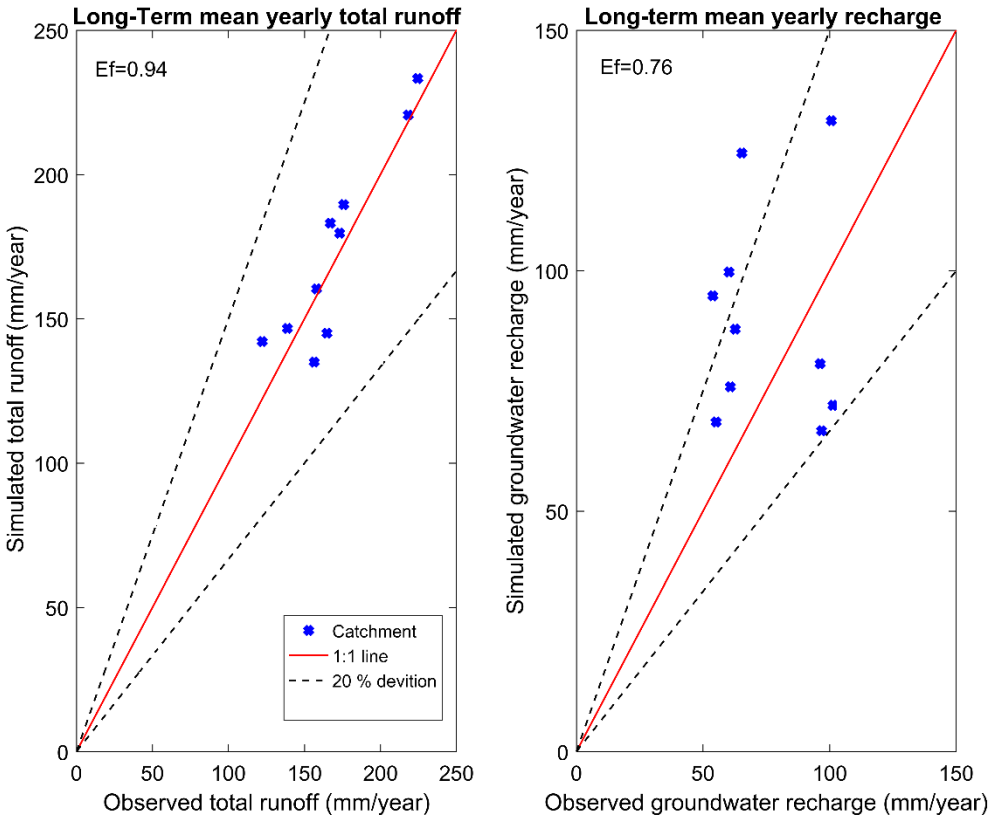

Figure 4. 13 The Recorded and Model-Calculated Total Runoff and Groundwater Recharge Comparison for Hydrological Reference of 1991-2010

4.3 The Recharge Controlling Factors

In this study, prior to the performance of the principal component analysis (PCA), the Pearson correlation approach was applied to provide the linear correlation among the basin attributes such as soils textures, land cover, area, topography, and climatic data together with the recharge. In a total of 20 basin characteristics were put together where some ArcGIS processing was done in order to gather their statistics. Table 4.1 presents the basin attributes, its attribute symbols, the related units and also the linear correlation when assembled together with the recharge. The basin attributes were generally expressed in percentage of their corresponding surface areas compared to the total area of the investigated area. Table 4.1, shows the correlation between the basin attributes together with recharge. The correlation analysis presented in Table 4.2 is the correlation existing in presented variables, where the significant linear correlations are also indicated. Accordingly, some basin attributes can be completely redundant, thus, provide a contribution to the identical driving principle in defining the spatially differentiated variance of the recharge.

In Table 4.1, the only 6 basin attributes are observed to possess a notable linear correlation with the recharge. The climatic data shows the influence on spatially differentiated groundwater recharge. As a result, the greatest positive linear correlation can be observed by precipitation with a correlation of 0.817, which is in the same agreement with many studies [31].

Table 4. 1 Basin Characteristics, Units and their Pearson Correlation with the Recharge

Catchment attributes	Abbreviation	Units	Correlation with the groundwater recharge
Soil types			
Alluvial soil	AS	%	**0.671**
Brown forest soils	BFS	%	-0.293
Brown forest soils without lime	BFSWL	%	**-0.752**
Rendzinas	R	%	-0.277
Brown soils without lime	BSWL	%	-0.020
Vertisol	V	%	0.302
Urban soils	US	%	-0.062
Land cover characteristics			
Artificial surface Land	ASL	%	0.130
Agriculture area	AA	%	**0.676**
Forest	F	%	**-0.659**
Semi natural area	ANA	%	-0.300
Wetland and water bodies	WWB	%	-0.072
Area and topography			
Basin drainage area	BDA	Km^2	0.541
Basin slope	BS	%	-0.058
Elevation	E	M	-0.469
Depth to the water table	DWT	M	0.185
Climate			
Precipitation	P	mm/year	**0.817**
Actual evapotranspiration	AE	mm/year	**-0.686**

[1] Values in bold represent correlation with a significance level alpha=0.05

The negative correlation was found between the actual evapotranspiration together with the groundwater recharge. This reveals that high actual evapotranspiration will stop the aquifer to have the maximum recharge and low actual evapotranspiration produce the increase in recharge. These results are in the same agreement with the study in [73]. This was followed by brown forest soils without lime, as it can be observed from Table 4.2, it is found to be negatively linear correlated with the recharge. For the soil groups, it can be seen that 2 groups are greatly correlated with the groundwater recharge. The alluvial group soil exhibits a great positive linear correlation together with the groundwater recharge. The alluvial zone existing in the investigated area is composed mainly by sandy soil group that is characterized by moderate and high hydraulic conductivity, therefore, the high ability of water penetration which may reach to the increase of the recharge in the investigated area.

The linear negative correlation with the groundwater recharge was also observed with the brown forest soils without lime. In this type of soil, the main component is formed by clay soil and possess a very low conductivity thus the water is not allowed to infiltrate easily into the aquifer.

According to the land cover types, only two from the five considered land cover types exhibited the noticeable linear correlation with the groundwater recharge. The land use types such as agriculture area and forest are observed to possess almost the similar correlation coefficient however a contrasting significant interdependence with groundwater recharge. The mass of the forest biomass can be expected to intensify the evapotranspiration and reduce the total runoff within the catchment, thus influence in a negative way the quantity of the water that can replenish the aquifer [74]. When considering the basin area and corresponding topography, there was no observed noticeable linear correlation between the recharge. Against this background, the principal component analysis (PCA) was used together with the highly linear correlated attributes with the recharge. During this study, it was noticed that the catchment attributes such as AS, BFSWL, AA, F, P, and AE exhibited the noticeable interdependency together with the groundwater

recharge. Table 4.3 presents the PCA of basin attributes that are expressing a great linear correlation together with the groundwater recharge.

In this study, the eigenvalues greater than one are taken into account in this study (Table 4.3). The area distributed variance of the groundwater recharge for the 2 principal components that were taken into account, is equivalent to almost 84%. It can be seen that the percentage of forest land use type show the largest loading factor, whereas the land covered by the agriculture become the second, and followed by the brown forest soils without lime together with the actual evapotranspiration, respectively, in principal component 1. The precipitation affects much more the groundwater recharge as it is indicated in principal component 2.

Table 4. 2 the Linear Correlation Assessment of Basin Attributes

Variables	GR	BSWL	AS	BFS	V	BFSWL	US	R	AS	AA	F	ANA	WWB	BDA	BS	P	AE	DWT	E
GR	**1.00**																		
BSWL	-0.02	**1.00**																	
AS	**0.67**	0.21	**1.00**																
BFS	-0.29	-0.61	0.11	**1.00**															
V	0.30	-0.04	-0.16	-0.43	**1.00**														
BFSWL	**-0.75**	-0.23	0.30	0.12	-0.53	**1.00**													
US	-0.06	0.20	0.47	-0.21	-0.25	0.23	**1.00**												
R	-0.28	-0.30	-0.42	0.41	-0.20	0.07	-0.16	**1.00**											
AS	0.13	0.43	0.55	-0.47	0.15	-0.13	0.62	-0.23	**1.00**										
AA	**0.68**	0.41	0.33	-0.34	**-0.73**	**-0.85**	-0.08	-0.46	-0.34	**1.00**									
F	**0.66**	-0.44	-0.37	-0.38	**-0.72**	**0.83**	-0.02	0.47	-0.42	**-1.00**	**1.00**								
ANA	-0.30	0.20	0.18	-0.33	-0.16	0.36	-0.03	-0.16	-0.18	-0.24	-0.20	**1.00**							
WWB	-0.07	0.29	-0.15	-0.57	0.45	-0.08	-0.27	-0.32	-0.16	-0.30	-0.29	-0.57	**1.00**						
BDA	**-0.54**	0.24	0.53	-0.28	0.14	-0.15	-0.28	-0.15	-0.37	-0.34	-0.36	-0.03	-0.06	**1.00**					
BS	-0.06	-0.39	-0.07	-0.49	-0.56	0.43	-0.25	-0.17	-0.59	-0.54	-0.58	-0.35	-0.08	-0.24	**1.00**				
P	**0.82**	-0.22	-0.51	-0.59	-0.01	-0.53	-0.35	-0.25	-0.33	-0.34	-0.29	-0.17	-0.07	-0.19	-0.44	**1.00**			
AE	**0.69**	-0.42	-0.60	-0.25	-0.43	**0.69**	-0.30	-0.30	**-0.72**	**-0.80**	**-0.83**	-0.25	-0.11	-0.57	**-0.64**	-0.19	**1.00**		
DWT	-0.19	0.31	-0.12	-0.52	**0.70**	-0.50	-0.06	-0.13	**-0.68**	**-0.64**	**-0.69**	-0.15	-0.28	-0.12	**-0.69**	-0.26	**-0.68**	**1.00**	
E	**-0.47**	-0.58	-0.39	-0.45	-0.57	**0.72**	-0.02	-0.40	-0.45	**-0.85**	**-0.87**	-0.24	-0.55	-0.23	-0.43	-0.17	**-0.68**	**-0.75**	**1.00**

Values in bold represent correlation with a significance level alpha=0.05

Basin attributes exhibiting great positive weighting on principal component 1 are alluvial soil (AS), agriculture area (AA) and precipitation (P) as it is indicated in table 4.3. Precipitation displayed the noticeable positive linear correlation with the groundwater recharge due to the reason that the precipitation becomes the main source recharge and this is in the same agreement with many pieces of research such as one presented in [9]. Alluvial soil types intensify the quantity of the groundwater

recharge, due to the reason that such sort of the soils is characterized by great existing of the sand particles that permit the water penetration to the alluvial aquifer type [20]. Thus, it is likely for the alluvial soil types are corresponding to the high rates in groundwater recharge. The observed positive linear correlation among the groundwater recharge and agriculture lands can contribute to the increase of the recharge based on the patterns existing in the infiltration and evapotranspiration, thus, without knowing specifically these corresponded land use types in details in the investigated area, the direct mechanism cannot be ascertained.

Table 4. 3 Principal Component Analysis (PCA) of Basin Variables that are most Correlated with Groundwater Recharge

		PC1	**PC2**
PC Analysis	Eigenvalue	3.946	1.090
	Variability (%)	65.774	18.174
	Cumulative (%)	65.774	83.948
Variables			
AS		0.582	0.621
BFSWL		**-0.894**	0.087
AA		**0.939**	-0.277
F		**-0.941**	0.289
P		0.516	**0.719**
AE		**-0.880**	0.139

Note: Bold type indicates variables with a loading factor greater than 0.70.

The results from principal component analysis reveal that groundwater recharge rates are small in an amount in the investigated area where the brown forest soils without lime, forest, and actual evapotranspiration control the area as it can be seen in Table 4.3. It can be observed also that the brown forest soils without lime are

likely to possess a high composition of clay soils which are strongly related to evapotranspiration and runoff, and this may result in a reduction of the groundwater recharge. Actual evapotranspiration affects negatively the groundwater recharge in diminishing the available quantity of the water for recharge. The forest land-use cover which is mostly known to increase the water infiltration and to have a relatively great quantity of evapotranspiration, therefore this results in the low groundwater recharge. In agreement with principal component analysis, it can be concluded that the groundwater recharge spatial patterns are influenced in order of significance by vegetation land-use, soil group types, and climatic data in Ergene river catchment.

Table 4. 4 Eigenvalues

	F1	F2	F3	F4	F5	F6
Eigenvalue	3.946	1.090	0.738	0.155	0.069	0.000
Variability (%)	65.774	18.174	12.306	2.586	1.154	0.006
Cumulative %	65.774	83.948	96.254	98.840	99.994	100.000

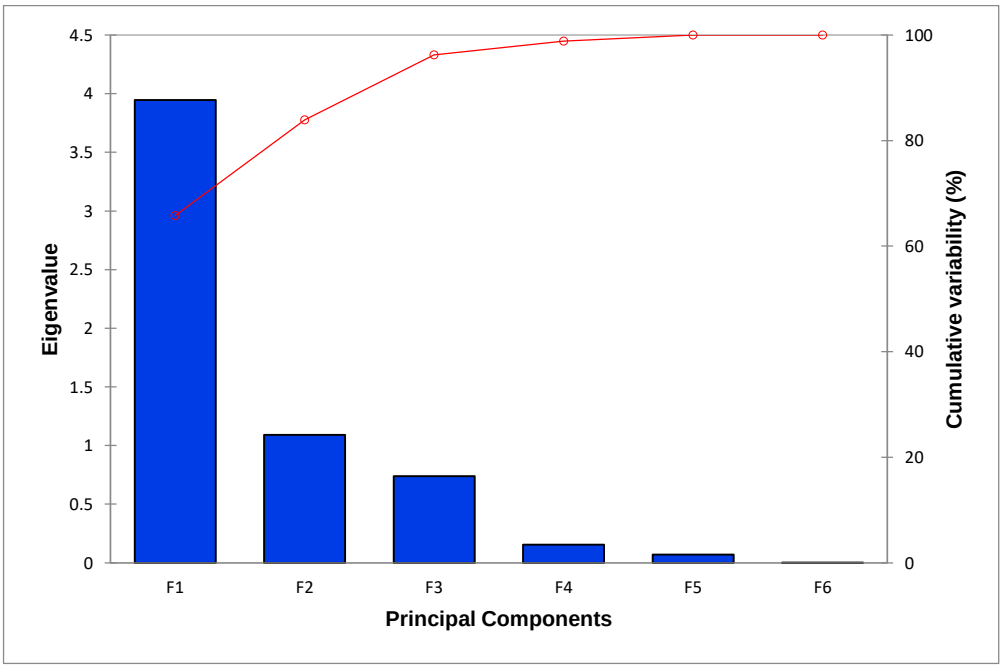

Figure 4. 14 Eigenvalue for every Principal Component and the Cumulative Variability

Table 4.4 and Figure 4.14 are related to a mathematical object called eigenvalues, which reflect the quality of the projection from the N-dimensional initial table (number of variables) to a lower number of dimensions. In the investigated area, the first eigenvalue is as 3.946 and displays a 65.774% of the total variability. This means that the first principal component contains the data which represents 65.774% of the total variability of the data. Each eigenvalue corresponds to a factor and each factor to one dimension. A factor is a linear combination of the initial variables, and all factors are uncorrelated. The eigenvalues and corresponding factors are sorted by descending order of how much of the initial variability they represent (in terms of percentages). The factor means the PCA dimension or PCA axis. Ideally, the first two eigenvalues will correspond to a high percentage of the variance, ensuring that the maps based the first two factors are a good quality projection of the initial multi-dimensional table of variables. In this study, the first 2 factors allow representing 83.95 % of the initial variability of the data.

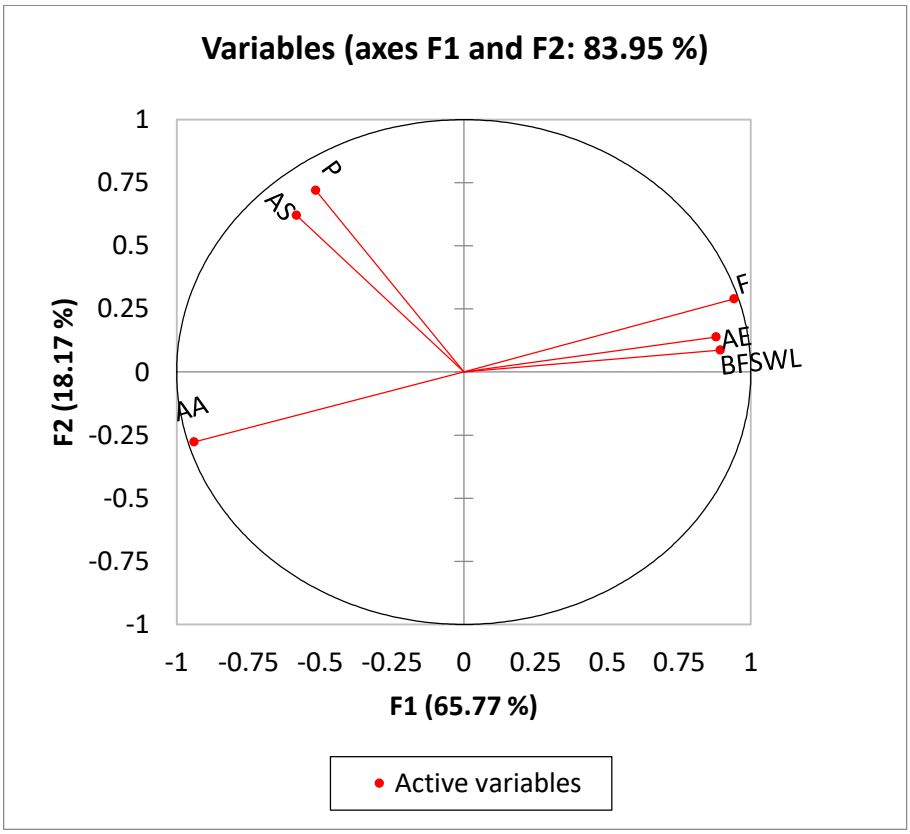

Figure 4. 15 Correlation Circle on Axes F1 and F2

Figure 4.15 presents a projection of the initial variables in the factors space. When two variables are far from the center, then, if they are close to each other, they are significantly positively correlated (e.g AS and P) (r = 1). If they are orthogonal, they are not correlated, if they are on the opposite side of the center, then they are significantly negatively correlated (r close to -1). When the variables are close to the center, some information is carried on the axes, and that any interpretation might be hazardous. In this case, this can be confirmed by either the correlation matrix or the correlation circle on axes F1 and F3. This correlation circle is useful in interpreting the meaning of the axes.

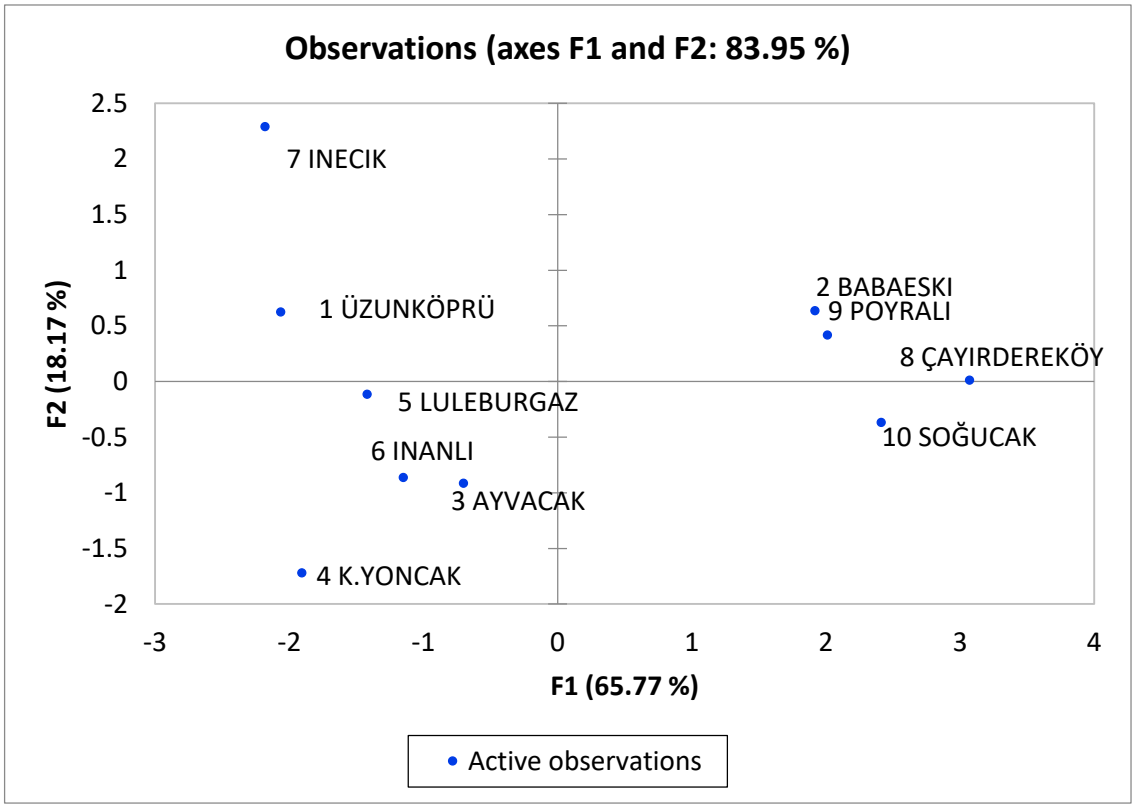

Figure 4. 16 Observations on the Two-Dimensional Map

This Figure 4.16 enables to identify trends in the observations. In this study, the groundwater recharge in İnecik and Çayırdereköy are unique as they can be seen from this Figure 4.16. coming back to the annual recharge values, Inecik displays the maximum value whereas the Çayırdeköy exhibits the minimum recharge. The axes were presented in terms of the factor of scores.

After a PCA analysis, a multiple linear regression analysis was done in order to identify the most controlling factors affecting the recharge and thus the regression model was generated. A multiple linear regression analysis was performed through XLSTAT software with the catchment ' attributes that were displaying high linear correlation with the recharge. The aim, of this action, was to create a model where the recharge can be explained by the basin characteristics with a high factor of loading in PCA and finally to verify the linear model in the Ergene River catchment (Table 4.5 and Figure 4.17). For the recharge with the principal component analysis with high loading catchment attributes (AS, E, BFSWL, AA, F, P, and AE) generated by two PC possessing an eigenvalue more than 1. Against this background, multiple linear regression analysis with the PC scores resulting from the principal component analysis. The groundwater recharge model possesses the 6 variables (AS, E, BFSWL, AA, F, and AE) that were obtained from the two uncorrelated PCs and account for 83.9% of the total variance. The equation of the model was generated and presented in equation (4.1).

$$GR = -217.3 + 0.5 * AS + 4.6E - 02 * BFSWL + 2.3 * AA + 2.25 * F + 0.69 * P - 0.75 * AE \quad (4.1)$$

Table 4. 5 Predictions and Residuals for Groundwater Recharge Model

Sub-basins	GR(mm/year)	Pred GR (mm/year)	Residual(mm/year)
ÜZUNKÖPRÜ	124.469	119.321	5.149
BABAESKI	68.553	67.430	1.123
AYVACAK	80.652	88.695	-8.043
K.YONCAK	99.740	95.229	4.511
LULEBURGAZ	94.801	95.632	-0.832
INANLI	87.852	89.997	-2.145
INECIK	131.205	133.592	-2.387
ÇAYIRDEREKÖY	66.756	70.612	-3.856
POYRALI	75.850	72.766	3.083
SOĞUCAK	72.021	68.625	3.396

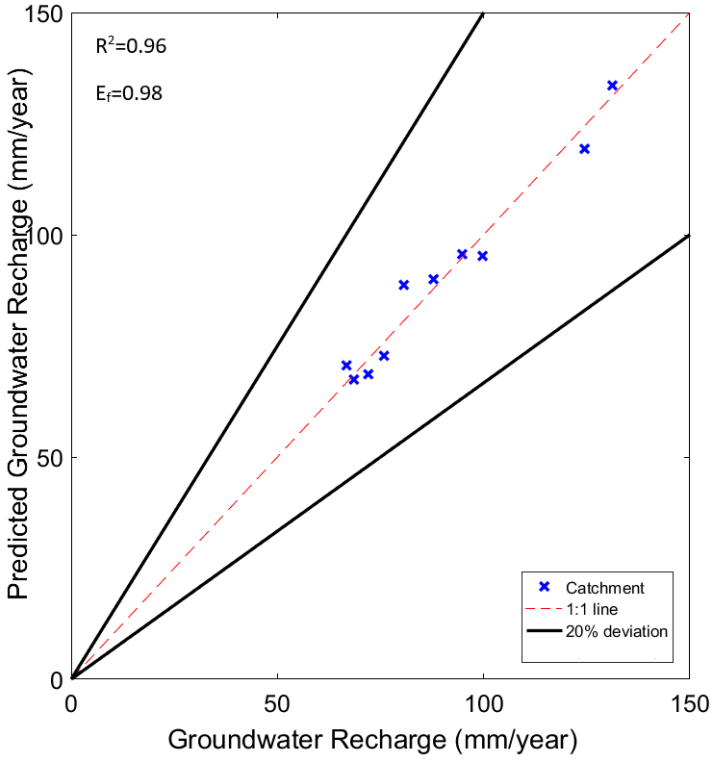

Figure 4. 17 Comparison of Predicted and Observed Recharge (mm/year)

Figure 4.17 shows the comparison of predicted groundwater recharge based on the model equation with observed recharge. The coefficient of determination or R squared and the Nash Sutcliffe coefficients were used to determine the fit of the goodness of the model where the model display 0.96 and 0.98 for R squared and the Nash Sutcliffe coefficients respectively. Thus 96% of the variability of the groundwater recharge is explained by catchment attributes (AS, E, BFSWL, AA, F, P, and AE).

4.4 Simulated Hydraulic Head

In the steady state groundwater flow simulation, the deep aquifers can be taken as confined aquifers where the transmissivities characteristics and saturated zone of the unconfined aquifer must be described in the model. In addition, the vertical exchange among the provided aquifer layers was considered. The investigated area is discretized into the grid cell of 100x100m. The MODFLOW calibration was performed in the steady state based on the observed mean hydraulic heads. The procedure firstly takes into account the observed hydraulic head, and it was manually performed by a trial and error approach. In this approach, the

transmissivity was changed until reaching the same or similar hydraulic heads when compared to the observed ones at different observing wells. Many iterations between mGROWA model and groundwater flow model MODFLOW were done, the simulated outputs were balanced in order to analyze the recharge and hydraulic heads as explained in coupling methodology.

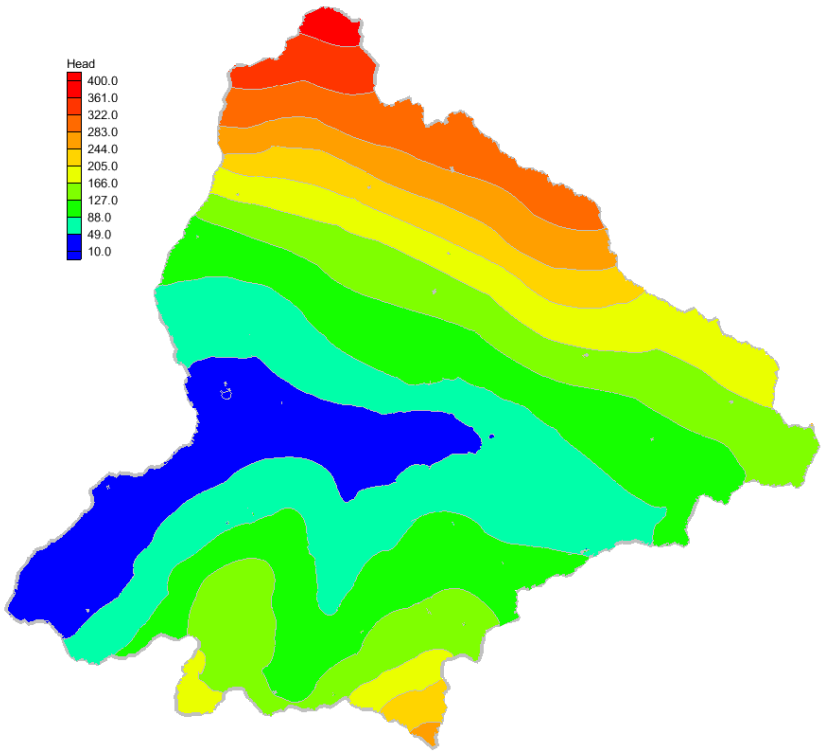

Figure 4. 18 Simulated Hydraulic Heads (m) for Ergene River Basin

Figure 4.18 shows the simulated hydraulic heads map for the Ergene river basin aquifer. As it can be observed from this figure, the calculated heads greatly change depending on the relief of the investigated area. It is noticed that the hydraulic heads vary in the range of 10 to 400 m where the highest head values are observed in the high altitudes in the northwest part on the study area up to 250 m. The lowest values were observed in the central part and west to southern part in the plains of the Ergene river with heads vary from 10 m. The moderate heads in the range of 45 m to 200 m were observed in the middle and south of the investigated area. Generally, it can be seen that the groundwater flows to the stream plains from the middle to the outlet of the catchment.

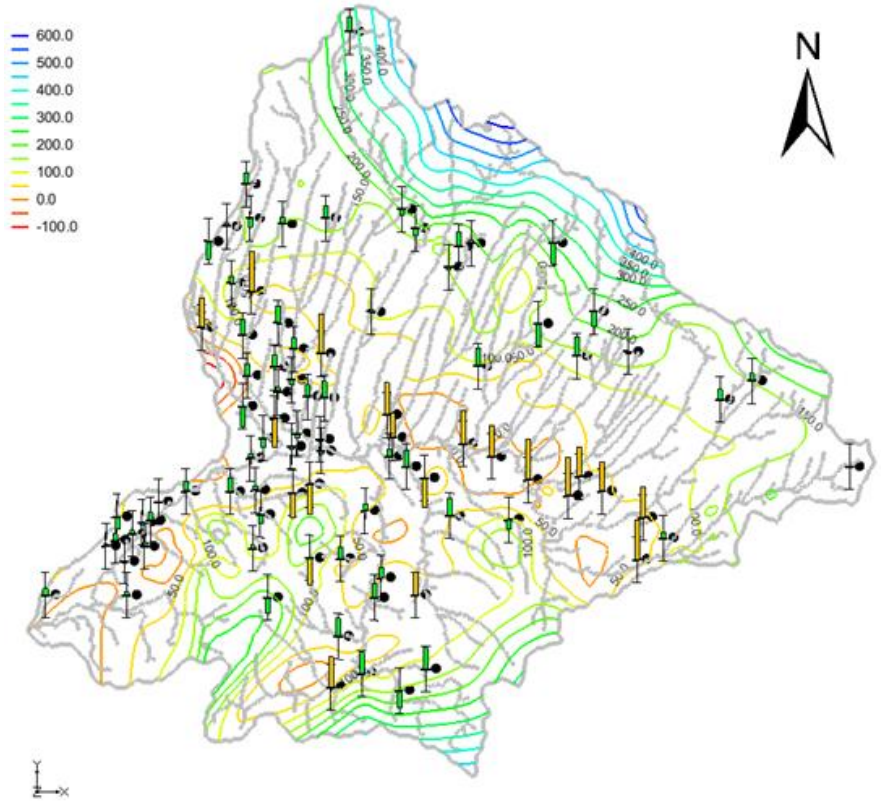

Figure 4. 19 Manual Calibration Result of Ergene River Groundwater Model for Steady-State Condition (heads are in m)

The post-processing was done in Groundwater model system (GMS) such as calibration and validation of the model. The measured data in spring from were divided into two groups in which one group were used for calibration and another part were used for validation and this was done by using observed point coverage in GMS. GMS is capable of using (parameter estimation (PEST) and stochastic method for doing the calibration. The results of calibration in this study were obtained manually. After the calibration model, some observed groundwater levels also were used to validate the model. The good adjustment was achieved as it can be seen in Figures 4.19, 4.20, 4.21 and 4.22.

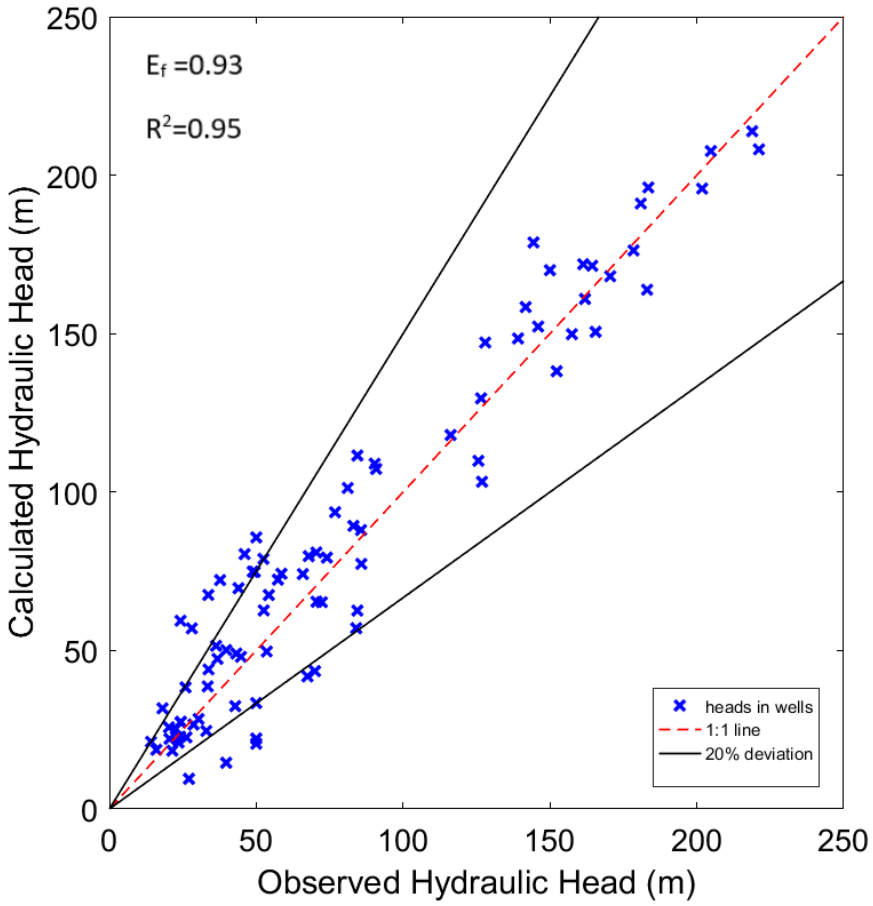

Figure 4. 20 Scatter Plot of Recorded and Computed Hydraulic Head in the Ergene River Basin(Calibration in Steady State Condition)

Figure 4.19 and 4.20 show the map and the scatter plot comparing the observed and computed hydraulic heads in 89 different monitoring wells existing in the Ergene river basin. Figure 4.21 and 4.22 shows the validation results performed in GMS model. R-Squared can be defined as a statistical measure of fit that shows how much variation of a dependent variable is explained by the independent variable in a regression model. An R-squared of 95.22 % and 84 %, respectively for calibration and validation, means that all modeled hydraulic heads are nearly completely explained by observed hydraulic heads. The Nash Sutcliffe coefficients were used to determine the fit of the goodness of the model where the model display 0.93 and 0.83 for the calibration and validation, respectively. Thus, the model validation shows that the model was performed very well and no inconsistency was observed in simulation.

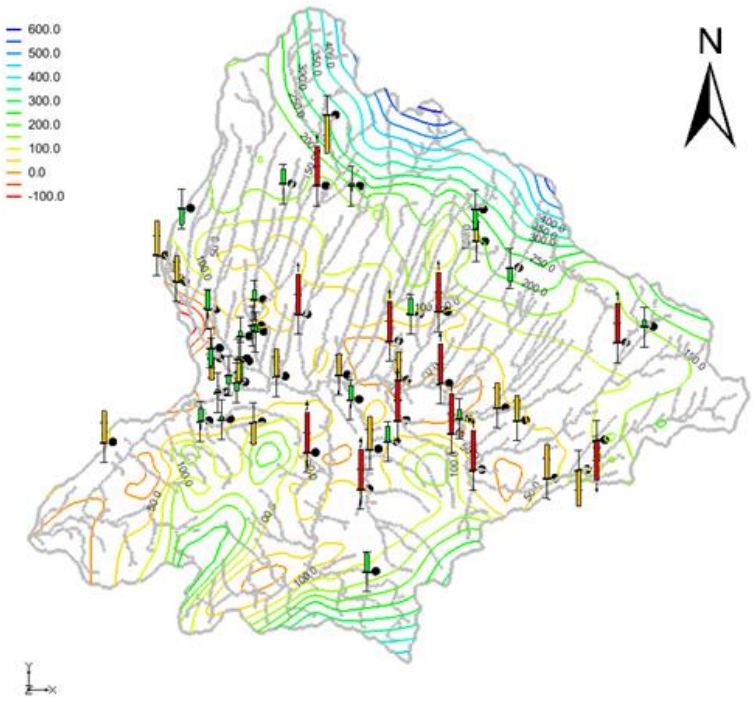

Figure 4. 21 Validation Result of Ergene River Groundwater Model for Steady-State Condition (heads are in m)

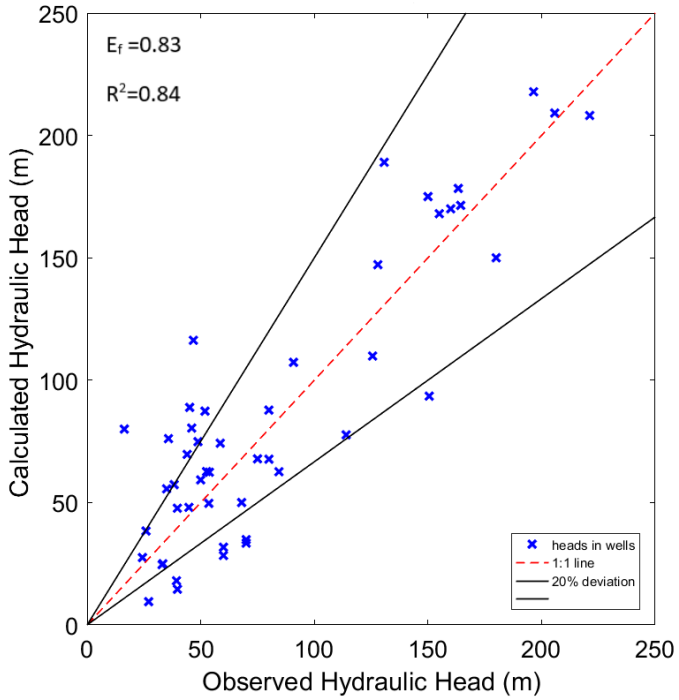

Figure 4. 22 Scatter Plot of Recorded and Computed Hydraulic Head in the Ergene River Basin (Validation in Steady State Condition)

4.5 Discussion of Results

In the comparison between the observed and the model-simulated outputs, there are obvious differences that continue to exist. These inaccuracies can be caused by unreliability in the complexity of model-data environments such as modeling approach, errors occurring in observation, uncertainties occurring in soils groups, land-use types, topography, and climatic data. In addition, the estimated groundwater divides into some considered sub-catchments might not be representative for real corresponding river drainage area due to artificial channels, irrigation practices, dams, and pumped groundwater wells that can perturb the natural water budget of a catchment. Besides, the fact of assuming that recharge, as it is equivalent to base flow, implies the equivalence between groundwater shed and the surface watershed, where the groundwater cannot discharge crosses boundary. Although, groundwater can run in aquifer even most of the time it can overlap many basins, within basins groundwater and surface water boundaries frequently may differ from each other, and this may alter in time. Therefore, to recognize the groundwater shed area which contributes to a river is hard work. Usually, a dissimilarity, between the observed base flow in the river and estimated recharge, may be caused by non-consideration of the lateral fluxes in such models that consider only vertical fluxes, and also the effect of scale.

The recorded base flow from the river gauging stations and its analysis can be used to estimate the level of groundwater recharge [13], [31] as a comparison method. Base flow is taken into account as a groundwater recession flow, where the portion of groundwater flows to the streams during the rainless seasons. The main consideration, in this approach, in order to determine the recharge levels, is that base flow is taken as equivalent to the total groundwater recharge of a basin and the groundwater discharge is roughly considered as the recharge [75]. The base flow analysis method does not consider the origin of the water, however, it considers that great rates of base flow are generated by flow coming from the groundwater reservoir. Thus, for a long period of time, base flow rates are generally taken as a watershed groundwater recharge [76]. This method is broadly useful to validate groundwater models which are based on empirical water balance techniques such as mGROWA model [77]. However, this approach possesses the complexity in directly comparing the recharge and base flow as the later one's approaches estimate the substitute of groundwater discharge and thus of real recharge [75].

In accordance with PCA, the recharge variation is controlled in order of significance by vegetation land-use, soil group types, and climate. The finding of high influence of vegetation on groundwater recharge was confirmed by [78], in their study about a global assessment of groundwater recharge for vegetation. Globally, vegetation possesses the greatest amount of water input such as precipitation and irrigation water that become recharge, and it presents around 1.3 and 3 times greater than potential evapotranspiration and soil hydraulic conductivity in recharge variation [78]. Regarding the finding on the influence of soil types that become the second significant factor for influencing most the groundwater recharge variation, in the coarse-textured soil, the recharge in much greater than in fine-textured soil, thus the movement of the water in the soil is highly controlled by soil texture and structure. This is the result is a confirmation of outputs of studies [31]. The finding of high influence of climate on variation of recharge was also confirmed by Jan et al. (2007), in their study [79] about the rainfall intensity and distribution impact on groundwater level changes and they found that mainly the increase or decrease in level of groundwater is a result of the presence or absence of precipitation, respectively. Thus the groundwater increment is directly relying on the accumulated precipitation. Stonestrom et al., 2007 in their study [80], showed that the recharge becomes much more depending on the quantity and intensity of precipitation, that influences the quantity of water to penetrate into the soil.

In the coupling, the mGROWA model simulates the groundwater recharge iteratively linked to the MODFLOW, in a manner that the modeled recharge can also be affected by the depth to the groundwater and vice versa. Generally, the regional groundwater flow models such as MODFLOW for the groundwater systems assessment e.g infiltration and discharge connections are usually the steady state and thus require the use of long term period groundwater recharge input data. Moreover, the area distributed recharge variation caused by the spatially differentiated soil groups, land use types, topography, etc., may be important and need to consequently be taken into account for these regional groundwater flow models.

Furthermore, the groundwater recharge values become each one of the essential poorly limited hydraulic variables in nearly all groundwater flow and transport models. As a result, the groundwater recharge is usually applied as an adjustable variable in performing a model calibration. Thus, unsatisfactory in the controlling accurately the recharge values

may conduct to a condition of model ‘s non–uniqueness for its outputs, which may return water resource management models useless. Despite that, by coupling the groundwater aquifer and stream masse budgets, the general calibration of a regional groundwater flow model may be enhanced. Against this background, by applying the long period term input data, the mGROWA model produces the temporal and spatial distributed area of runoff, actual evapotranspiration, and recharge. Considering the evapotranspiration from the shallow zones (wetlands), the depth to groundwater table needs to be accounted and considered in the calculations of the groundwater recharge. Thus, in this study, mGROWA is iteratively linked to the MODFLOW that produces the depth to the groundwater, and in accordance with this, the mGROWA model returns the computed recharge to MODFLOW. In the modeling of recharge, the groundwater levels were considered with a view of preventing additional uncertainty and vagueness in optimizing hydraulic conductivities by inverse modeling.

5

Conclusion

The study was conducted in Ergene River basin classified as the among most important catchments exposed to a high level of groundwater exploitation because of the existing of the industrial and agricultural activities. Therefore, the determination of the groundwater recharge was necessary for its sustainable management. But also, in groundwater modeling, the spatial pattern of the groundwater recharge is rarely considered, even though inadequate input recharge data may rise uncertainty in simulation's outputs and calibration, particularly in computing the hydraulic conductivity and groundwater dynamics. The methodology of baseflow estimation in investigated area denotes a considerable spatial pattern of groundwater recharge, and this exhibits the necessity of determining the spatially differentiated recharge on Ergene river basin. The GIS grid-based mGROWA technique was proven to be able to determine the spatial patterns of groundwater recharge.

This study aimed to develop a new approach that strongly relies on the impact of soil groups, land-use types, topography, and climatic conditions in order to calculate spatially distributed recharge and generate at the same time the sub-surface water flow dynamics by coupling mGROWA and MODFLOW models. The accurate estimate of recharge at the regional scale is the leading variable required for exploring the recharge-discharge systems along with providing the authenticity in sub-surface water flow models calibration and validation. The groundwater recharge and dynamics are a prerequisite to the sustainable sub-surface water quantity and quality management.

In the first objective of this study, the novel grid-based water balance model mGROWA results and the dominant factors influencing groundwater recharge in Ergene catchment is discussed. Five sequential tasks were performed during this study. In the first task, (1) a regular and reliable GIS input database made up of the

climate, land-use, soils types, geology, and topography information was created. This was followed as the second step (2) by a water budget analysis with the aim of estimating the renewable water resources such as total runoff at macroscale catchment. Then (3) the dominant runoff components (direct runoff and groundwater recharge) were determined by adopting the concept of base flow index (BFI), and (4) the reliability of the long-term spatially distributed runoffs was verified by comparing the modelled and observed runoffs (total runoff and baseflow obtained from Wundt-Kille separation techniques) from the 10 available gauging stations, (5) finally principal component analysis method was applied in the purpose of determining the dominant catchment and climate factors influencing groundwater recharge.

The mGROWA model outputs have been presented in the form of maps. The lowest actual evapotranspiration (less than 300 mm/y) was observed in urbanized areas. High actual evapotranspiration in the range of 400-450 mm/y appeared in the highest altitudes of the northern part of the study area where the land is covered by forest. The arithmetic average value of the actual evapotranspiration was noticed to be 450 mm/y. The urbanized areas displayed the high total runoff values, hence the high direct runoff level in the range between 350 and 400 mm/y, and 200 and 300 mm/y respectively. The total runoff levels steadily decrease in the high altitude land located in the northern part of Ergene catchment due to the forest cover which generates high actual evapotranspiration (lesser than 150 mm/y). The generated direct runoff shows similar spatial patterns as the total runoff and both are highly influenced by the land-use type. Across the study area (approx. 1,091,645 grid cells) the arithmetic averages for total runoff and direct runoff are 200 mm/y and 85 mm/y respectively. The alluvial plains in the lowland of the catchment prevail a high net groundwater recharge levels up to 600 mm/y, because of high infiltration rates in such unconsolidated sand aquifers. In the northern zone of the catchment, the net groundwater recharge rates are generally diminishing up to the lowest values (less than 50 mm/y). The calculated long-term average net groundwater recharge level over the Ergene catchment amounts 95 mm/y. It could be seen that the groundwater recharge rates starts to occur in November and ends in April. The highest rates of groundwater recharge were observed in January and start to decrease in April as

the vegetation time begins. In accordance with PCA, the spatial groundwater recharge variation is controlled in order of significance by vegetation land-use, soil group types, and climate.

In the second objective of the study, the calculated groundwater recharge in the investigated area as the output of the mGROWA is integrated into a groundwater flow model (MODFLOW) as upper boundary layer in order to determine groundwater dynamics e.g. the hydraulic heads distribution. The calculated heads greatly change depending on the relief of the investigated area. It is noticed that the hydraulic heads vary in the range of 10 to 400 m where the highest head values are observed in the high altitudes in the northwest part of the study area. The outputs of this approach are tested and validated by comparing the recorded and calculated hydraulics heads. The approach developed in this study is recommended to be applied in different catchments across Turkey. The outputs so generated may conclusively contribute to the establishment of the quantitative status of groundwater water reservoir exploitation and enhancement of water resource management and policy of the region.

This study has achieved all the significant issues such as estimating different water balance components including the recharge and its controlling factors, and the integration of the water balance model and groundwater flow in the Ergene River basin, which has been a significant contribution for both groundwater and surface water resources. Despite this achievement, this research can be further improved by considering below-mentioned points, which are not fully implemented in this study resources. (i) Drilling more observation wells distributed over the investigated area for significantly improving the model calibration. Against this background, these wells will provide the groundwater database which will provide the ability to run the current model and any future groundwater model by a transient flow. (ii) Including the water quality analysis for the Ergene River basin, to investigate its suitability for drinking purposes in addition to the agricultural and industrial uses, to reduce the dependence on the surface water source through the maximum benefit from the available groundwater source. (iii) mGROWA simulations can be performed based on climate data, land-use, and soils data as well, against this background, the land use and climate change attribute are very necessary for the context of water resources management for simulations considering climate data from

regional climate models and land use change. By applying this, it can enable the projection of the effect of climate and land use change on the discharge of the Ergene River and recharge as a precondition for the execution of groundwater management strategies.

References

[1] T. B. Shah, J.; Villholth, K.; Angelica, M.; Custodio, E.; Daibes, F.; Hoogesteger, J.; Giordano, Mark; Girman, J.; van der Gun, J.; Kendy, E.; Kijne, J.; Llamas, R.; Masiyandima, M.; Margat, J.; Marin, L.; Peck, J.; Rozelle, S.; Sharma, B. R.; Vincent, L.; Wang, J. , Groundwater: a global assessment of scale and significance. Supriyo Das, India: International Water Management Institute (IWMI), 2007.

[2] A. W. Yenehum, K.; Betelaan, O. , "Spatial and temporal variability of groundwater recharge in Geba bain. Northern Ethiopia," Journal of africa Earth Sciences, vol. 134, pp. 198-212, 2017.

[3] K. P. G. Seiler, J.R., Groundwater recharge from run-off, infiltration and percolation vol. 55: Water Science and Technology Library, 2007.

[4] Simmers., Estimation of natural groundwater recharge vol. 70. D. Reidel, Dordrecht, Holland., 1988.

[5] O. Arkoc, "Heavy metal concentrations of groundwater in the east of Ergene Basin, Turkey," Bull Environ Contam Toxicol, vol. 93, pp. 429-33, Oct 2014.

[6] E. Füsun and B. Zehra, "Linear Alkylbenzene Sulfonates in the Groundwater and Surface Waters: Ergene Basin Case Study," Journal of Agricultural Science and Technology A, vol. 7, 2017.

[7] O. Arkoç, "Assessment of scaling properties of groundwater with elevated sulfate concentration: a case study from Ergene Basin, Turkey," Arabian Journal of Geosciences, vol. 6, pp. 4377-4385, 2012.

[8] C. Santhi, P. M. Allen, R. S. Muttiah, J. G. Arnold, and P. Tuppad, "Regional estimation of base flow for the conterminous United States by hydrologic landscape regions," Journal of Hydrology, vol. 351, pp. 139-153, 2008.

[9] C. A. Rumsey, M. P. Miller, D. D. Susong, F. D. Tillman, and D. W. Anning, "Regional scale estimates of baseflow and factors influencing baseflow in the

Upper Colorado River Basin," Journal of Hydrology: Regional Studies, vol. 4, pp. 91-107, 2015.

[10] M. L. Sharma, "Measurement and prediction of natural groundwater recharge -An overview," Journal of Hydrology, vol. 25, pp. 49-56, 1989.

[11] K. A. Assefa and A. D. Woodbury, "Transient, spatially varied groundwater recharge modeling," Water Resources Research, vol. 49, pp. 4593-4606, 2013.

[12] T. R. Arnold, "Procedural knowledge for integrated modelling: Towards the Modelling Playground," Environmental Modelling & Software, vol. 39, pp. 135-148, 2013.

[13] F. Herrmann, L. Keller, R. Kunkel, H. Vereecken, and F. Wendland, "Determination of spatially differentiated water balance components including groundwater recharge on the Federal State level – A case study using the mGROWA model in North Rhine-Westphalia (Germany)," Journal of Hydrology: Regional Studies, vol. 4, pp. 294-312, 2015.

[14] M. H. McDonald, A.W, A modular three-dimensional finite difference ground-water flow model vol. 6. USA: Tech. Water-Resources Investig., 1988.

[15] J. A. Guzman, D. N. Moriasi, P. H. Gowda, J. L. Steiner, P. J. Starks, J. G. Arnold, et al., "A model integration framework for linking SWAT and MODFLOW," Environmental Modelling & Software, vol. 73, pp. 103-116, 2015.

[16] E. Rukundo and A. Dogan, "Assessment of Climate and Land Use Change Projections and their Impacts on Flooding," Polish Journal of Environmental Studies, vol. 25, pp. 2541-2551, 2016.

[17] B. H. Scanlon, W. R.; Cook, G.P, "Choosing appropriate techniques for quantifying groundwater recharge," Hydrogeology Journal, vol. 10, pp. 18-39, 2002.

[18] L. Ehlers, F. Herrmann, M. Blaschek, R. Duttmann, and F. Wendland, "Sensitivity of mGROWA-simulated groundwater recharge to changes in soil and land use parameters in a Mediterranean environment and conclusions in

view of ensemble-based climate impact simulations," Sci Total Environ, vol. 543, pp. 937-51, Feb 1 2016.

[19] M. Bakker, V. Post, C. D. Langevin, J. D. Hughes, J. T. White, J. J. Starn, et al., "Scripting MODFLOW Model Development Using Python and FloPy," Ground Water, vol. 54, pp. 733-739, Sep 2016.

[20] D. M. Wolock, T. C. Winter, and G. McMahon, "Delineation and Evaluation of Hydrologic-Landscape Regions in the United States Using Geographic Information System Tools and Multivariate Statistical Analyses," Environmental Management, vol. 34, pp. S71-S88, 2004.

[21] J. J. de Vries and I. Simmers, "Groundwater recharge: an overview of processes and challenges," Hydrogeology Journal, vol. 10, pp. 5-17, 2002.

[22] D. N. I. Lerner, A.S, Simmers, I, Groundwater Recharge: a Guide to Understanding and Estimating Natural Recharge. Germany: Heise Hannover, 1990.

[23] R. M. U. Varni, J.E, "Simulation of regional-scale groundwater flow in the Azul River basin, Buenos Aires Province, Argentina," Hydrogeology Journal, vol. 7, pp. 180 -189, 1996.

[24] C. B. Zheng, G.D, Applied Contaminant Transport Modeling, 2nd Edn. New York: John Wiley and Sons, Inc, 2002.

[25] R. W. Kunkel, F, "The GROWA98 model for water balance analysis in large river basins-the river Elbe case study," Journal of Hydrology, vol. 259, pp. 152-162, 2002.

[26] H. K. Bogena, R.; Montzka, C.; Wendland, F, "Uncertainties in the simulation of groundwater recharge at different scales," Advances in Geosciences, vol. 5, pp. 25 - 30, 2005.

[27] M. A. Karpuzcu, N.; Alpaslan, N.; Engin, G; Görmann, H.; Gunduz, M.; Kocal, M.; Oncel, S.; Pekdeger, A.; Voigt, H.; Kuhr, P.; Montzka, C.; Tetzlaff, H.; Vereecken, H.; Wendland, F, Integrated modelling of nutrients in selected rşver basins of Turkey vol. 17. Germany: Forschungszentrum Jülich GmbH, 2008.

[28] F. J. Herrmann, C.; Jenn, F.; Kunkel, R.; Voigt, H.J.; Voigt, J.; Wendaland, F, "Groundwater recharge rates for regional groundwater modelling: a case study using GROWA in the Lower Rhine lignite mining area, Germany," Hydrogeology Journal, vol. 17, pp. 2049 - 2060, 2009.

[29] A. A. Panagopoulos, G.; Kuhr, P.; Tziritis, E.; Wendland, F, "Area-differentiated modeling of water balance in Pinios river basin, central Greece," Global NEST, vol. 17, pp. 221-235, 2015.

[30] B. Tetzlaff, M. Andjelov, P. Kuhr, J. Uhan, and F. Wendland, "Model-based assessment of groundwater recharge in Slovenia," Environmental Earth Sciences, vol. 74, pp. 6177-6192, 2015.

[31] Z. Zomlot, B. Verbeiren, M. Huysmans, and O. Batelaan, "Spatial distribution of groundwater recharge and base flow: Assessment of controlling factors," Journal of Hydrology: Regional Studies, vol. 4, pp. 349-368, 2015.

[32] F. B. Herrmann, N.; Blaschek, M.; Deidda, R.; Duttmann, R.; Wendland, F., "Simulation of future groundwater recharge using a climate modelensemble and SAR-image based soil parameter distributions—Acasestudy in an intensively-used Mediterranean catchment," Science of the Total Environment, vol. 543, pp. 889-905, 2016.

[33] F. Herrmann, R. Kunkel, U. Ostermann, H. Vereecken, and F. Wendland, "Projected impact of climate change on irrigation needs and groundwater resources in the metropolitan area of Hamburg (Germany)," Environmental Earth Sciences, vol. 75, 2016.

[34] A. E. V. Cheo, H. J.; Wendland, F, "Modeling groundwater recharge through rainfall in the Far-North region of Cameroon," Groundwater for sustainable development, vol. 5, pp. 118-130, 2017.

[35] G. Hegen, "Ueber die bewegung des wassers in engen cylindrischen röhren. ," Annalen der Physik und Chemie, vol. 122, pp. 423 - 442, 1839.

[36] J. L. M. Poiseuille, "Recherches experimentales sur Ie mouvement des liquids dans les tubes de tres petits diametres; Influence de la pression sur la

quantite de Iiquide qui traverse les tubes de tres petits diametres.," C. R. Acad. Sci., vol. 11, pp. 61 - 67, 1840.

[37] H. Darcy, Les Fontains Publiques de la Ville de Dijon. . Paris.: Victor Dalmont, 1958.

[38] H. Harbaugh, MODFLOW-2005: The U.S. Geological Survey modular groundwater model—the ground-water flow process. Techniques and Methods. USA: U.S. Geological Survey, 2000.

[39] M. W. Anderson, W, Applied groundwater modeling: Simulation of Flow and advective transport. San Diego, California: Academic Press Inc., 1992.

[40] M. W. Anderson, W; Hunt, R. J, Applied groundwater modeling, simulation of flow and advective transport. . London: Academic Press, 2015.

[41] E. H. Poeter, M, "Inverse Models: a necessary next step in groundwater modeling," Journal of Groundwater, vol. 35, pp. 250 - 260, 1997.

[42] D. Loudyi, "A 2d finite volume model for groundwater flow simulations: integrating nonorthogonal grid capability into MODFLOW," PhD, Carfiff University, 2005.

[43] K. S. Abdalla Mg, "Groundwater Modeling of Multi-Aquifer Systems Using GMS," Journal of Waste Water Treatment & Analysis, vol. 06, 2015.

[44] S. Qiu, X. Liang, C. Xiao, H. Huang, Z. Fang, and F. Lv, "Numerical Simulation of Groundwater Flow in a River Valley Basin in Jilin Urban Area, China," Water, vol. 7, pp. 5768-5787, 2015.

[45] M. B. Rahnama and A. Zamzam, "Quantitative and qualitative simulation of groundwater by mathematical models in Rafsanjan aquifer using MODFLOW and MT3DMS," Arabian Journal of Geosciences, vol. 6, pp. 901-912, 2011.

[46] R. T. Bailey, T. C. Wible, M. Arabi, R. M. Records, and J. Ditty, "Assessing regional-scale spatio-temporal patterns of groundwater-surface water interactions using a coupled SWAT-MODFLOW model," Hydrological Processes, 2016.

[47] A. Qadir, Z. Ahmad, T. Khan, M. Zafar, A. Qadir, and M. Murata, "A spatio-temporal three-dimensional conceptualization and simulation of Dera Ismail Khan alluvial aquifer in visual MODFLOW: a case study from Pakistan," Arabian Journal of Geosciences, vol. 9, 2016.

[48] A. S. Becker, P, Hydrological Models for Water-Resources System Design and Operation. : World Meteorological Organisation, 1990.

[49] G. F. Wessolek, M, "Standorteigenschaften und Wasserhaushalt von versiegelten Flächen.," Pflanzenernähr. Bodenk., vol. 160, pp. 41-46, 1997.

[50] D. Shepard, "A two-dimensional interpolation function for irregularly-spaced data," ed: Proceedings - 1968 ACM National Conference, 1968.

[51] H. Bogena, R. Kunkel, T. Schöbel, H. P. Schrey, and F. Wendland, "Distributed modeling of groundwater recharge at the macroscale," Ecological Modelling, vol. 187, pp. 15-26, 2005.

[52] W. Wundt, Die Kleinstwasserf¨ uhrung der Fl¨ usse als Maß f¨ ur die verf¨ ugbaren Grundwassermengen. vol. 104. Germany, 1958.

[53] K. Kille, "Das Verfahren MoMNQ, ein Beitrag zur Berechnung der mittleren langjährigen Grundwasserneubildung mit Hilfe der monatlichen Niedrigwasserabflüsse. ," Zeitschrift der Dtsch. Geol. Gesellschaft Sonderba, vol. 122, pp. 89-95, 1970.

[54] S. Demuth, Untersuchung zum Niedrigwasser in West-Europa. Freiburger Schriften xur Hydrologie. Freiburg, Germany: Universitat Freiburg, 1993.

[55] R. W. Kunkel, F, Der Landschaftswasserhaushalt im Flubeinzugsgebiet der Elbe - Verfahren. Datengrundlagen und Bilanzgröben. vol. 12. Jülich, Germany: Schr. d. FZJ. Reine Umwelt., 1998.

[56] G. J. Dörhöfer, V, "Eine Methode zur flächendifferenzierten Ermittlung der Grundwasserneubildungsrate," Geol. Jb., vol. 27, pp. 45-65, 1980.

[57] V. Hennings, Methodendokumentation Bodenkunde – Auswertemethoden zur Beurteilung der Empfindlichkeit und Belastbarkeit von Böden. Hannover: - Geologisches Jahrbuch, Reihe F, 2000.

[58] J. E. S. Nash, J.V "River flow forecasting through conceptual models part I -A discussion of principles," Journal of Hydrology, vol. 10, pp. 282-290, 1970.

[59] R. H. K. McCuen, Z.; Cutter, G.A, "Evaluation of the Nash-Sutcliffe Efficiency Index," Journal of hydrologic engineering, vol. 11, pp. 597-602, 2006.

[60] H. Abdi and L. J. Williams, "Principal component analysis," Wiley Interdisciplinary Reviews: Computational Statistics, vol. 2, pp. 433-459, 2010.

[61] E. J. D. Knudson, D.L.; Christian, G.D, "Application of Factor Analysis to the Study of Rain Chemistry in the Puget Sound Region," in ACS Symposium Series 52, Washington., D.C, USA, 1977, pp. 80-116.

[62] Y. Wang, M. a. Shao, Z. Liu, and R. Horton, "Regional-scale variation and distribution patterns of soil saturated hydraulic conductivities in surface and subsurface layers in the loessial soils of China," Journal of Hydrology, vol. 487, pp. 13-23, 2013.

[63] B. Abou Zakhem, A. Al-Charideh, and B. Kattaa, "Using principal component analysis in the investigation of groundwater hydrochemistry of Upper Jezireh Basin, Syria," Hydrological Sciences Journal, vol. 62, pp. 2266-2279, 2017.

[64] H. H. George and A. S. Zohrab, "Reference Crop Evapotranspiration from Temperature," Applied Engineering in Agriculture, vol. 1, pp. 96-99, 1985.

[65] A. Berti, G. Tardivo, A. Chiaudani, F. Rech, and M. Borin, "Assessing reference evapotranspiration by the Hargreaves method in north-eastern Italy," Agricultural Water Management, vol. 140, pp. 20-25, 2014.

[66] M. Cobaner, H. Citakoğlu, T. Haktanir, and O. Kisi, "Modifying Hargreaves–Samani equation with meteorological variables for estimation of reference evapotranspiration in Turkey," Hydrology Research, vol. 48, pp. 480-497, 2017.

[67] G. Y. Lu and D. W. Wong, "An adaptive inverse-distance weighting spatial interpolation technique," Computers & Geosciences, vol. 34, pp. 1044-1055, 2008.

[68] C. R. Dudgeon, "Effects of non-Darcy flow and partial penetration on water levels near open-pit excavations.," in In: Proceedings of the 18th Congress of the International Association of Hydrogeologists, Cambridge, England., 1985, pp. 122-132.

[69] P. L. B. Younger, S.A; Hedin, R.S, Mine water. Hdrology, Pollution, Remediation: Environmental Pollution, 2002.

[70] J. M. Buttle, P. W. Hazlett, C. D. Murray, I. F. Creed, D. S. Jeffries, and R. Semkin, "Prediction of groundwater characteristics in forested and harvested basins during spring snowmelt using a topographic index," Hydrological Processes, vol. 15, pp. 3389-3407, 2001.

[71] K. Price, "Effects of watershed topography, soils, land use, and climate on baseflow hydrology in humid regions: A review," Progress in Physical Geography: Earth and Environment, vol. 35, pp. 465-492, 2011.

[72] D. N. A. Moriasi, J.G.; Van Liew, M.W.; Bingner, R.L.; Harmel, D.; Veith, T.L, "Model evaluation guidelines for systematic quantification of accuracy in watershed simulations," American Society of Agriculture and biological Engineers, vol. 50, pp. 885-900, 2007.

[73] K. Richard, "Development of Groundwater Recharge Model for the <i>Sumanpa</i> Catchment at Ashanti-Mampong-Ashanti Area in Ghana," Science Research, vol. 3, p. 289, 2015.

[74] J. Krishnaswamy, M. Bonell, B. Venkatesh, B. K. Purandara, K. N. Rakesh, S. Lele, et al., "The groundwater recharge response and hydrologic services of tropical humid forest ecosystems to use and reforestation: Support for the “infiltration-evapotranspiration trade-off hypothesis”," Journal of Hydrology, vol. 498, pp. 191-209, 2013.

[75] D. W. Risser, W. J. Gburek, and G. J. Folmar, "Comparison of recharge estimates at a small watershed in east-central Pennsylvania, USA," Hydrogeology Journal, vol. 17, pp. 287-298, 2008.

[76] S. C. Meyer, "Analysis of base flow trends in urban streams, northeastern Illinois, USA," Hydrogeology Journal, vol. 13, pp. 871-885, 2004.

[77] G. N. Delin, R. W. Healy, D. L. Lorenz, and J. R. Nimmo, "Comparison of local- to regional-scale estimates of ground-water recharge in Minnesota, USA," Journal of Hydrology, vol. 334, pp. 231-249, 2007.

[78] J. H. Kim and R. B. Jackson, "A Global Analysis of Groundwater Recharge for Vegetation, Climate, and Soils," Vadose Zone Journal, vol. 11, p. 0, 2012.

[79] C. D. Jan, T.-H. Chen, and W.-C. Lo, "Effect of rainfall intensity and distribution on groundwater level fluctuations," Journal of Hydrology, vol. 332, pp. 348-360, 2007.

[80] A. C. Stonestrom, J.; Leake, S.A, Groundwater recharge in the arid and semiarid southwestern united states. Reston, Virginia: U.S. Geological Survey, 2007.

A

Mgrowap Script

```
<xml version="1.0" encoding="UTF-8">
    <job name="Mgrowap">

        <!-- model cells -->
        <modelgrid
        modelgridcellcode="1">E:/PhD/Thesis/mGROWA/mGROWA/r2mgrowap4/Ascii/modelgrid.asc<
        /modelgrid>

        <!-- constants -->
        <nodatavalue value="-9999.0"></nodatavalue>
        <missingcalculationmode value="-7772"></missingcalculationmode>

        <!-- processing -->
        <nprocessors number="4"></nprocessors>

        <!-- geometry & global parameter-->
        <cellStructure layerThickness_dm="3" numberOfLayers="5"></cellStructure>
        <dissefunction r="5"></dissefunction>
        <percolationwaterformation pwbf="0.6" plTH="2"></percolationwaterformation>
        <initialSoilMoisture type="1" initialRelativeSoilMoisture="1.0"
        files=""></initialSoilMoisture>

        <!-- time steps -->

        <timeline>E:/PhD/Thesis/mGROWA/mGROWA/r2mgrowap4/Mgrowap/sp1/timeline.txt</timeli
        ne>

        <!-- reports -->
        <reportfolder
        maxErrorPointsPerFile="1000">E:/PhD/Thesis/mGROWA/mGROWA/r2mgrowap4/reports/sp1</
        reportfolder>

        <!-- control points-->

        <controlpoints>E:/PhD/Thesis/mGROWA/mGROWA/r2mgrowap4/Mgrowap/cp.txt</controlpoin
        ts>

        <controlpointsResultFolder>E:/PhD/Thesis/mGROWA/mGROWA/r2mgrowap4/output/cp/sp1/<
        /controlpointsResultFolder>
        <controlpointsClimateStationSortSequenceFolder
        write="true">E:/PhD/Thesis/mGROWA/mGROWA/r2mgrowap4/output/cp/sortsequences/sp1/
        </controlpointsClimateStationSortSequenceFolder>

        <!-- input timelines -->

        <timelineP>E:/PhD/Thesis/mGROWA/mGROWA/r2mgrowap4/Mgrowap/sp1/timelineP.txt</time
        lineP>

            <timelinePFolder>E:/PhD/Thesis/mGROWA/mGROWA/r2mgrowap4/input/p/month/</timel
            inePFolder>

        <timelineEt0>E:/PhD/Thesis/mGROWA/mGROWA/r2mgrowap4/Mgrowap/sp1/timelineEt0.txt</
        timelineEt0>

            <timelineEt0Folder>E:/PhD/Thesis/mGROWA/mGROWA/r2mgrowap4/input/et0/month/</t
            imelineEt0Folder>
        <timelineActualIrrigation read="false"></timelineActualIrrigation>
            <actualIrrigationFolder></actualIrrigationFolder>

        <!-- station-based climate data -->
        <stations>E:/PhD/Thesis/mGROWA/mGROWA/r2mgrowap4/Mgrowap/stations.txt</stations>
        <stationsP
        nodata="NA">E:/PhD/Thesis/mGROWA/mGROWA/r2mgrowap4/Mgrowap/stations_p.txt</statio
        nsP>

            <stationsPFolder>E:/PhD/Thesis/mGROWA/mGROWA/r2mgrowap4/input/stations/p/sp1/
            </stationsPFolder>
```

```
44          <stationsEt0
            nodata="NA">E:/PhD/Thesis/mGROWA/mGROWA/r2mgrowap4/Mgrowap/stations_et0.txt</stat
            ionsEt0>
45
                <stationsEt0Folder>E:/PhD/Thesis/mGROWA/mGROWA/r2mgrowap4/input/stations/et0/
                spl/</stationsEt0Folder>
46
47          <!-- parameter timelines -->
48
            <timelineTopoFactor>E:/PhD/Thesis/mGROWA/mGROWA/r2mgrowap4/Mgrowap/timelineTopoFa
            ctor.txt</timelineTopoFactor>
49
                <timelineTopoFactorFolder>E:/PhD/Thesis/mGROWA/mGROWA/r2mgrowap4/input/</time
                lineTopoFactorFolder>
50
            <timelineLanduse>E:/PhD/Thesis/mGROWA/mGROWA/r2mgrowap4/Mgrowap/timelineLanduse.t
            xt</timelineLanduse>
51
                <timelineLanduseFolder>E:/PhD/Thesis/mGROWA/mGROWA/r2mgrowap4/input/</timelin
                eLanduseFolder>
52
                <parameterLanduseClass1>E:/PhD/Thesis/mGROWA/mGROWA/r2mgrowap4/Mgrowap/land_u
                se_parameter1.txt</parameterLanduseClass1>
53
                <parameterLanduseClass2>E:/PhD/Thesis/mGROWA/mGROWA/r2mgrowap4/Mgrowap/land_u
                se_parameter2.txt</parameterLanduseClass2>
54
                <modesLanduse>E:/PhD/Thesis/mGROWA/mGROWA/r2mgrowap4/Mgrowap/land_use_modes.t
                xt</modesLanduse>
55
                <parameterLanduseLayerConsumptionFactors>E:/PhD/Thesis/mGROWA/mGROWA/r2mgrowa
                p4/Mgrowap/land_use_consumption3dmLayer.txt
56              </parameterLanduseLayerConsumptionFactors>
57
                <percentageImperviousness>E:/PhD/Thesis/mGROWA/mGROWA/r2mgrowap4/Mgrowap/perc
                entageImperviousness.txt</percentageImperviousness>
58
                <rainStorageCapacity>E:/PhD/Thesis/mGROWA/mGROWA/r2mgrowap4/Mgrowap/rainStora
                geCapacity.txt</rainStorageCapacity>
59
            <timelineSoil>E:/PhD/Thesis/mGROWA/mGROWA/r2mgrowap4/Mgrowap/timelineSoil.txt</ti
            melineSoil>
60
                <timelineSoilFolder>E:/PhD/Thesis/mGROWA/mGROWA/r2mgrowap4/input/</timelineSo
                ilFolder>
61
                <soilprofiles>E:/PhD/Thesis/mGROWA/mGROWA/r2mgrowap4/Mgrowap/soilprofiles.txt
                </soilprofiles>
62
                <soilTypeGroupsParameter1>E:/PhD/Thesis/mGROWA/mGROWA/r2mgrowap4/Mgrowap/soil
                typegroups_parameter1.txt</soilTypeGroupsParameter1>
63
                <soilTypeGroupsParameter2>E:/PhD/Thesis/mGROWA/mGROWA/r2mgrowap4/Mgrowap/soil
                typegroups_parameter2.txt</soilTypeGroupsParameter2>
64
                <soilTypeParameter1>E:/PhD/Thesis/mGROWA/mGROWA/r2mgrowap4/Mgrowap/soiltype_p
                arameter1.txt</soilTypeParameter1>
65
                <soilTypeParameter2>E:/PhD/Thesis/mGROWA/mGROWA/r2mgrowap4/Mgrowap/soiltype_p
                arameter2.txt</soilTypeParameter2>
66
                <soilTypeParameter3>E:/PhD/Thesis/mGROWA/mGROWA/r2mgrowap4/Mgrowap/soiltype_p
                arameter3.txt</soilTypeParameter3>
67
            <timelineDepthToWaterTable>E:/PhD/Thesis/mGROWA/mGROWA/r2mgrowap4/Mgrowap/timelin
            eDepthToWaterTable.txt</timelineDepthToWaterTable>
68
```

```
            <timelineDepthToWaterTableFolder>E:/PhD/Thesis/mGROWA/mGROWA/r2mgrowap4/input
            /</timelineDepthToWaterTableFolder>
69          <!-- irrigation -->
70          <timelineIrrigationFunction></timelineIrrigationFunction>
71              <timelineIrrigationFunctionFolder></timelineIrrigationFunctionFolder>
72              <irrigationTimingParameters></irrigationTimingParameters>
73              <irrigationLayerThresholds></irrigationLayerThresholds>
74
75          <!-- output timelines -->
76          <timelineEta
            write="true">E:/PhD/Thesis/mGROWA/mGROWA/r2mgrowap4/Mgrowap/sp1/timelineEta.txt</
            timelineEta>
77
                <timelineEtaFolder>E:/PhD/Thesis/mGROWA/mGROWA/r2mgrowap4/output/eta/month/</
                timelineEtaFolder>
78          <timelineQ
            write="true">E:/PhD/Thesis/mGROWA/mGROWA/r2mgrowap4/Mgrowap/sp1/timelineQ.txt</ti
            melineQ>
79
                <timelineQFolder>E:/PhD/Thesis/mGROWA/mGROWA/r2mgrowap4/output/q/month/</time
                lineQFolder>
80          <timelineQu
            write="true">E:/PhD/Thesis/mGROWA/mGROWA/r2mgrowap4/Mgrowap/sp1/timelineQu.txt</t
            imelineQu>
81
                <timelineQuFolder>E:/PhD/Thesis/mGROWA/mGROWA/r2mgrowap4/output/qu/month/</ti
                melineQuFolder>
82          <timelineCwb
            write="true">E:/PhD/Thesis/mGROWA/mGROWA/r2mgrowap4/Mgrowap/sp1/timelineCwb.txt</
            timelineCwb>
83
                <timelineCwbFolder>E:/PhD/Thesis/mGROWA/mGROWA/r2mgrowap4/output/cwb/month/</
                timelineCwbFolder>
84          <timelineE
            write="true">E:/PhD/Thesis/mGROWA/mGROWA/r2mgrowap4/Mgrowap/sp1/timelineE.txt</ti
            melineE>
85
                <timelineEFolder>E:/PhD/Thesis/mGROWA/mGROWA/r2mgrowap4/output/e/month/</time
                lineEFolder>
86          <timelineMi write="false"></timelineMi>
87              <timelineMiFolder></timelineMiFolder>
88
89          <timelineDaysQ write="false"></timelineDaysQ>
90              <timelineDaysQFolder></timelineDaysQFolder>
91          <timelineDaysEwc write="false"></timelineDaysEwc>
92              <timelineDaysEwcFolder></timelineDaysEwcFolder>
93          <timelineDaysSwd write="false"></timelineDaysSwd>
94              <timelineDaysSwdFolder></timelineDaysSwdFolder>
95          <timelineDaysLwc write="true true true true true" prefix="wc"
            suffix=".asc">E:/PhD/Thesis/mGROWA/mGROWA/r2mgrowap4/Mgrowap/sp1
            /timelineDaysLwc.txt</timelineDaysLwc>
96
97
                <timelineDaysLwcFolder>E:/PhD/Thesis/mGROWA/mGROWA/r2mgrowap4/output/lwc/day/
                </timelineDaysLwcFolder>
98
99          <!-- statistics -->
100         <timelinePeriodsSoilWaterDeficit write="true"
            threshold="60">E:/PhD/Thesis/mGROWA/mGROWA/r2mgrowap4/Mgrowap/sp1/timelinePeriods
            SoilWaterDeficit.txt
101         </timelinePeriodsSoilWaterDeficit>
102
                <gridnamesPeriodsSoilWaterDeficit>E:/PhD/Thesis/mGROWA/mGROWA/r2mgrowap4/Mgro
                wap/sp1/gridnamesNdswd.txt</gridnamesPeriodsSoilWaterDeficit>
103
                    <gridnamesPeriodsSoilWaterDeficitFolder>E:/PhD/Thesis/mGROWA/mGROWA/r2mgr
                    owap4/output/statistics/ndswd/</gridnamesPeriodsSoilWaterDeficitFolder>
104
                <gridnamesPeriodsMaxConsecutiveDaysSoilWaterDeficit>E:/PhD/Thesis/mGROWA/mGRO
                WA/r2mgrowap4/Mgrowap/sp1/gridnamesMdswd.txt
105             </gridnamesPeriodsMaxConsecutiveDaysSoilWaterDeficit>
106
                    <gridnamesPeriodsMaxConsecutiveDaysSoilWaterDeficitFolder>E:/PhD/Thesis/m
                    GROWA/mGROWA/r2mgrowap4/output/statistics/mdswd/
107                 </gridnamesPeriodsMaxConsecutiveDaysSoilWaterDeficitFolder>
108
109         <!-- daily catchment statistics -->
110         <dailyCatchmentStatisticsFolder write="false"
            file=""></dailyCatchmentStatisticsFolder>
111         <catchmentsGrid></catchmentsGrid>
112     </job>

</xml>
```

B

Mgrowap Runoff Separation Script

```
<xml version="1.0" encoding="UTF-8">
    <!-- runoff separation -->
    <job name="MgrowaRunoffSeparation">

        <!-- model cells -->
        <modelgrid
        modelgridcellcode="1">E:/PhD/Thesis/mGROWA/mGROWA/r2mgrowap4/Ascii/modelgrid.asc<
        /modelgrid>

        <!-- processing mode -->
        <processingMode mode="timesteps"></processingMode>
        <!-- mode 1: rows -->
        <!-- mode 2: timesteps -->

        <!-- constants -->
        <nodatavalue value="-9999.0"></nodatavalue>

        <!-- time steps -->

        <timeline>E:/PhD/Thesis/mGROWA/mGROWA/r2mgrowap4/Mgrowap/sp1/timeline.txt</timeli
        ne>

        <!-- reports -->
        <reportfolder
        maxErrorPointsPerFile="5000">E:/PhD/Thesis/mGROWA/mGROWA/r2mgrowap4/reports/sp1/<
        /reportfolder>

        <!-- control points-->

        <controlpoints>E:/PhD/Thesis/mGROWA/mGROWA/r2mgrowap4/Mgrowap/cp.txt</controlpoin
        ts>

        <controlpointsResultFolder>E:/PhD/Thesis/mGROWA/mGROWA/r2mgrowap4/output/cp/sp1/<
        /controlpointsResultFolder>

        <!-- intput timelines -->

        <timelineQ>E:/PhD/Thesis/mGROWA/mGROWA/r2mgrowap4/Mgrowap/sp1/timelineQ.txt</time
        lineQ>

            <timelineQFolder>E:/PhD/Thesis/mGROWA/mGROWA/r2mgrowap4/output/q/month/</time
            lineQFolder>

        <timelineE>E:/PhD/Thesis/mGROWA/mGROWA/r2mgrowap4/Mgrowap/sp1/timelineE.txt</time
        lineE>

            <timelineEFolder>E:/PhD/Thesis/mGROWA/mGROWA/r2mgrowap4/output/e/month/</time
            lineEFolder>

        <timelineQu>E:/PhD/Thesis/mGROWA/mGROWA/r2mgrowap4/Mgrowap/sp1/timelineQu.txt</ti
        melineQu>

            <timelineQuFolder>E:/PhD/Thesis/mGROWA/mGROWA/r2mgrowap4/output/qu/month/</ti
            melineQuFolder>

        <!-- parameter timelines -->

        <timelineLanduse>E:/PhD/Thesis/mGROWA/mGROWA/r2mgrowap4/Mgrowap/timelineLanduse.t
        xt</timelineLanduse>

            <timelineLanduseFolder>E:/PhD/Thesis/mGROWA/mGROWA/r2mgrowap4/input/</timelin
            eLanduseFolder>
            <modesLanduse
            modeFreeWaterSurface="1">E:/PhD/Thesis/mGROWA/mGROWA/r2mgrowap4/Mgrowap/land_
            use_modes.txt</modesLanduse>

        <timelineSlope>E:/PhD/Thesis/mGROWA/mGROWA/r2mgrowap4/MgrowaRunoffSeparation/time
```

```
lineSlope.txt</timelineSlope>
39
    <timelineSlopeFolder>E:/PhD/Thesis/mGROWA/mGROWA/r2mgrowap4/input/</timelineS
    lopeFolder>
40
    <bfiSlopeClasses>E:/PhD/Thesis/mGROWA/mGROWA/r2mgrowap4/MgrowaRunoffSeparatio
    n/bfiSlopeClasses.txt</bfiSlopeClasses>
41
<timelinePermeabilityClasses>E:/PhD/Thesis/mGROWA/mGROWA/r2mgrowap4/MgrowaRunoffS
eparation/timelinePermeabilityClasses.txt</timelinePermeabilityClasses>
42
    <timelinePermeabilityClassesFolder>E:/PhD/Thesis/mGROWA/mGROWA/r2mgrowap4/inp
    ut/</timelinePermeabilityClassesFolder>
43
    <bfiPermeabilityClasses>E:/PhD/Thesis/mGROWA/mGROWA/r2mgrowap4/MgrowaRunoffSe
    paration/bfiPermeabilityClasses.txt</bfiPermeabilityClasses>
44
<timelineDepthToWaterTable>E:/PhD/Thesis/mGROWA/mGROWA/r2mgrowap4/Mgrowap/timelin
eDepthToWaterTable.txt</timelineDepthToWaterTable>
45
    <timelineDepthToWaterTableFolder>E:/PhD/Thesis/mGROWA/mGROWA/r2mgrowap4/input
    /</timelineDepthToWaterTableFolder>
46
<timelineWaterLoggingTendencyClasses>E:/PhD/Thesis/mGROWA/mGROWA/r2mgrowap4/Mgrow
aRunoffSeparation/timelineWaterLoggingTendencyClasses.txt</timelineWaterLoggingTe
ndencyClasses>
47
    <timelineWaterLoggingTendencyClassesFolder>E:/PhD/Thesis/mGROWA/mGROWA/r2mgro
    wap4/input/</timelineWaterLoggingTendencyClassesFolder>
48
    <bfiWaterLoggingTendencyClasses>E:/PhD/Thesis/mGROWA/mGROWA/r2mgrowap4/Mgrowa
    RunoffSeparation/bfiWaterLoggingTendencyClasses.txt</bfiWaterLoggingTendencyC
    lasses>
49
<timelineDrainageClasses>E:/PhD/Thesis/mGROWA/mGROWA/r2mgrowap4/MgrowaRunoffSepar
ation/timelineDrainageClasses.txt</timelineDrainageClasses>
50
    <timelineDrainageClassesFolder>E:/PhD/Thesis/mGROWA/mGROWA/r2mgrowap4/input/<
    /timelineDrainageClassesFolder>
51
    <bfiDrainageClasses>E:/PhD/Thesis/mGROWA/mGROWA/r2mgrowap4/MgrowaRunoffSepara
    tion/bfiDrainageClasses.txt</bfiDrainageClasses>
52
53  <!-- output timelines -->
54  <timelineQr write="false"></timelineQr>
55      <timelineQrFolder></timelineQrFolder>
56  <timelineQrn
    write="true">E:/PhD/Thesis/mGROWA/mGROWA/r2mgrowap4/MgrowaRunoffSeparation/sp1/ti
    melineQrn.txt</timelineQrn>
57
    <timelineQrnFolder>E:/PhD/Thesis/mGROWA/mGROWA/r2mgrowap4/output/qrn/month/</
    timelineQrnFolder>
58  <timelineQd
    write="true">E:/PhD/Thesis/mGROWA/mGROWA/r2mgrowap4/MgrowaRunoffSeparation/sp1/ti
    melineQd.txt</timelineQd>
59
    <timelineQdFolder>E:/PhD/Thesis/mGROWA/mGROWA/r2mgrowap4/output/qd/month/</ti
    melineQdFolder>
60  <timelineQad
    write="true">E:/PhD/Thesis/mGROWA/mGROWA/r2mgrowap4/MgrowaRunoffSeparation/sp1/ti
    melineQad.txt</timelineQad>
61
    <timelineQadFolder>E:/PhD/Thesis/mGROWA/mGROWA/r2mgrowap4/output/qad/month/</
    timelineQadFolder>
62  <timelineBFI
    write="true">E:/PhD/Thesis/mGROWA/mGROWA/r2mgrowap4/MgrowaRunoffSeparation/sp1/ti
    melineBFI.txt</timelineBFI>



63
    <timelineBFIFolder>E:/PhD/Thesis/mGROWA/mGROWA/r2mgrowap4/output/bfi/month/</
    timelineBFIFolder>
64  <timelineQn
    write="true">E:/PhD/Thesis/mGROWA/mGROWA/r2mgrowap4/MgrowaRunoffSeparation/sp1/ti
    melineQn.txt</timelineQn>
65
    <timelineQnFolder>E:/PhD/Thesis/mGROWA/mGROWA/r2mgrowap4/output/qn/month/</ti
    melineQnFolder>
66  </job>

</xml>
```

C

Script of Time Series at Control Point

```
## script: time series (days) at control points

## R version 2.9.0

## libraries
library(zoo);

## root folder
root.folder <- "E:/PhD/Thesis/mGROWA/mGROWA/r2mgrowap1/"

## id's
rid = 2;
pid = 20;

## control point result folder
cp.folder = paste(root.folder,"output/cp/sp3/",sep="");
cp.filename.prefix = "cpDayValues_";
cp.filename.suffix = ".txt";
timeline.file = paste(root.folder,"Mgrowap/sp3/timeline.txt",sep="");
cp.file = paste(root.folder,"Mgrowap/cp.txt",sep="");
plot.folder = paste(root.folder,"cpResults/pdf/",sep="");
dir.create(plot.folder);

##
month <- c("11","12","01","02","03","04","05","06","07","08","09","10");
shift.wry <- c(-1,-1,0,0,0,0,0,0,0,0,0,0);
n.days <- c(30,31,31,28,31,30,31,30,31,31,30,31);

## control point ids
## timeline
cp.ids <- read.table(cp.file, header=F, sep="\t", dec=".",
                     col.names=c("cpid","short_name","easting","northing"),
                     colClasses=c("integer","character","numeric","numeric"),
                     stringsAsFactors=F);

## timeline
timeline <- read.table(timeline.file, header=F, sep="\t", dec=".",
                       col.names=c("did","day","month","mid","year","wry"),

                       colClasses=c("integer","integer","integer","integer","integer","int
                       eger"),
                       stringsAsFactors=F);

## control point data

for (i in 1:length(cp.ids[,1])) {

    if (file.exists(paste(cp.folder,cp.filename.prefix,cp.ids[i,1],cp.filename.suffix,
    sep="")) == T)   {
    cp.data <-
    read.table(paste(cp.folder,cp.filename.prefix,cp.ids[i,1],cp.filename.suffix,
    sep=""), header=TRUE, sep="\t", dec=".",
    col.names=c("control_point_id","timestep_days_index","interpolated_precipitation","in
    terpolated_et0","daily_precipitation","daily_et0","daily_eta","daily_q","daily_cwb","
    awc_ex_mm","pwp_ex_mm","tfc_ex_mm","daily_gwe","daily_irr_mm"),
                        stringsAsFactors=F);
    colnames(cp.data) <-
    c("cpid","di","ip","iet0","p","et0","eta","q","cwb","awc","pwp","fc","gwe","irr");

    if (length(cp.data[,1]) > 0)    {

      cp.data <- merge(cp.data, timeline, by.x=c("di"), by.y=c("did"));
      cp.data <- cbind(cp.data,
      date=strptime(paste(cp.data$year,"-",cp.data$month,"-",cp.data$day, sep=""),
      "%Y-%m-%d"));

      pdf(file=paste(plot.folder,"cpid_",cp.ids[i,1],".pdf", sep=""), width=12.4,
      height=9.8, onefile=TRUE, family="Helvetica", title="cp_timeseries_days",
      fonts=NULL, version="1.1");
```

```
op <- par();
for (j in 1:length(unique(cp.data$wry)))  {

  x.labels <- data.frame()
  for (k in 1:12) {

    x.labels[k,1] <-
    format(paste(unique(cp.data$wry)[j]+shift.wry[k],"-",month[k],"-01",sep=""));

  }
  strptime(x.labels[,1],format="%Y-%m-%d");
x.lim <-
as.POSIXct(c(strptime(paste(unique(cp.data$wry)[j]+shift.wry[1],"-",month[1],"-01",
sep=""),format="%Y-%m-%d"),

           strptime(paste(unique(cp.data$wry)[j]+shift.wry[12],"-",month[12],"-",n.
           days[12],sep=""),format="%Y-%m-%d")));


  par(mai=c(0,0.8,0,0.2));
  nf <- layout(matrix(c(1:8),8,1, byrow=TRUE), widths=c(12,12,12,12,12,12,12,12),
  heights=c(1.0,1.0,1.0,1.0,1.0,1.0,1.0,1.0), TRUE);

  p <- plot(cp.data[cp.data$wry == unique(cp.data$wry)[j],"date"],
  cp.data[cp.data$wry == unique(cp.data$wry)[j],"p"], type="s", xlab="", ylab="p
  in mm", main="", ylim=c(0,max(cp.data$p)), xlim=x.lim, xaxt='n');
  axis.POSIXct(1, at=strptime(x.labels[,1],format="%Y-%m-%d"),
  labels=x.labels[,1], side=3);
  axis.POSIXct(1, at=strptime(x.labels[,1],format="%Y-%m-%d"), labels=F, side=1);

  abline(a = 0, b = 0, col="gray");
  mtext(toString(paste(unique(cp.data$wry)[j])), side=3, line=3, adj=0.5,
  col="black");
  mtext(toString(paste("control point: ",cp.ids[i,1], "   ", cp.ids[i,2],
  sep="")), side=3, line=3, adj=0, col="black");
  mtext(toString(paste("mgrowa run ",rid," - Ergene",sep="")), side=3, line=3,
  adj=1, cex=0.8);
  mtext("   Precipitation  ", side=3, line=-2.2, adj=0, cex=0.8, font=2);
  mtext(paste("  ",round(sum(cp.data[cp.data$wry ==
  unique(cp.data$wry)[j],"p"]),digits=0), " mm   "), side=3, line=-2.2, adj=1,
  cex=0.8, font=2, col="blue4");


  et0 <- plot(cp.data[cp.data$wry == unique(cp.data$wry)[j],"date"],
  cp.data[cp.data$wry == unique(cp.data$wry)[j],"et0"], type="s", xlab="",
  ylab=expression(et[0] * " in mm"), main="", ylim=c(0,8), xlim=x.lim, xaxt='n');
  axis.POSIXct(1, at=strptime(x.labels[,1],format="%Y-%m-%d"), labels=F);
  abline(a = 0, b = 0, col="gray");
  mtext("   Grass reference evapotranspiration  ", side=3, line=-2.2, adj=0,
  cex=0.8, font=2);
  mtext(paste("  ",round(sum(cp.data[cp.data$wry ==
  unique(cp.data$wry)[j],"et0"]),digits=0), " mm   "), side=3, line=-2.2, adj=1,
  cex=0.8, font=2);


  eta <- plot(cp.data[cp.data$wry == unique(cp.data$wry)[j],"date"],
  cp.data[cp.data$wry == unique(cp.data$wry)[j],"eta"], type="s", xlab="",
  ylab=expression(et[a] * " in mm"), main="", ylim=c(0,8), xlim=x.lim, xaxt='n');
  axis.POSIXct(1, at=strptime(x.labels[,1],format="%Y-%m-%d"), labels=F);
  abline(a = 0, b = 0, col="gray");
  mtext("   Actual evapotranspiration  ", side=3, line=-2.2, adj=0, cex=0.8,
  font=2);
  mtext(paste("  ",round(-sum(cp.data[cp.data$wry ==
  unique(cp.data$wry)[j],"eta"]),digits=0), " mm   "), side=3, line=-2.2, adj=1,
  cex=0.8, font=2, col="darkred");


  det <- plot(cp.data[cp.data$wry == unique(cp.data$wry)[j],"date"],
```

```
(cp.data[cp.data$wry == unique(cp.data$wry)[j],"eta"]-cp.data[cp.data$wry ==
unique(cp.data$wry)[j],"et0"]), type="s", xlab="", ylab=expression(et[a] * " -
" * et[0] * " in mm"), main="", ylim=c(-7,6), xlim=x.lim, xaxt='n');
axis.POSIXct(1, at=strptime(x.labels[,1],format="%Y-%m-%d"), labels=F);
abline(a = 0, b = 0, col="gray");
par(new=T);
det <- plot(cp.data[cp.data$wry == unique(cp.data$wry)[j],"date"],
(cp.data[cp.data$wry == unique(cp.data$wry)[j],"eta"]-cp.data[cp.data$wry ==
unique(cp.data$wry)[j],"et0"]), type="s", xlab="", ylab="", main="",
ylim=c(-7,6), xlim=x.lim, xaxt='n');
par(new=F);
mtext("   eta-et0  ", side=3, line=-2.2, adj=0, cex=0.8, font=2);
mtext(paste("  ",round(sum((cp.data[cp.data$wry ==
unique(cp.data$wry)[j],"eta"]-cp.data[cp.data$wry ==
unique(cp.data$wry)[j],"et0"])),digits=0), " mm   "), side=3, line=-2.2, adj=1,
cex=0.8, font=2);


q <- plot(cp.data[cp.data$wry == unique(cp.data$wry)[j],"date"],
cp.data[cp.data$wry == unique(cp.data$wry)[j],"q"], type="s", xlab="", ylab="q
in mm", main="", ylim=c(0,max(cp.data$q)), xlim=x.lim, xaxt='n');
axis.POSIXct(1, at=strptime(x.labels[,1],format="%Y-%m-%d"), labels=F);
abline(a = 0, b = 0, col="gray");
mtext("   Percolation water  ", side=3, line=-2.2, adj=0, cex=0.8, font=2);
mtext(paste("  ",round(-sum(cp.data[cp.data$wry ==
unique(cp.data$wry)[j],"q"]),digits=0), " mm   "), side=3, line=-2.2, adj=1,
cex=0.8, font=2, col="darkred");



awc.ylim <- c(0,1.5*max(c(cp.data$awc,cp.data$fc)));
awc.xmin <- min(cp.data[cp.data$wry == unique(cp.data$wry)[j],"date"]);
awc <- plot(cp.data[cp.data$wry == unique(cp.data$wry)[j],"date"],
cp.data[cp.data$wry == unique(cp.data$wry)[j],"awc"], type="s", xlab="",
ylab=expression(theta * " in mm"), main="", ylim=awc.ylim, xlim=x.lim, xaxt='n');
axis.POSIXct(1, at=strptime(x.labels[,1],format="%Y-%m-%d"), labels=F);
par(new=T);
plot(cp.data[cp.data$wry == unique(cp.data$wry)[j],"date"], cp.data[cp.data$wry
== unique(cp.data$wry)[j],"awc"], type="s", xlab="", ylab="", main="",
ylim=awc.ylim, xlim=x.lim, xaxt='n');
lines(cp.data[cp.data$wry == unique(cp.data$wry)[j],"date"],
cp.data[cp.data$wry == unique(cp.data$wry)[j],"pwp"], type="s",
col="chocolate4");
lines(cp.data[cp.data$wry == unique(cp.data$wry)[j],"date"],
cp.data[cp.data$wry == unique(cp.data$wry)[j],"fc"], type="s", col="royalblue4");
par(new=F);
mtext("   Water content in the root zone  ", side=3, line=-2.2, adj=0, cex=0.8,
font=2);
awc.a <- cp.data[cp.data$wry == unique(cp.data$wry)[j],"awc"][1];
awc.e <- cp.data[cp.data$wry ==
unique(cp.data$wry)[j],"awc"][length(cp.data[cp.data$wry ==
unique(cp.data$wry)[j],"awc"])];
if((awc.e-awc.a)>=0){
  mtext(paste("  ",round(awc.e-awc.a,digits=0), " mm   "), side=3, line=-2.2,
  adj=1, cex=0.8, font=2, col="blue4");
}
if((awc.e-awc.a)<0){
  mtext(paste("  ",round(awc.e-awc.a,digits=0), " mm   "), side=3, line=-2.2,
  adj=1, cex=0.8, font=2, col="darkred");
}


gwe <- plot(cp.data[cp.data$wry == unique(cp.data$wry)[j],"date"],
cp.data[cp.data$wry == unique(cp.data$wry)[j],"gwe"], type="s", xlab="",
ylab="ib in mm", main="", ylim=c(0,8), xlim=x.lim, xaxt='n');
axis.POSIXct(1, at=strptime(x.labels[,1],format="%Y-%m-%d"), labels=F);
abline(a = 0, b = 0, col="gray");
mtext("   Capillary rise and direct evapotranspiration from groundwater /
surface water", side=3, line=-2.2, adj=0, cex=0.8, font=2);
```

```
143           mtext(paste("  ",round(sum(cp.data[cp.data$wry ==
              unique(cp.data$wry)[j],"gwe"]),digits=0), " mm   "), side=3, line=-2.2, adj=1,
              cex=0.8, font=2, col="blue4");
144
145
146
147           irr <- plot(cp.data[cp.data$wry == unique(cp.data$wry)[j],"date"],
              cp.data[cp.data$wry == unique(cp.data$wry)[j],"irr"], type="s", xlab="",
              ylab="Irrigation in mm", main="", ylim=c(0,30), xlim=x.lim, xaxt='n');
148         axis.POSIXct(1, at=strptime(x.labels[,1],format="%Y-%m-%d"), labels=x.labels[,1]);
149           abline(a = 0, b = 0, col="gray");
150           mtext("   Irrigation  ", side=3, line=-2.2, adj=0, cex=0.8, font=2);
151           mtext(paste("  ",round(sum(cp.data[cp.data$wry ==
              unique(cp.data$wry)[j],"irr"]),digits=0), " mm   "), side=3, line=-2.2, adj=1,
              cex=0.8, font=2, col="blue4");
152
153           legend(x=as.POSIXct(x.labels[1,1]), y=-15, c("Water content in the root zone at
              permanent wilting point", "Water content in the root zone at field capacity"),
              lwd=0.5, col=c("chocolate4","royalblue4"), cex=0.8, bty="n", xpd=NA);
154           ##legend(x=awc.xmin, y=-4, c("Water content in the root zone at permanent
              wilting point", "Water content in the root zone at field capacity"), lwd=0.5,
              col=c("chocolate4","royalblue4"), cex=0.8, bty="n", xpd=NA);
155         ##legend(x=awc.xmin, y=-0.4*max(c(cp.data$awc,cp.data$fc)), c("Water content in
            the root zone at permanent wilting point", "Water content in the root zone at
            field capacity"), lwd=0.5, col=c("chocolate4","royalblue4"), cex=0.8, bty="n",
            xpd=NA);
156
157
158         }
159
160         par(op);
161         dev.off();
162     }
163       }
164
165   }
166
```

D

Python Script for Groundwater Flow Model

```
import flopy
import os
import flopy.utils.binaryfile as bf
import numpy as np
from osgeo import gdal
import matplotlib.pyplot as plt
```

```
modelname = "model1"
modelpath = "../Model/"
#Modflow Nwt
mf1 = flopy.modflow.Modflow(modelname, exe_name="../Exe/MODFLOW-NWT_64.exe", vers
nwt = flopy.modflow.ModflowNwt(mf1 ,maxiterout=150,linmeth=2)
```

```
#Raster paths
demPath ="../Rst/DEM_200.tif"
crPath = "../Rst/CR.tif"
bot_1Path = "../Rst/bottom1.tif"
bot_2Path = "../Rst/bottom2.tif"
bot_3Path = "../Rst/bottom3.tif"
bot_4Path = "../Rst/bottom4.tif"
rechargePath = "../Rst/recharge.tif"

#Open files
demDs = gdal.Open(demPath)
crDs = gdal.Open(crPath)
bot_1Ds = gdal.Open(bot_1Path)
bot_2Ds = gdal.Open(bot_2Path)
bot_3Ds = gdal.Open(bot_3Path)
bot_4Ds = gdal.Open(bot_4Path)
rechargeDs= gdal.Open(rechargePath)
geot = crDs.GetGeoTransform() #Xmin, deltax, ?, ymax, ?, delta y

geot
```

```
# Get data as arrays
demData = demDs.GetRasterBand(1).ReadAsArray()
crData = crDs.GetRasterBand(1).ReadAsArray()
bot_1Data = bot_1Ds.GetRasterBand(1).ReadAsArray()
bot_2Data = bot_2Ds.GetRasterBand(1).ReadAsArray()
bot_3Data = bot_2Ds.GetRasterBand(1).ReadAsArray()
bot_4Data = bot_2Ds.GetRasterBand(1).ReadAsArray()
rechargeData = rechargeDs.GetRasterBand(1).ReadAsArray()
# Get statistics
stats = demDs.GetRasterBand(1).GetStatistics(0,1)
stats
```

```
#Elevation of Layers
Layer1 = bot_1Data
Layer2 = bot_1Data
Layer3 = bot_3Data
Layer4 = bot_4Data
```

```
#Boundaries for Dis = Create discretization object, spatial/temporal discretizati
ztop = demData
zbot = [Layer1, Layer2, Layer3, Layer4]
nlay = 4
nrow = demDs.RasterYSize
ncol = demDs.RasterXSize
delr = geot[1]
delc = abs(geot[5])
```

```
dis = flopy.modflow.ModflowDis(mf1, nlay,nrow,ncol,delr=delr,delc=delc,top=ztop,b
```

```
# Variables for the BAS package
iboundData = np.zeros(demData.shape, dtype=np.int32)
iboundData[crData > 0 ] = 1
bas = flopy.modflow.ModflowBas(mf1,ibound=iboundData,strt=ztop, hnoflo=-2.0E+020)
```

```
# Array of hydraulic heads per layer
hk = [1E-4, 1E-7, 1E-8, 1E-9]
```

```
#Add the recharge package (RCH) to the MODFLOW model
rch = rechargeData
rch = flopy.modflow.ModflowRch(mf1, nrchop=3, rech =rch_data)
```

```
#Add the evapotranspiration package (EVT) to the MODFLOW model
evtr = np.ones((nrow, ncol), dtype=np.float32) * 1/365/86400
evtr_data = {0: evtr}
evt = flopy.modflow.ModflowEvt(mf1,nevtop=1,surf=ztop,evtr=evtr_data, exdp=0.5)
```

```
#Add the drain package (DRN) to the MODFLOW model
river = np.zeros(demData.shape, dtype=np.int32)
river[crData == 3 ] = 1
list = []
for i in range(river.shape[0]):
    for q in range(river.shape[1]):
        if river[i,q] == 1:
            list.append([0,i,q,ztop[i,q],0.001]) #layer,row,column,elevation(floa
rivDrn = {0:list}

drn = flopy.modflow.ModflowDrn(mf1, stress_period_data=rivDrn)
```

```
# Add OC package to the MODFLOW model
oc = flopy.modflow.ModflowOc(mf1) #ihedfm= 1, iddnfm=1
```

```
#Write input files -> write file with extensions
mf1.write_input()

#run model -> gives the solution
mf1.run_model()
```

```
#Import model
ml = flopy.modflow.Modflow.load('../Model/model1.nam')
```

```
# First step is to set up the plot
fig = plt.figure(figsize=(15, 15))
ax = fig.add_subplot(1, 1, 1, aspect='equal')

# Next we create an instance of the ModelMap class
modelmap = flopy.plot.ModelMap(sr=ml.dis.sr)

# Then we can use the plot_grid() method to draw the grid
# The return value for this function is a matplotlib LineCollection object,
# which could be manipulated (or used) later if necessary.
linecollection = modelmap.plot_grid(linewidth=0.4)
```

```
fig = plt.figure(figsize=(15, 6))
ax = fig.add_subplot(1, 1, 1)
# Next we create an instance of the ModelCrossSection class
#modelxsect = flopy.plot.ModelCrossSection(model=ml, line={'Column': 5})
modelxsect = flopy.plot.ModelCrossSection(model=ml, line={'Row': 99})

# Then we can use the plot_grid() method to draw the grid
# The return value for this function is a matplotlib LineCollection object,
# which could be manipulated (or used) later if necessary.
linecollection = modelxsect.plot_grid(linewidth=0.4)
t = ax.set_title('Column 6 Cross-Section - Model Grid')
```

```
fig = plt.figure(figsize=(15, 15))
ax = fig.add_subplot(1, 1, 1, aspect='equal')
modelmap = flopy.plot.ModelMap(model=ml, rotation=0)
quadmesh = modelmap.plot_ibound(color_noflow='cyan')
linecollection = modelmap.plot_grid(linewidth=0.4)
```

```
fig = plt.figure(figsize=(15, 6))
ax = fig.add_subplot(1, 1, 1)
modelxsect = flopy.plot.ModelCrossSection(model=ml, line={'Column': 5})
patches = modelxsect.plot_ibound(color_noflow='cyan')
linecollection = modelxsect.plot_grid(linewidth=0.4)
t = ax.set_title('Column 6 Cross-Section with IBOUND Boundary Conditions')
```

Publications from the thesis

Contact Information: emmyruk7bc@gmail.com

Papers

E. Rukundo and A. Doğan, "Dominant Influencing Factors of Groundwater Recharge Spatial Patterns in Ergene River Catchment, Turkey," *Water*, vol. 11, no. 4, p. 653, Mar. 2019.